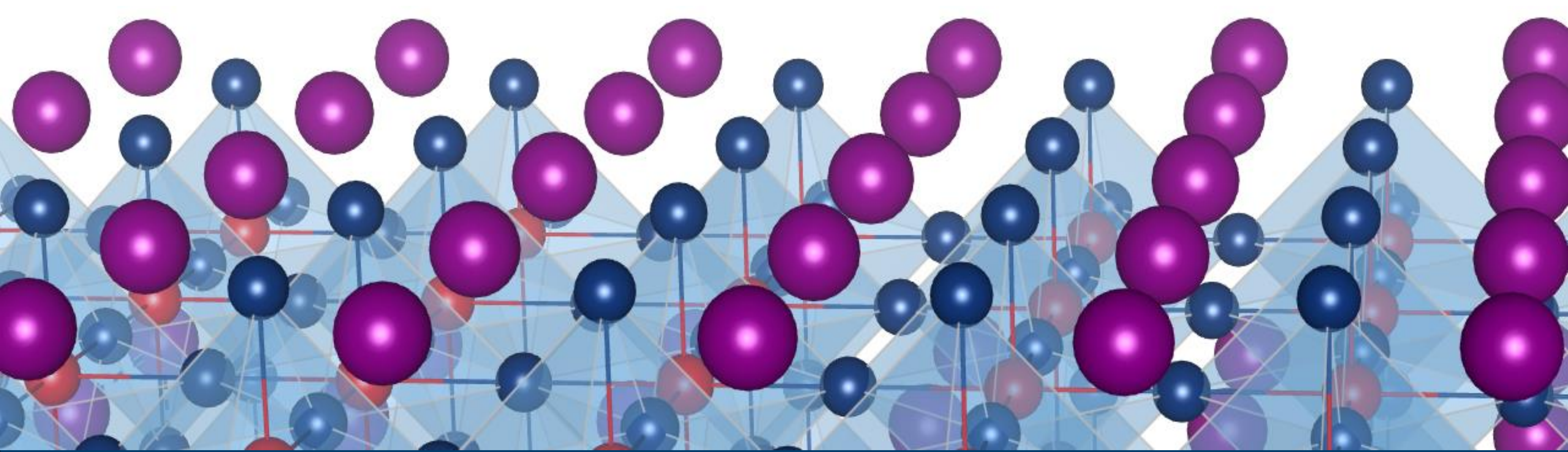

DETERMINING DEFECT DENSITIES AND CHARGE EXTRACTION LOSSES IN PEROVSKITE SOLAR CELLS

Sandheep Ravishankar, Uwe Rau and Thomas Kirchartz

IMD-3 Photovoltaik, Forschungszentrum Jülich

determining doping and defect densities using capacitance measurements

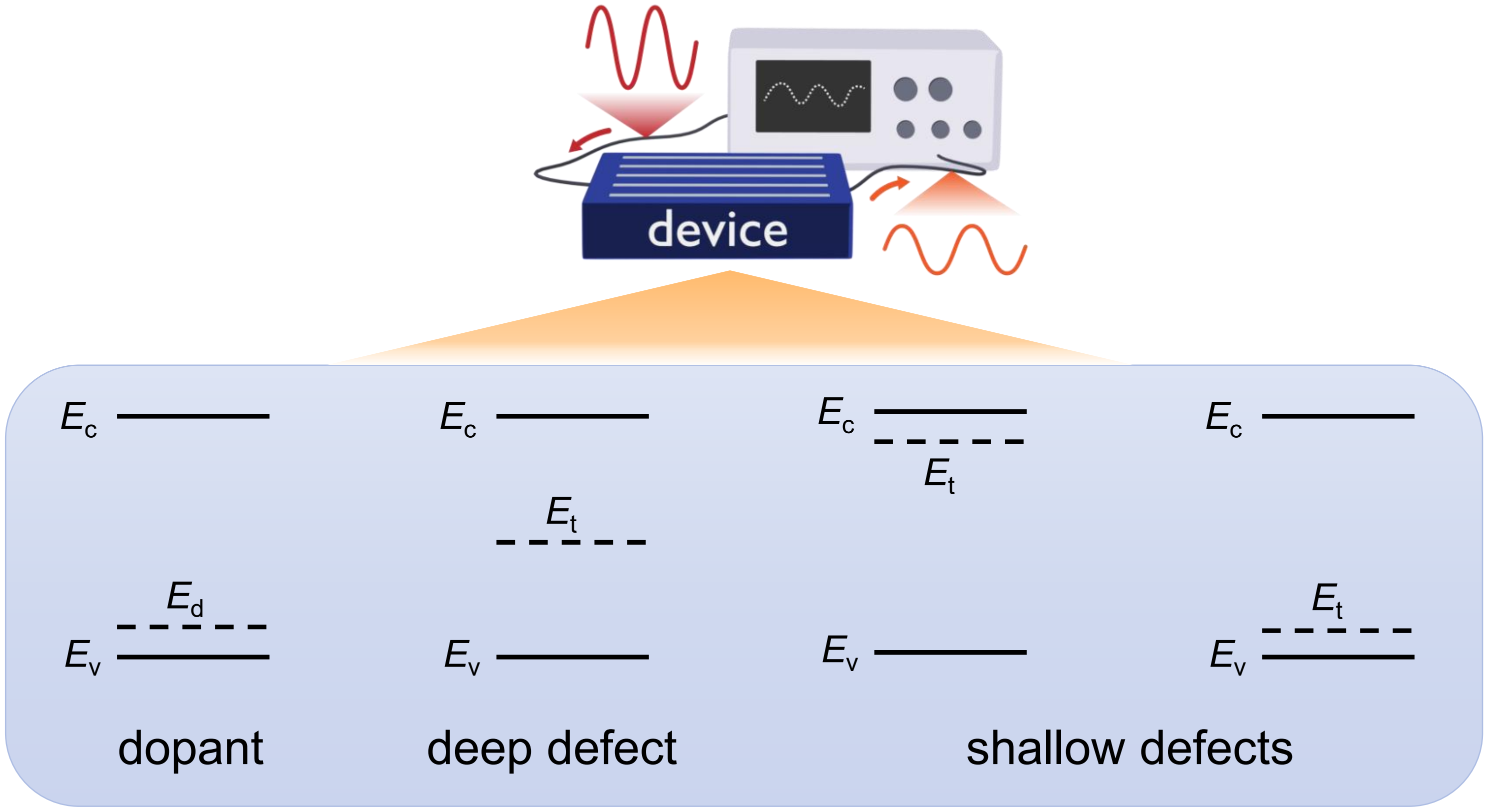

depletion layer capacitance

density of negatively-charged dopants N_a (cm^{-3})

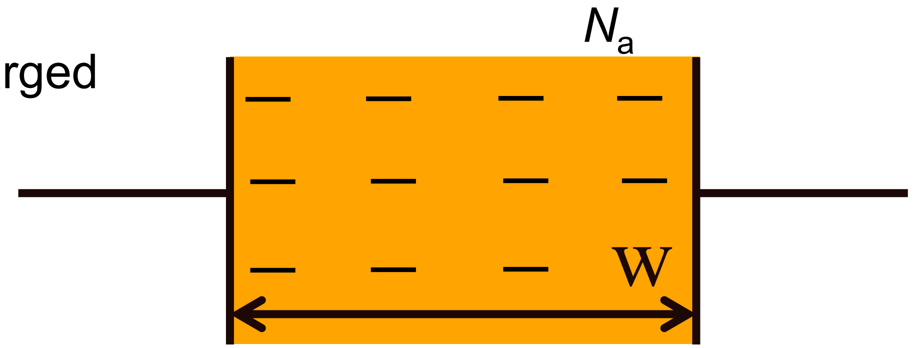

$$C = \frac{\varepsilon_r \varepsilon_0}{w}$$

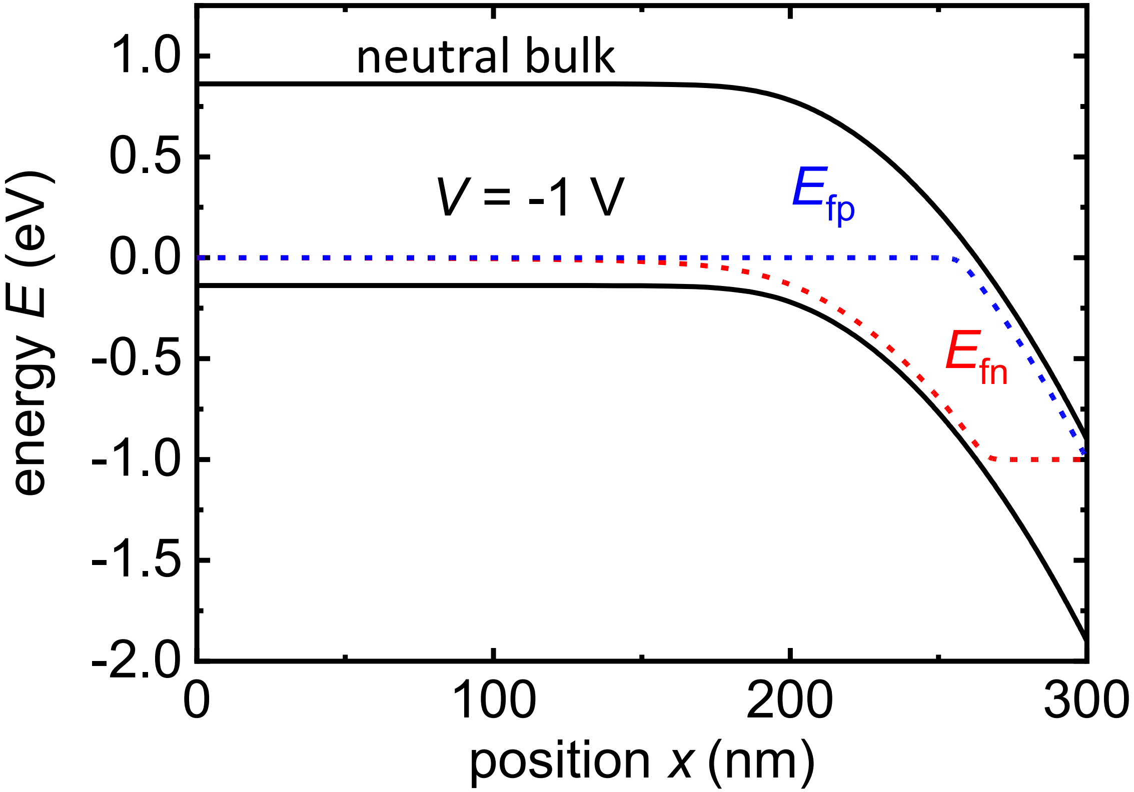

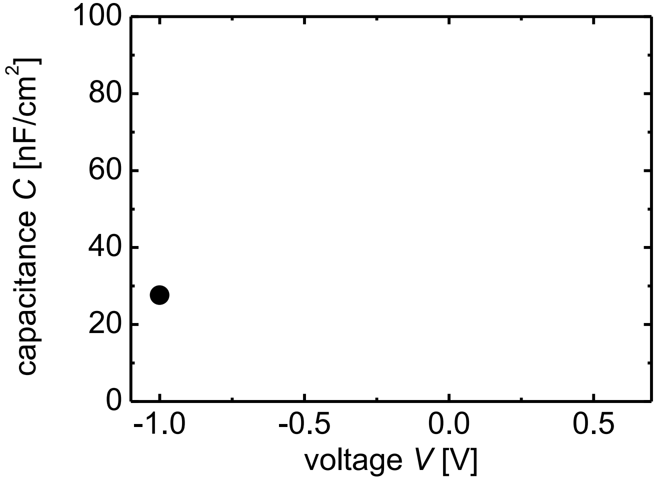

depletion layer capacitance

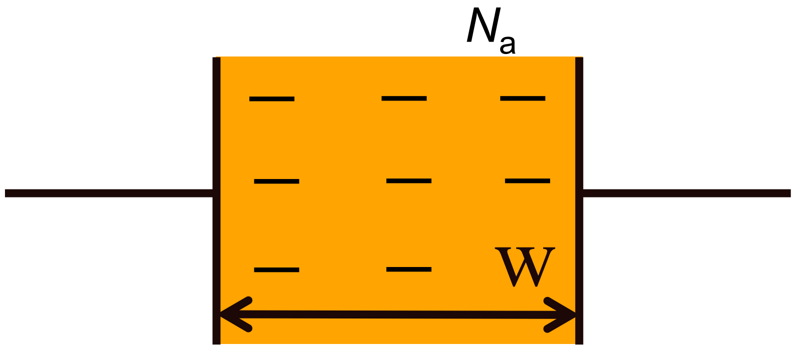

$$C = \frac{\varepsilon_r \varepsilon_0}{w}$$

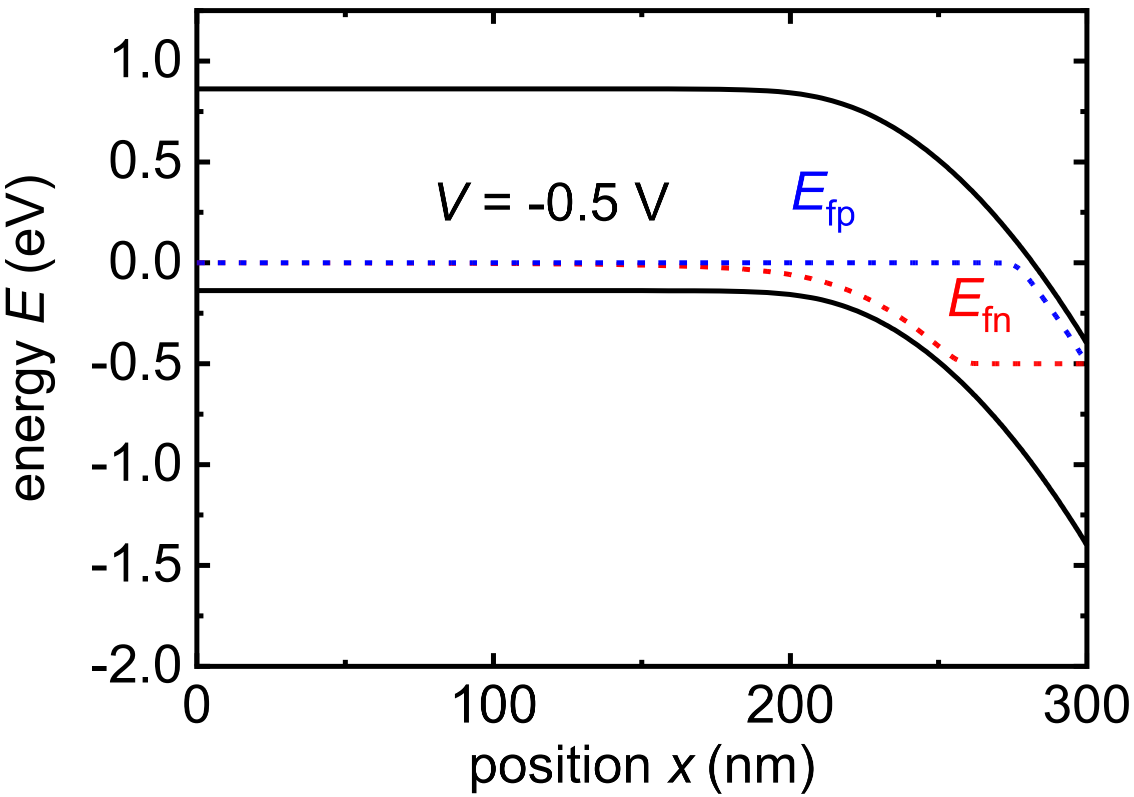

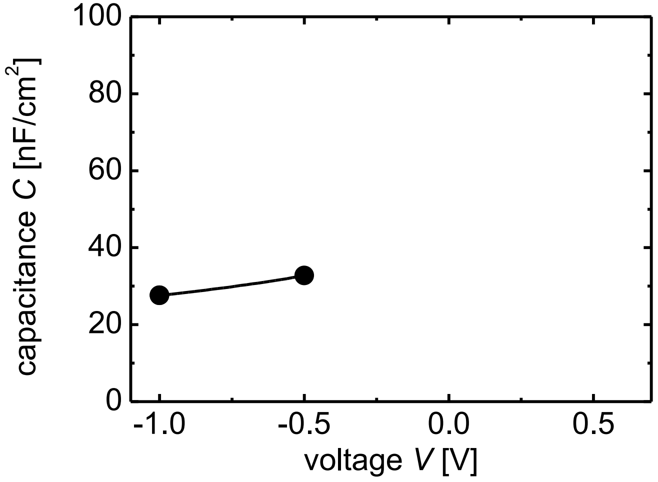

depletion layer capacitance

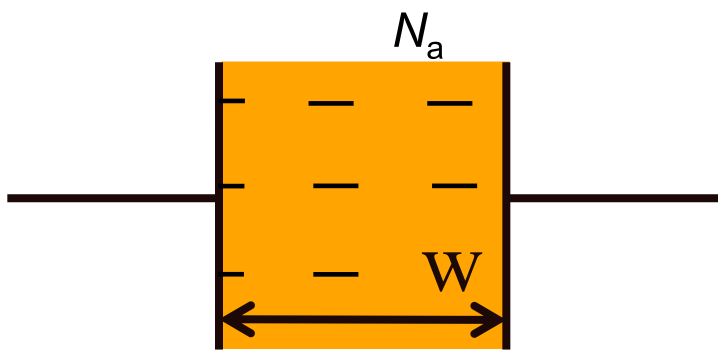

$$C = \frac{\varepsilon_r \varepsilon_0}{w}$$

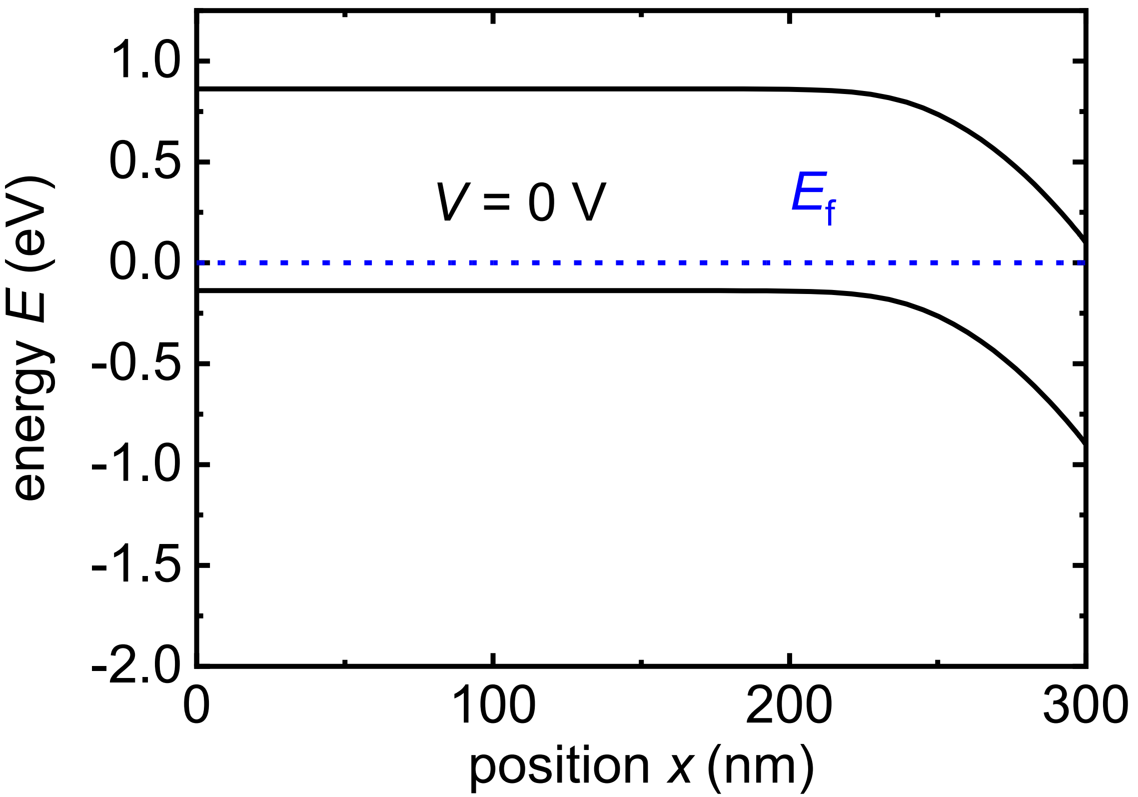

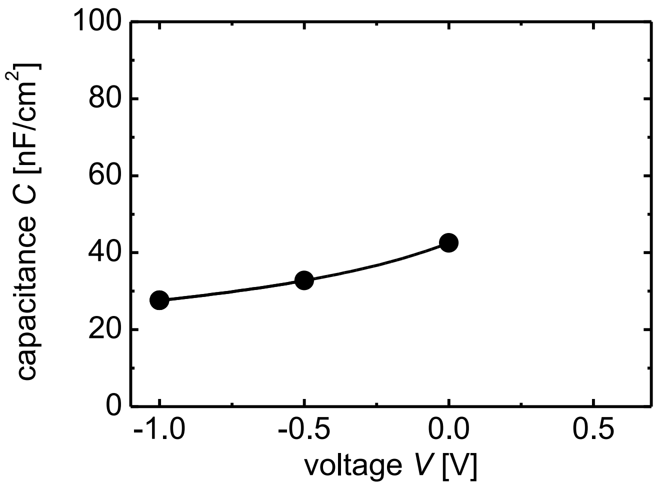

depletion layer capacitance

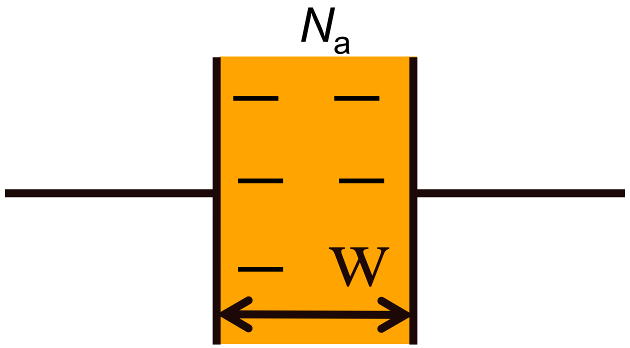

$$C = \frac{\varepsilon_r \varepsilon_0}{w}$$

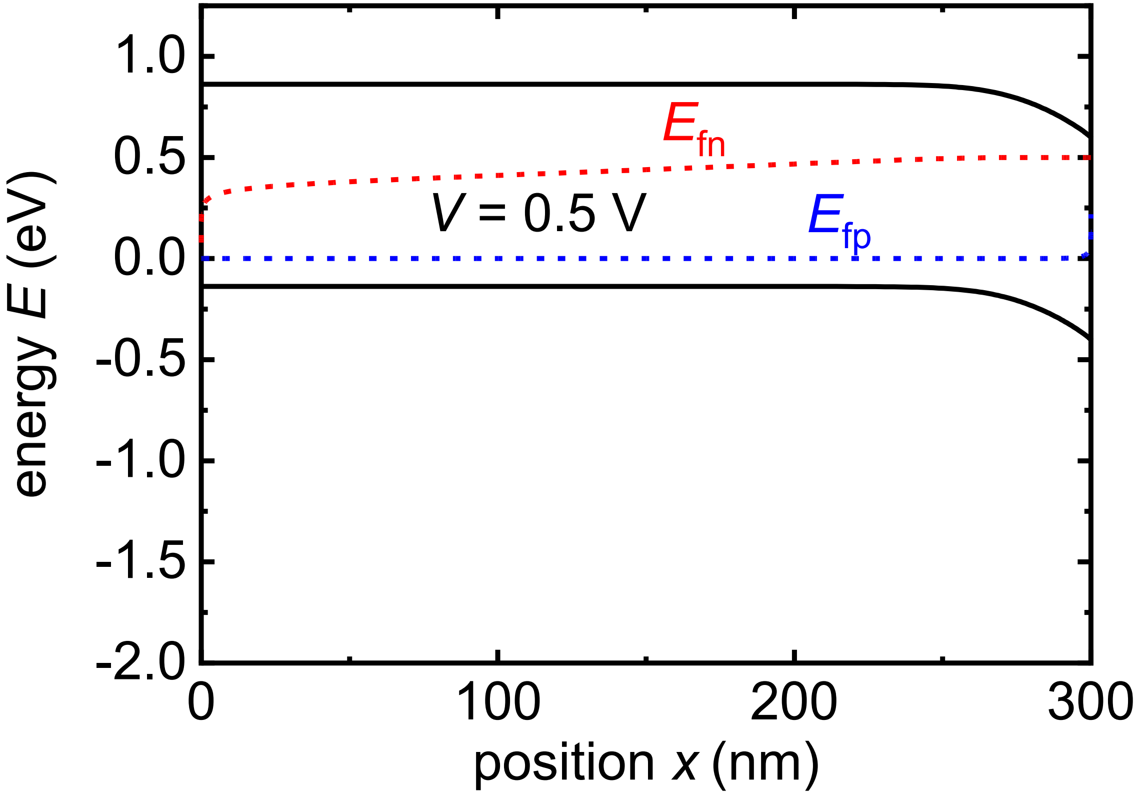

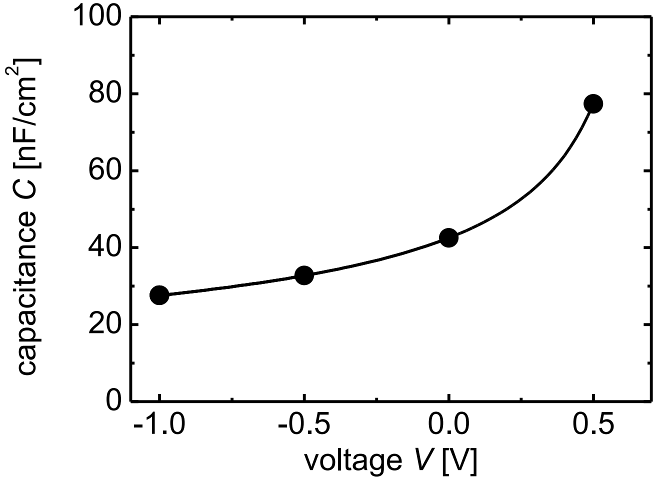

capacitance analysis

$$C(V) = \sqrt{\frac{q\epsilon_r\epsilon_0 N_d}{2(V_{bi} - V)}}$$

$$C^{-2}(V) = \frac{2}{q\epsilon_r\epsilon_0 N_d}(V_{bi} - V)$$

$$N_d(V) = \frac{-2(dC^{-2}/dV)^{-1}}{q\epsilon_r\epsilon_0}$$

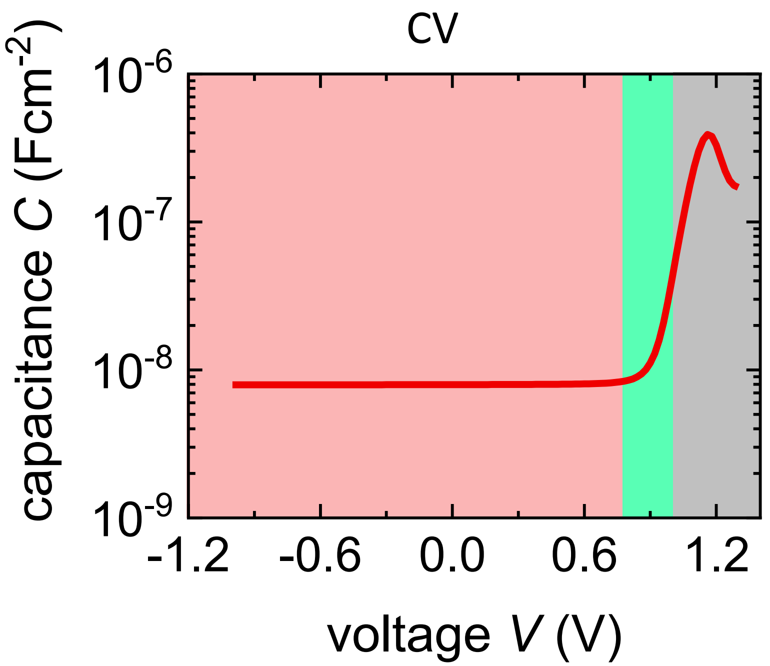

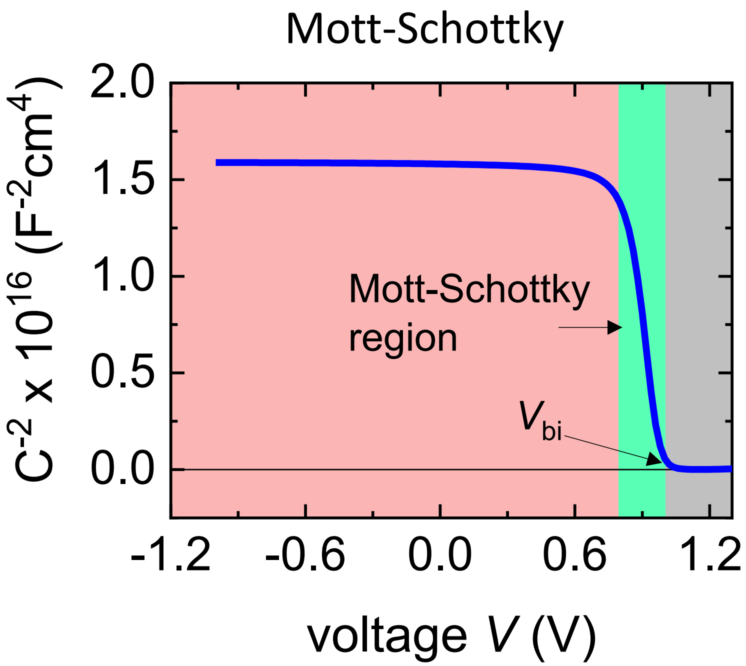

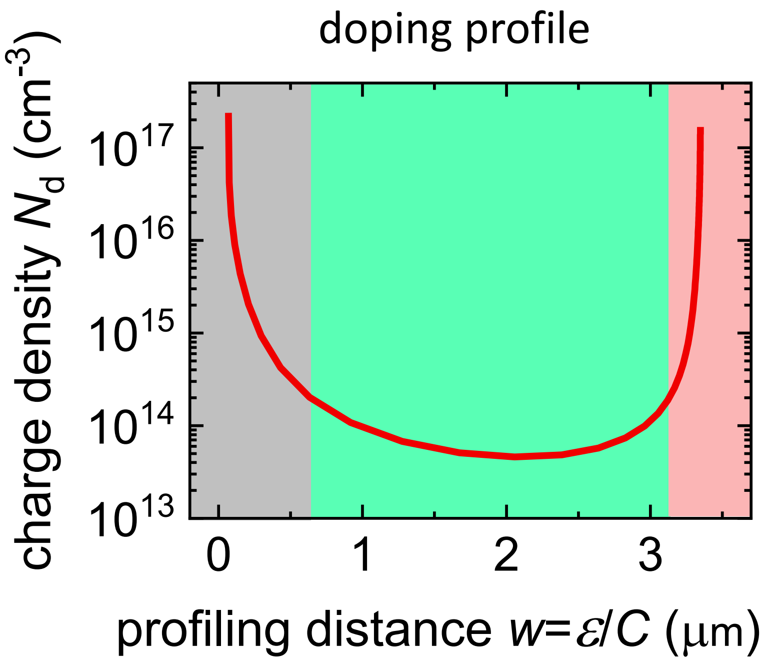

allows estimation of doping/defect density and built-in voltage

experimental Mott-Schottky plots

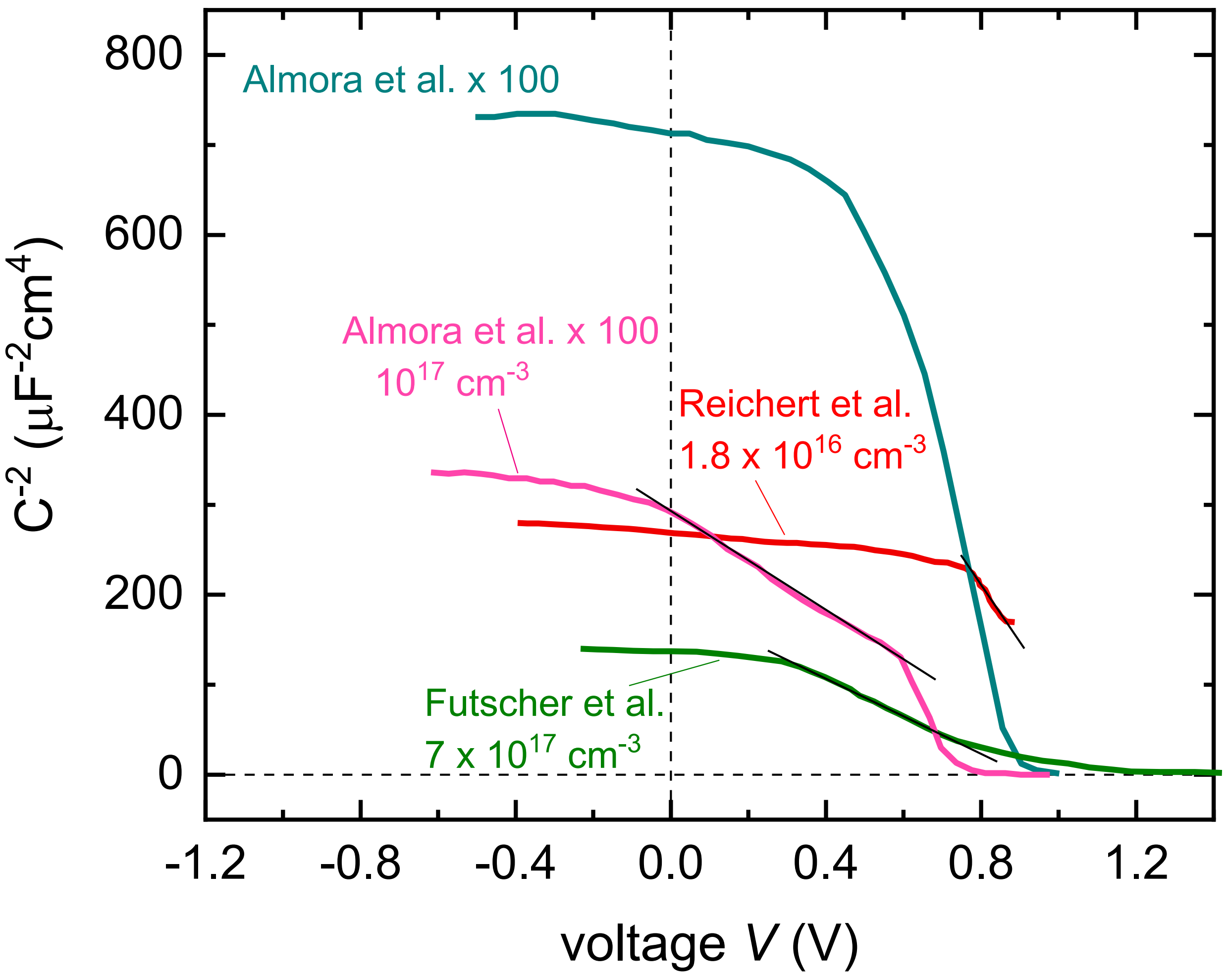

O. Almora et al., 2016, DOI: 10.1063/1.4966127.
M. H. Futscher et al., 2020, DOI: 10.1063/1.5132754.
S. Reichert et al., 2020, DOI: 10.1103/PhysRevApplied.13.034018.

experimental Mott-Schottky plots

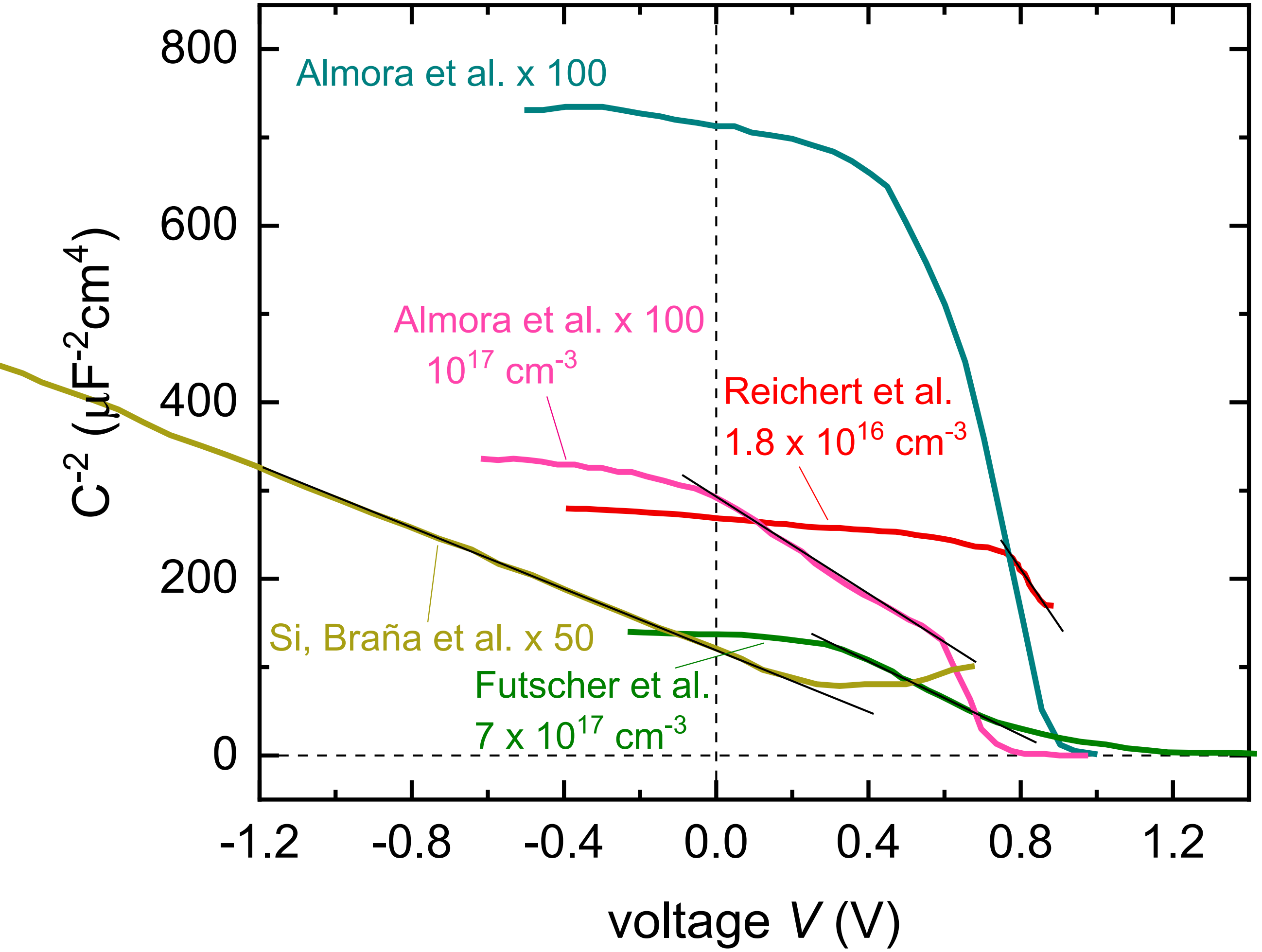

A. F. Braña et al., 2015, DOI: 10.1088/1742-6596/647/1/012069.

experimental Mott-Schottky plots

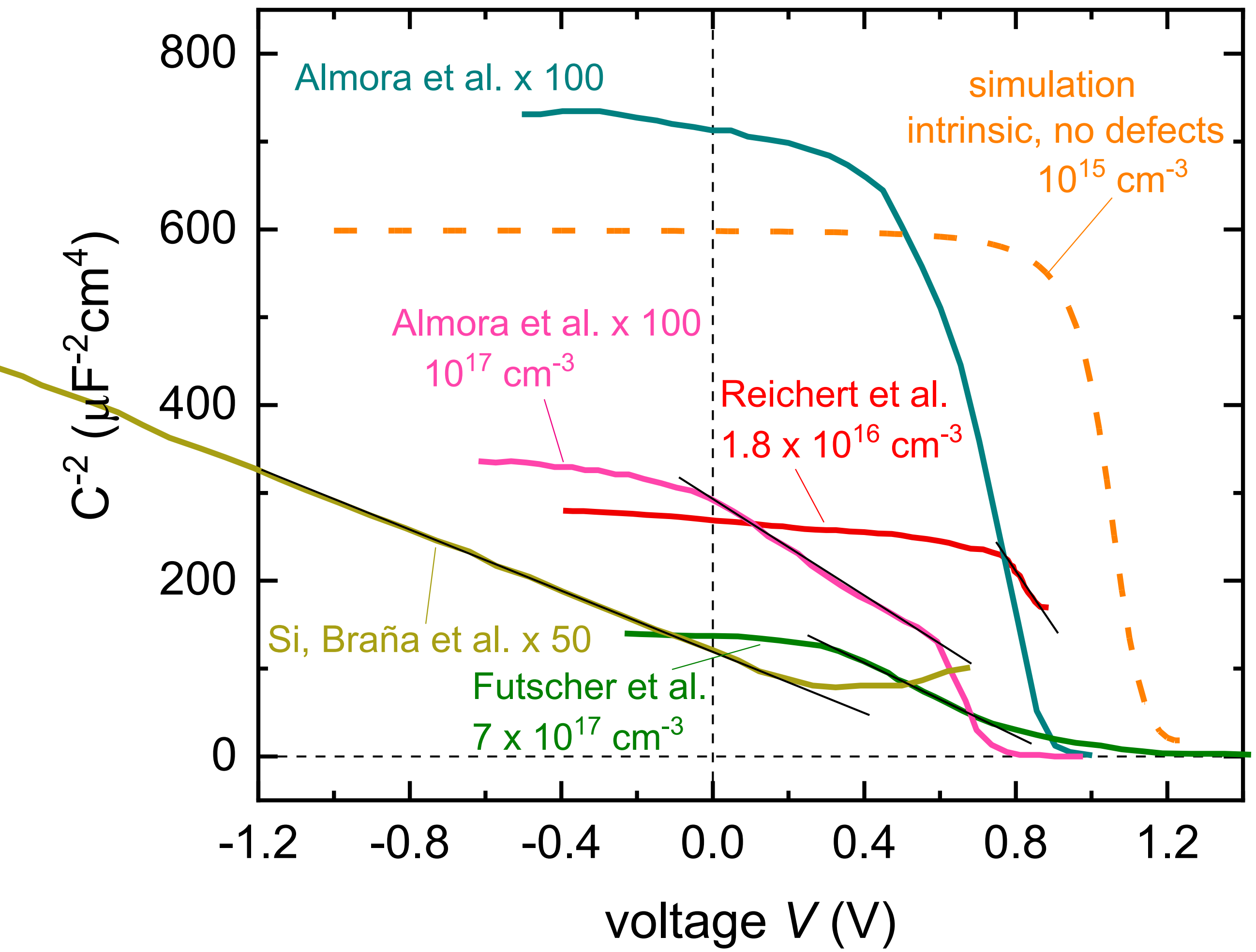

why does an intrinsic semiconductor make a Mott-Schottky behaviour?

competition between surface charge and bulk charge

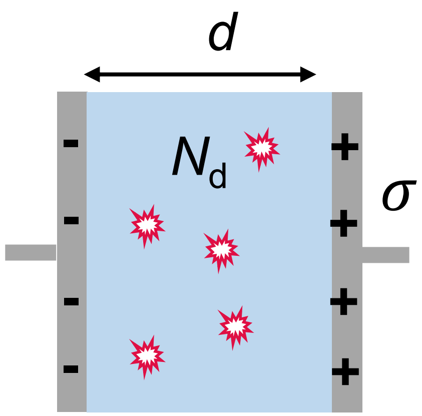

detection of a density of charged dopants/traps N_d requires

$$qdN_d \gg \sigma$$

volume charge — surface charge

competition between surface charge and bulk charge

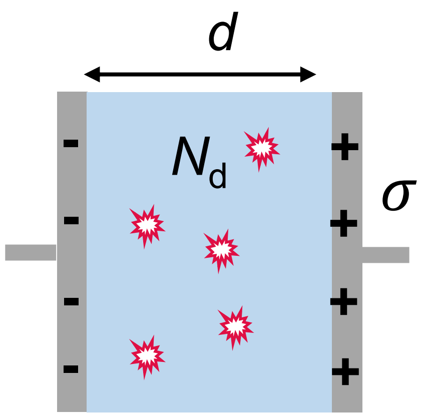

detection of a density of charged dopants/traps N_d requires

$$qdN_d \gg \sigma$$

volume charge surface charge

$$N_d \gg \frac{\varepsilon V_{bi}}{qd^2}$$

competition between surface charge and bulk charge

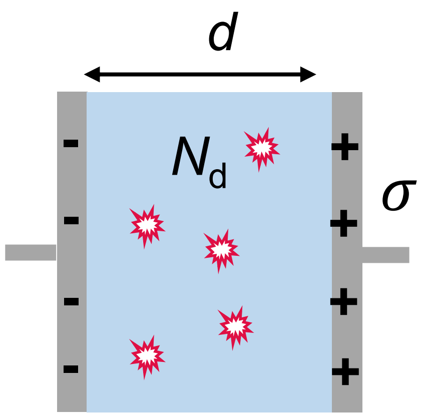

detection of a density of charged dopants/traps N_d requires

$$qdN_d \gg \sigma$$

volume charge — surface charge

$$\rightarrow \quad N_d \gg \frac{\varepsilon V_{bi}}{qd^2}$$

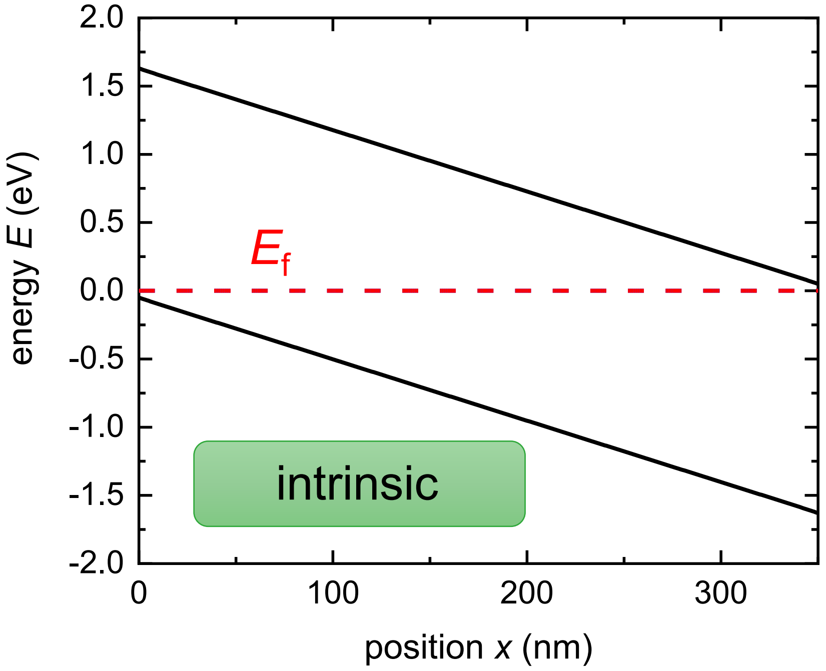

competition between surface charge and bulk charge

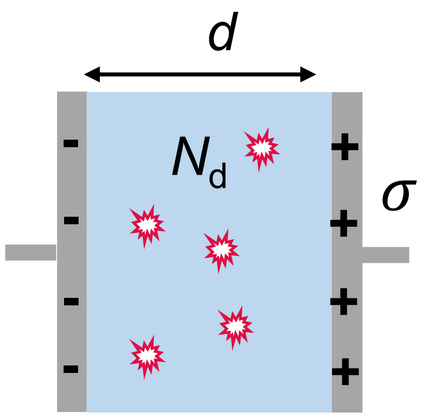

detection of a density of charged dopants/traps N_d requires

$$q d N_d \gg \sigma$$

volume charge — surface charge

$$N_d \gg \frac{\varepsilon V_{bi}}{q d^2}$$

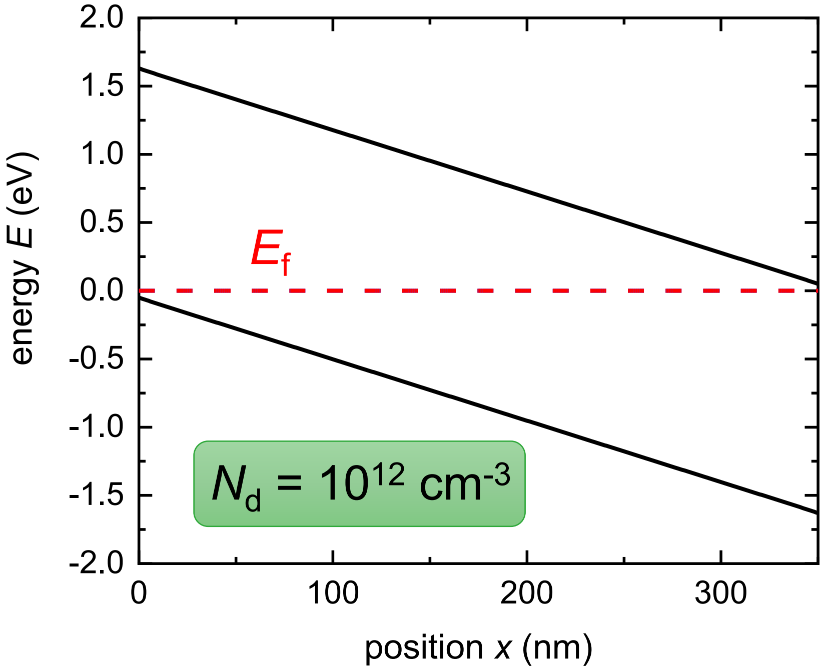

competition between surface charge and bulk charge

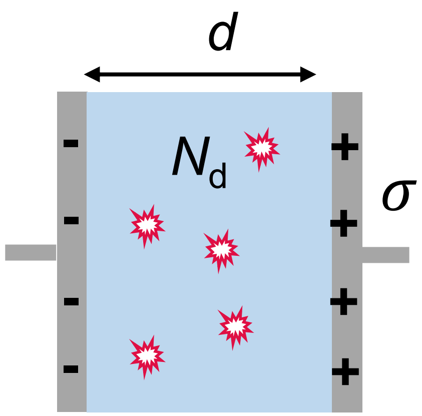

detection of a density of charged dopants/traps N_d requires

$$q d N_d \gg \sigma$$

volume charge   surface charge

$$N_d \gg \frac{\varepsilon V_{bi}}{q d^2}$$

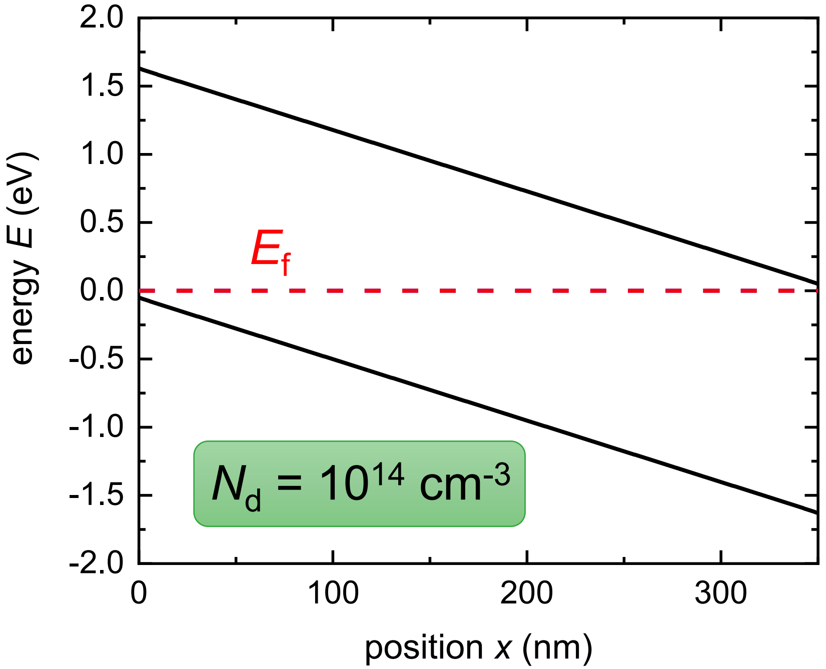

competition between surface charge and bulk charge

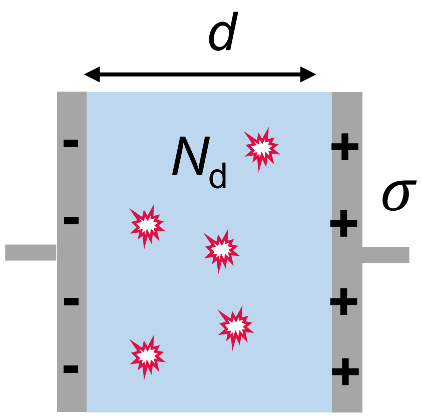

detection of a density of charged dopants/traps N_d requires

$$qdN_d \gg \sigma$$

volume charge | surface charge

$$\Rightarrow N_d \gg \frac{\varepsilon V_{bi}}{qd^2}$$

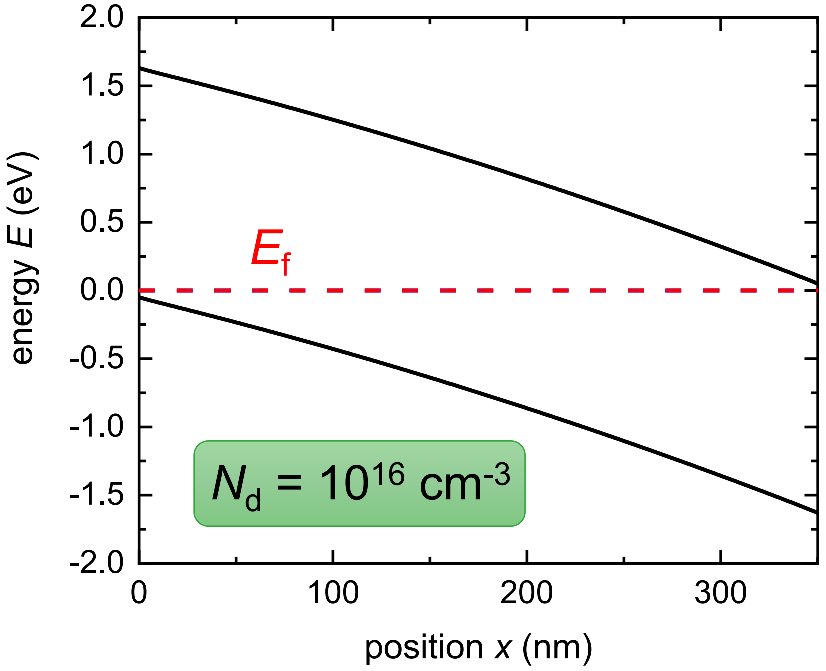

competition between surface charge and bulk charge

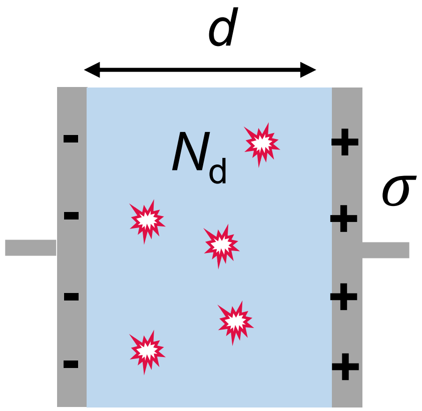

detection of a density of charged dopants/traps N_d requires

$$qdN_\mathrm{d} \gg \sigma$$

volume charge | surface charge

$$N_\mathrm{d} \gg \frac{\varepsilon V_\mathrm{bi}}{qd^2}$$

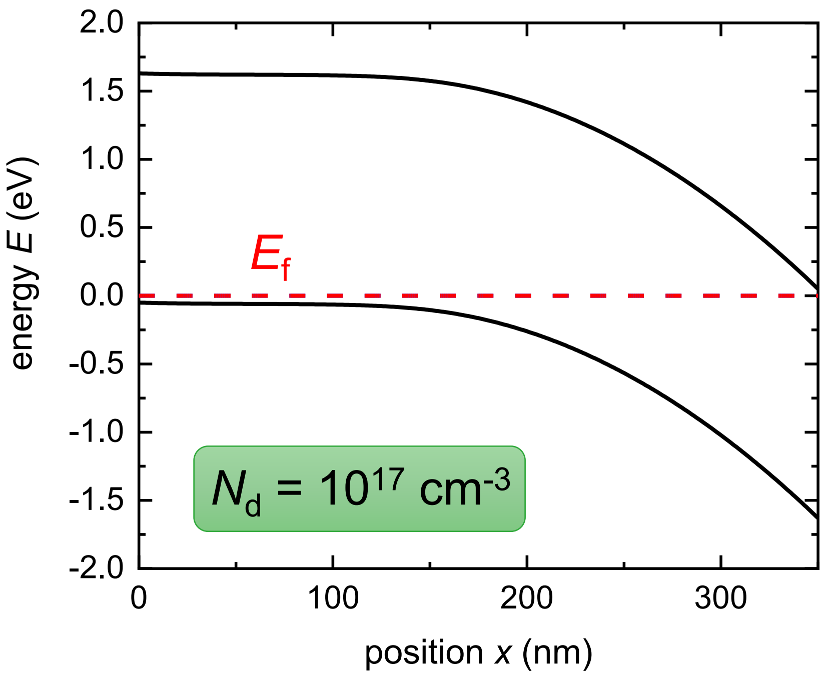

competition between surface charge and bulk charge

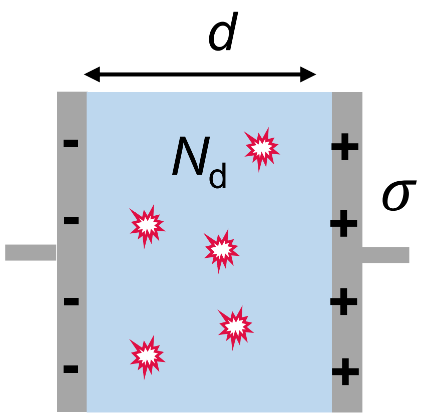

detection of a density of charged dopants/traps N_d requires

$$qdN_d \gg \sigma$$

volume charge   surface charge

$$N_d \gg \frac{\varepsilon V_{bi}}{qd^2}$$

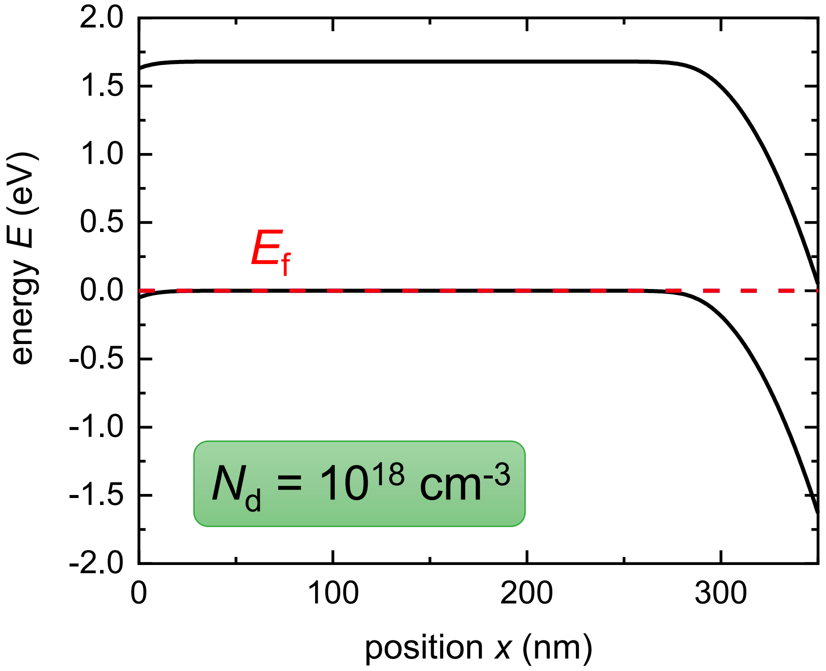

charge injection at forward bias

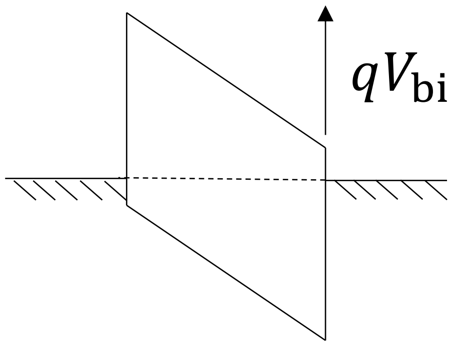

chemical capacitance

$$C_\mu = C_0 \exp \frac{qV}{m_{CV} k_B T}$$

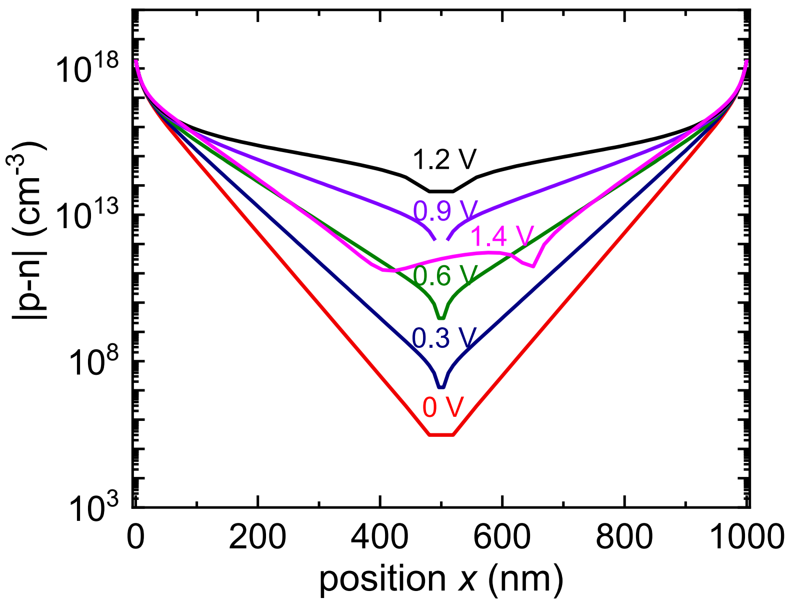

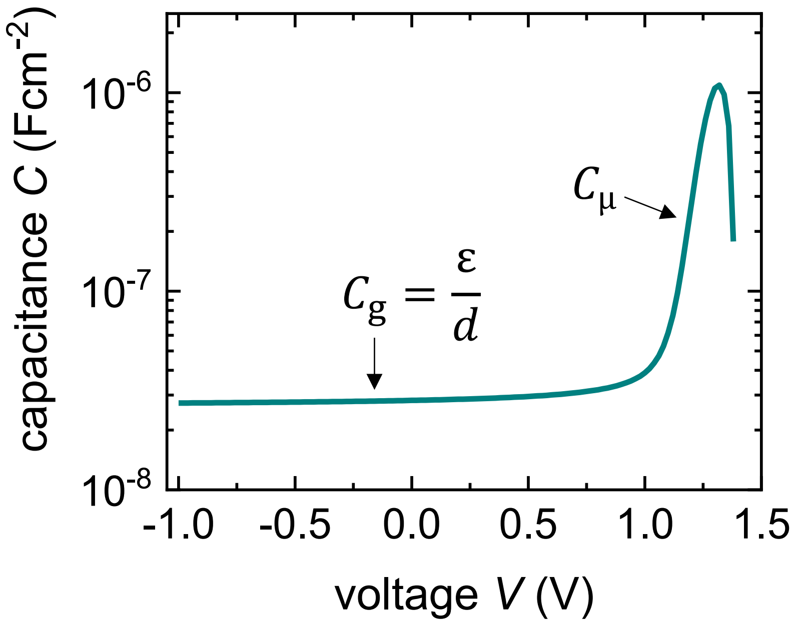

charge injection at forward bias

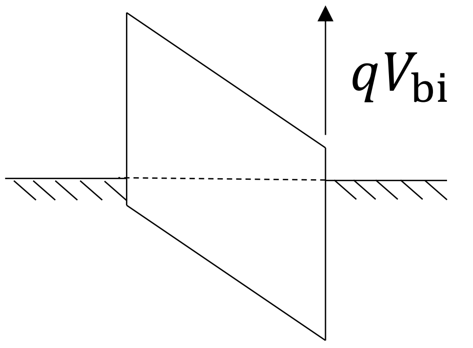

chemical capacitance

$$C_{\mu} = C_0 \exp \frac{qV}{m_{CV} k_B T}$$

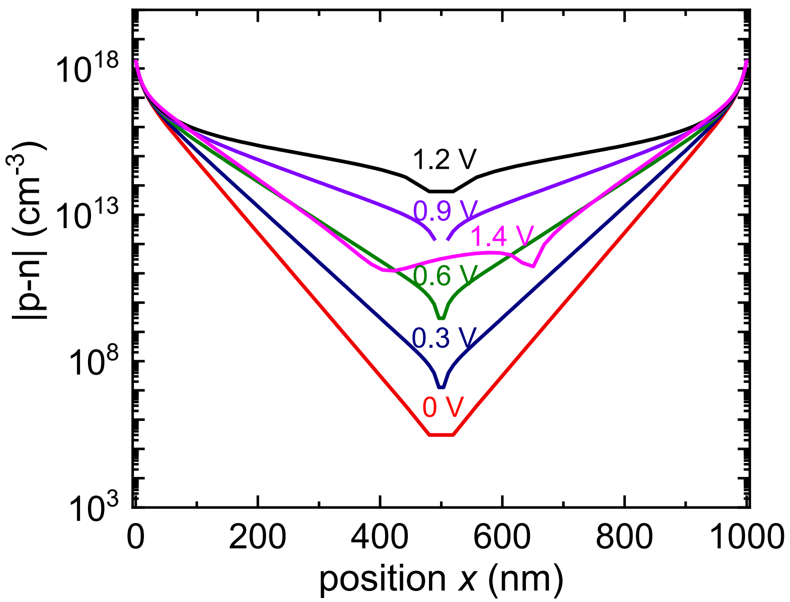

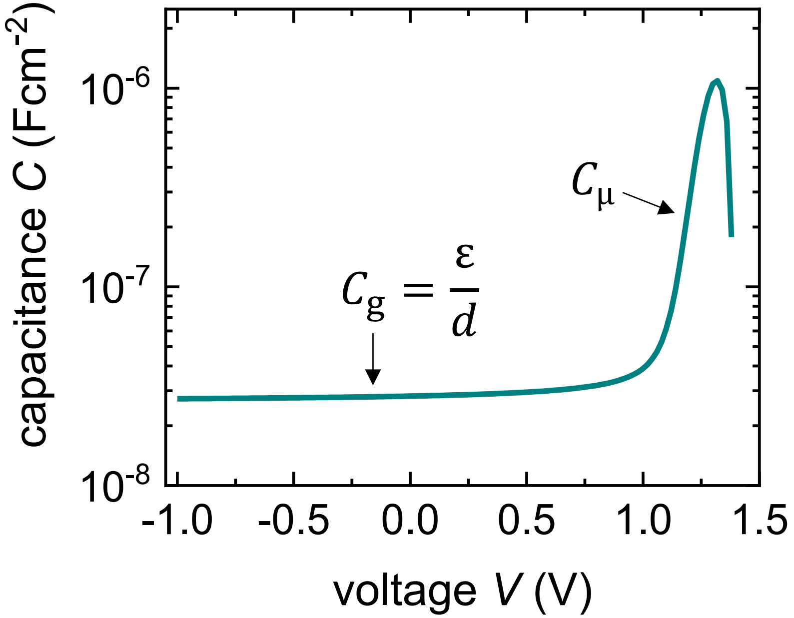

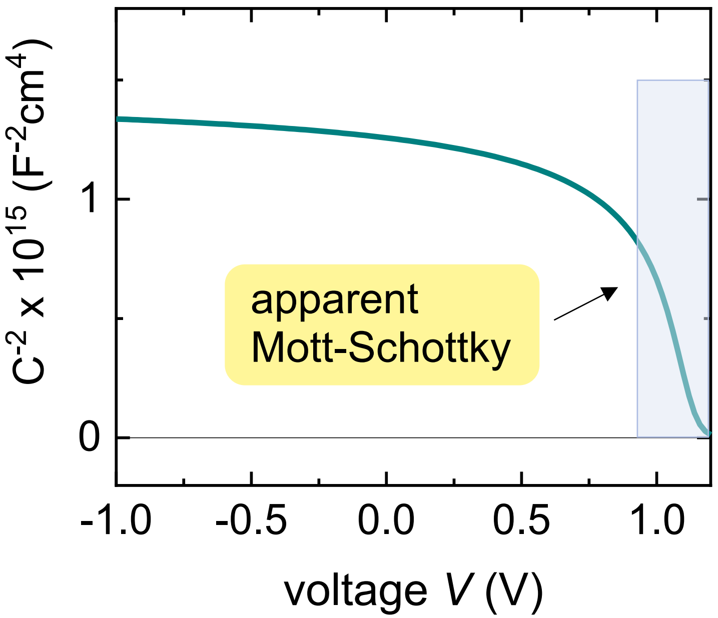

key question

can we resolve doping and defect densities from overlapping mechanisms in capacitance measurements?

resolution limit

can we resolve doping and defect densities from overlapping mechanisms in capacitance measurements?

$$C(V) = C_\mathrm{g} + C_0 \exp \frac{qV}{m_\mathrm{CV} k_\mathrm{B} T}$$

resolution limit

can we resolve doping and defect densities from overlapping mechanisms in capacitance measurements?

$$C(V) = C_g + C_0 \exp \frac{qV}{m_{CV} k_B T}$$

↓

$$N_d(V) = \frac{-2}{q \varepsilon_r \varepsilon_0} \left(\frac{dC^{-2}}{dV} \right)^{-1}$$

resolution limit

can we resolve doping and defect densities from overlapping mechanisms in capacitance measurements?

$$C(V) = C_g + C_0 \exp \frac{qV}{m_{CV} k_B T}$$

↓

$$N_d(V) = \frac{-2}{q \varepsilon_r \varepsilon_0} \left(\frac{dC^{-2}}{dV} \right)^{-1}$$

↓

$$N_{d,min} = \frac{27 m_{CV} k_B T \epsilon_r \epsilon_0}{4 q^2 d^2}$$

minimum defect or doping density resolvable in a capacitance measurement

S. Ravishankar et al., Science **371**, eabd8014 (2021).

analysis of doping profiles

drive-level capacitance profiling (DLCP)

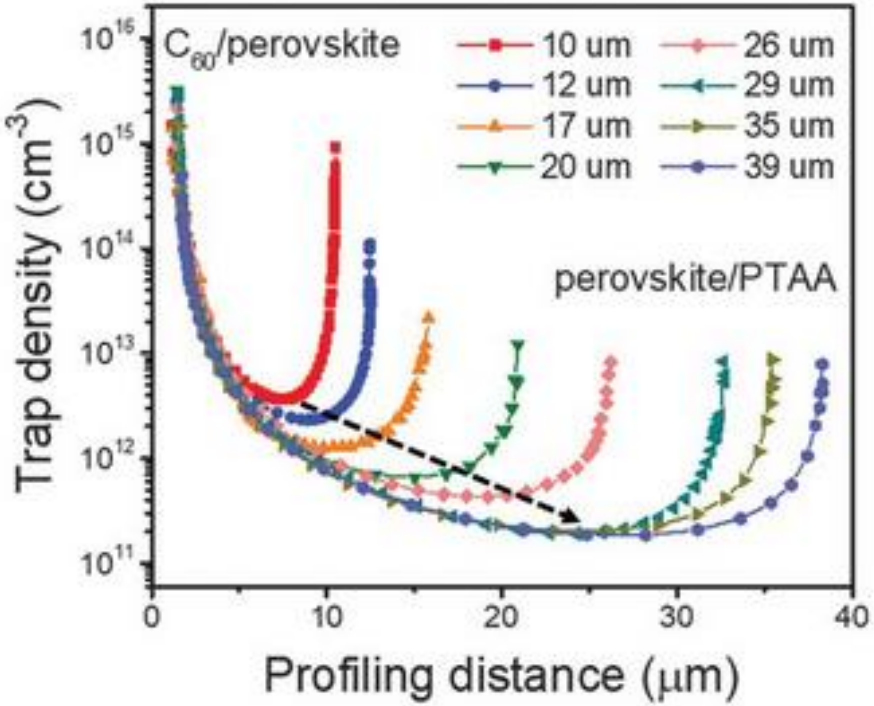

Perovskite material	Minimal bulk trap density ($N_{T\,min}$) (cm^{-3})	Interface trap density (cm^{-3})	
$MAPbBr_3$ single crystal (bulk)	6.5×10^{10}	1.8×10^{12} (C_{60})	1.8×10^{12} (Au)
$MAPbI_3$ single crystal (bulk)	1.8×10^{11}	1.2×10^{12} (C_{60})	1.2×10^{12} (Au)
$MAPbI_3$ single crystal (thin)	1.9×10^{11} to 3.2×10^{12}	2.0×10^{13} to 1.1×10^{16} (C_{60})	1.5×10^{13} to 1.0×10^{15} (PTAA)
$Cs_{0.05}FA_{0.70}MA_{0.25}PbI_3$ film	4.3×10^{14}	8.6×10^{15} (C_{60})	1.2×10^{17} (PTAA)
$Rb_{0.05}Cs_{0.05}FA_{0.75}MA_{0.15}Pb(I_{0.95}Br_{0.05})_3$ film	5.7×10^{14}	2.0×10^{16} (C_{60})	1.1×10^{17} (PTAA)
$FA_{0.92}MA_{0.08}PbI_3$ film	7.9×10^{14}	1.9×10^{16} (C_{60})	9.0×10^{16} (PTAA)
$MAPbI_3$ film	9.2×10^{14}	2.2×10^{16} (C_{60})	1.2×10^{17} (PTAA)
$Cs_{0.05}FA_{0.8}MA_{0.15}Pb_{0.5}Sn_{0.5}(I_{0.85}Br_{0.15})_3$ film	1.2×10^{15}	1.5×10^{16} (C_{60})	1.1×10^{17} (PTAA)

Z. Ni et al., 2020. *Science*, *367*(6484), pp.1352-1358.

analysis of doping profiles

drive-level capacitance profiling (DLCP)

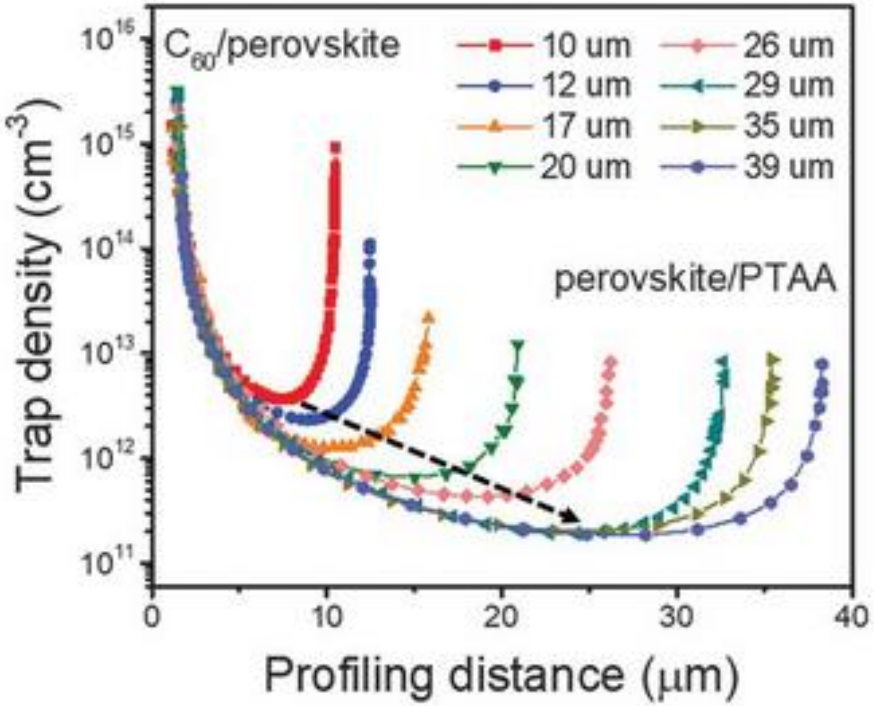

simulation: dopant-and-trap-free PSC

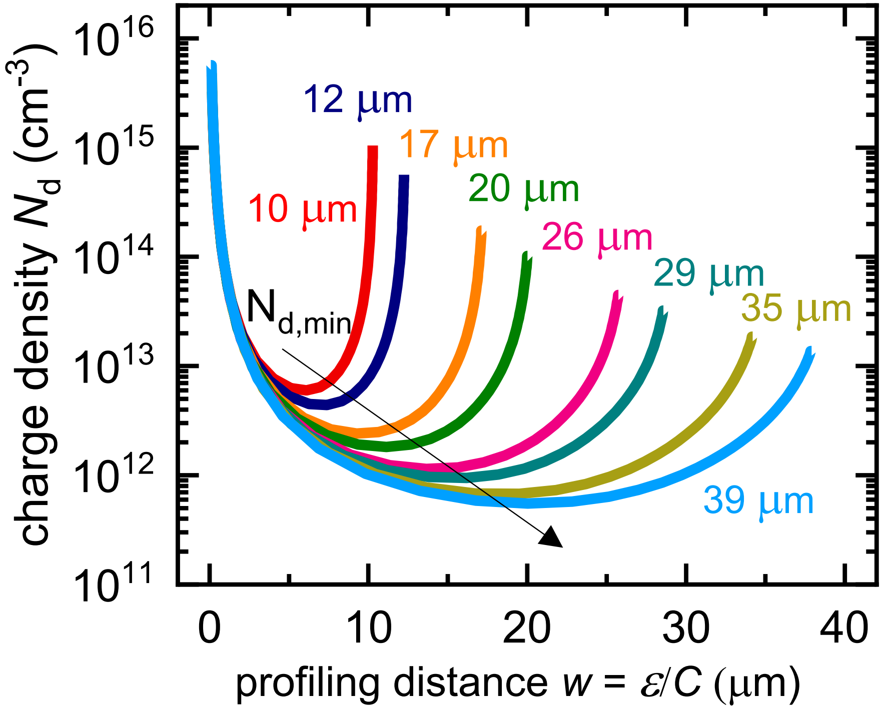

Perovskite material	Minimal bulk trap density ($N_{T\,min}$) (cm^{-3})	Interface trap density (cm^{-3})	
$MAPbBr_3$ single crystal (bulk)	6.5×10^{10}	1.8×10^{12} (C_{60})	1.8×10^{12} (Au)
$MAPbI_3$ single crystal (bulk)	1.8×10^{11}	1.2×10^{12} (C_{60})	1.2×10^{12} (Au)
$MAPbI_3$ single crystal (thin)	1.9×10^{11} to 3.2×10^{12}	2.0×10^{13} to 1.1×10^{16} (C_{60})	1.5×10^{13} to 1.0×10^{15} (PTAA)
$Cs_{0.05}FA_{0.70}MA_{0.25}PbI_3$ film	4.3×10^{14}	8.6×10^{15} (C_{60})	1.2×10^{17} (PTAA)
$Rb_{0.05}Cs_{0.05}FA_{0.75}MA_{0.15}Pb(I_{0.95}Br_{0.05})_3$ film	5.7×10^{14}	2.0×10^{16} (C_{60})	1.1×10^{17} (PTAA)
$FA_{0.92}MA_{0.08}PbI_3$ film	7.9×10^{14}	1.9×10^{16} (C_{60})	9.0×10^{16} (PTAA)
$MAPbI_3$ film	9.2×10^{14}	2.2×10^{16} (C_{60})	1.2×10^{17} (PTAA)
$Cs_{0.05}FA_{0.8}MA_{0.15}Pb_{0.5}Sn_{0.5}(I_{0.85}Br_{0.15})_3$ film	1.2×10^{15}	1.5×10^{16} (C_{60})	1.1×10^{17} (PTAA)

S. Ravishankar et al., Science **371**, eabd8014 (2021).

analysis of doping profiles

drive-level capacitance profiling (DLCP)

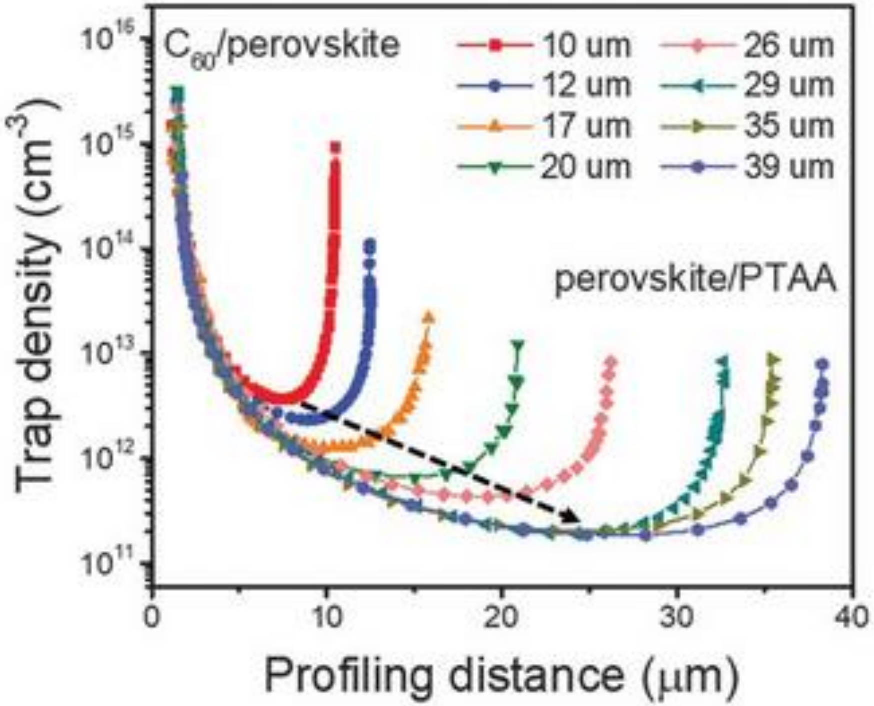

simulation: dopant-and-trap-free PSC

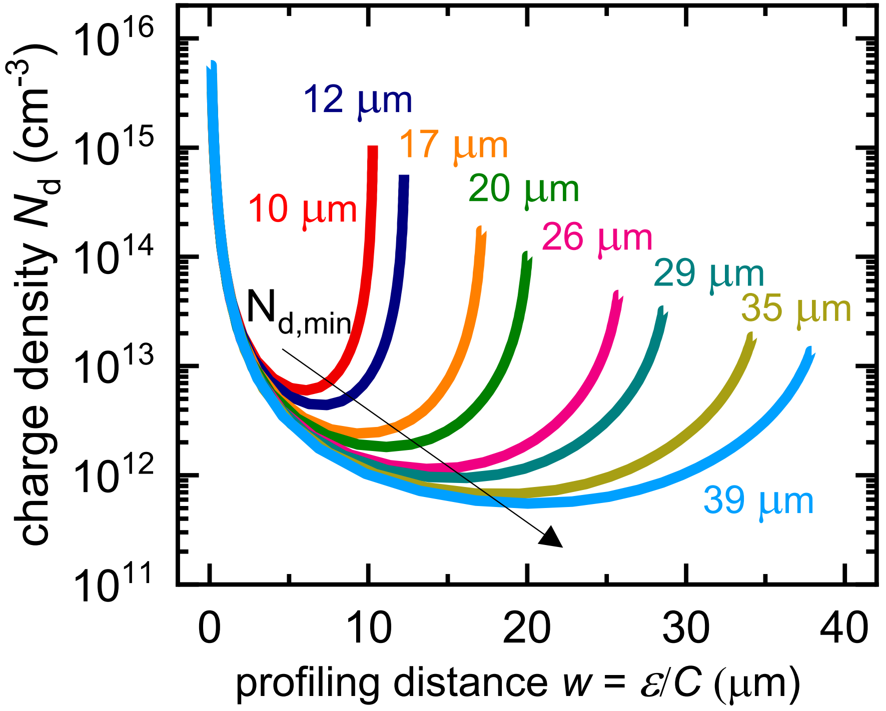

Perovskite material	Minimal bulk trap density ($N_{T\,min}$) (cm^{-3})	Interface trap density (cm^{-3})	
$MAPbBr_3$ single crystal (bulk)	6.5×10^{10}	1.8×10^{12} (C_{60})	1.8×10^{12} (Au)
$MAPbI_3$ single crystal (bulk)	1.8×10^{11}	1.2×10^{12} (C_{60})	1.2×10^{12} (Au)
$MAPbI_3$ single crystal (thin)	1.9×10^{11} to 3.2×10^{12}	2.0×10^{13} to 1.1×10^{16} (C_{60})	1.5×10^{13} to 1.0×10^{15} (PTAA)
$Cs_{0.05}FA_{0.70}MA_{0.25}PbI_3$ film	4.3×10^{14}	8.6×10^{15} (C_{60})	1.2×10^{17} (PTAA)
$Rb_{0.05}Cs_{0.05}FA_{0.75}MA_{0.15}Pb(I_{0.95}Br_{0.05})_3$ film	5.7×10^{14}	2.0×10^{16} (C_{60})	1.1×10^{17} (PTAA)
$FA_{0.92}MA_{0.08}PbI_3$ film	7.9×10^{14}	1.9×10^{16} (C_{60})	9.0×10^{16} (PTAA)
$MAPbI_3$ film	9.2×10^{14}	2.2×10^{16} (C_{60})	1.2×10^{17} (PTAA)
$Cs_{0.05}FA_{0.8}MA_{0.15}Pb_{0.5}Sn_{0.5}(I_{0.85}Br_{0.15})_3$ film	1.2×10^{15}	1.5×10^{16} (C_{60})	1.1×10^{17} (PTAA)

← NOT real defect densities

S. Ravishankar et al., Science **371**, eabd8014 (2021).

analysis of doping profiles

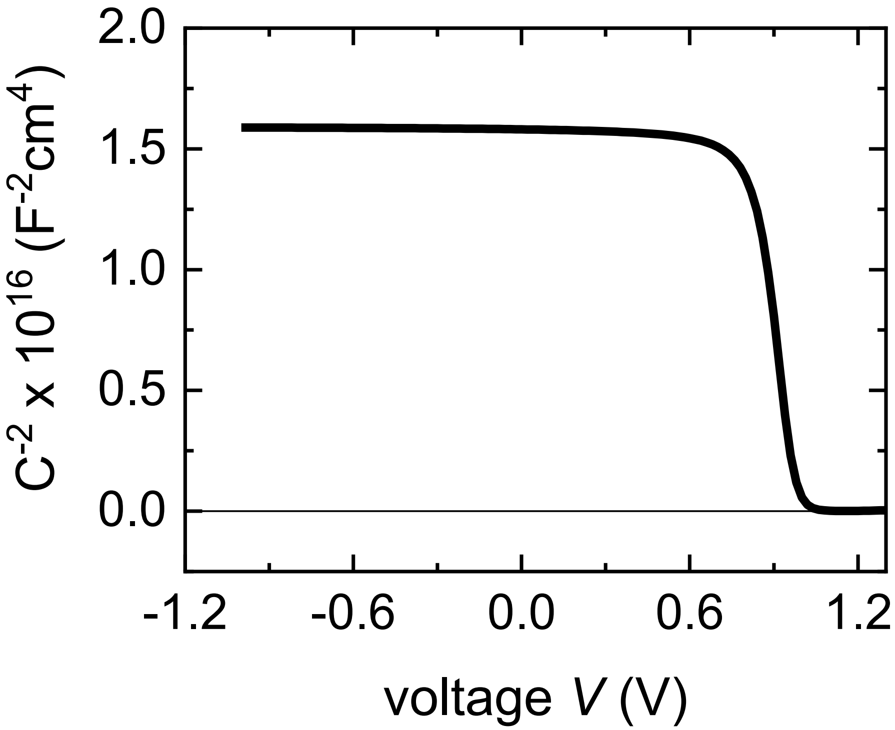

$$C(V) = C_g + C_0 \exp \frac{qV}{mk_B T}$$

analysis of doping profiles

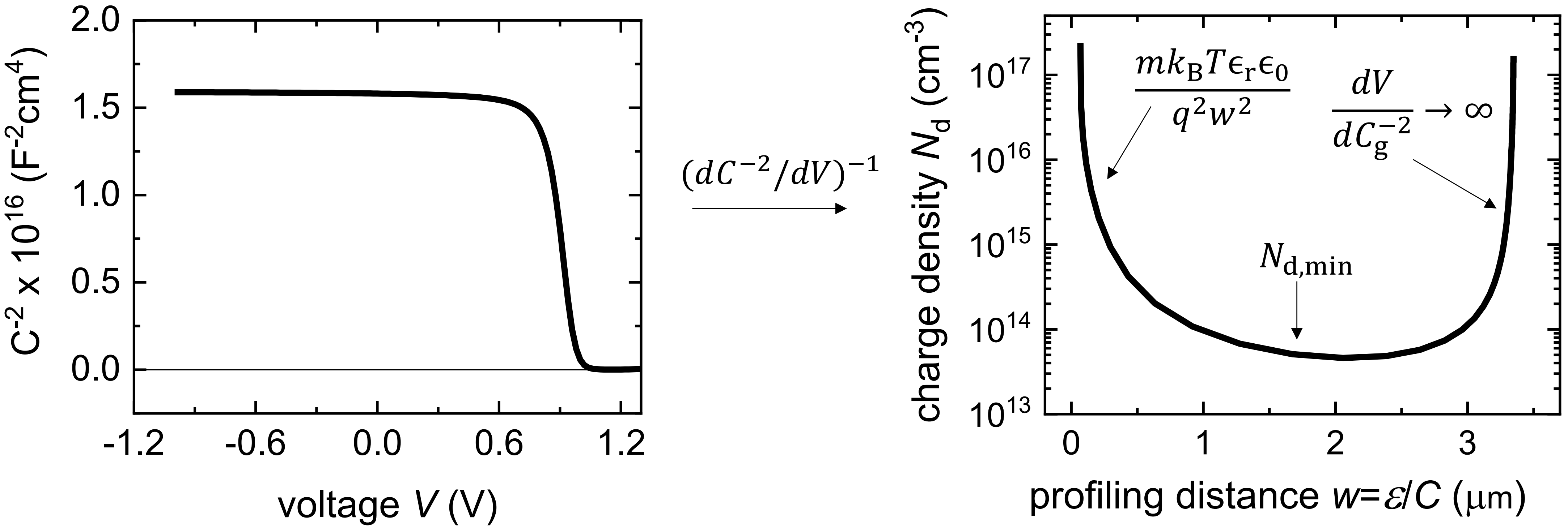

$$C(V) = C_g + C_0 \exp\frac{qV}{mk_BT}$$

$$N_d(w) = N_{d,min} + \frac{mk_BT\epsilon_r\epsilon_0}{q^2w^2}$$

apparent defect densities – infinite rise due to C_g, minimum determined by resolution limit

other photovoltaic technologies

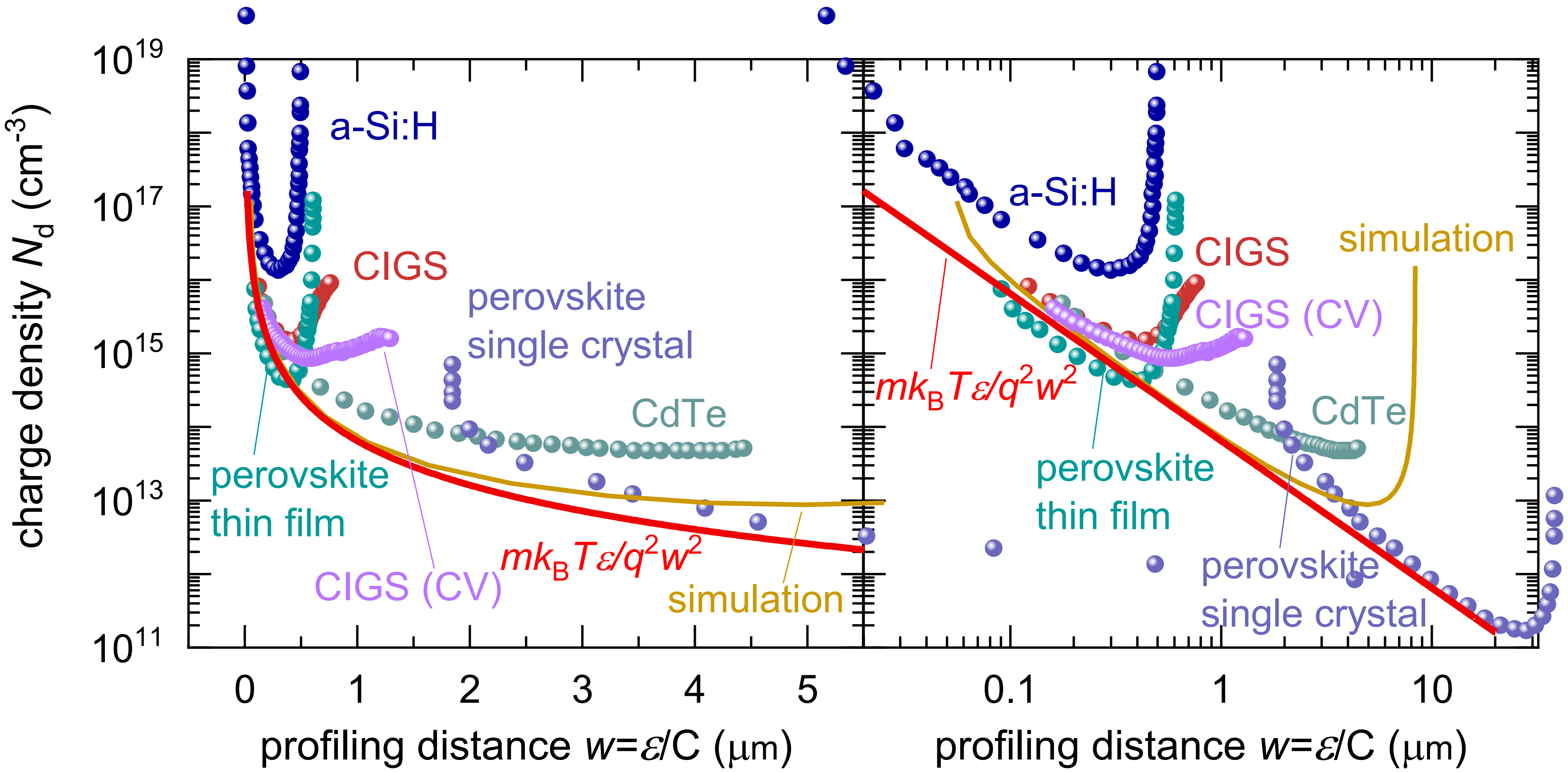

S. Ravishankar et al., Science **371**, eabd8014 (2021).

measured defect densities in literature

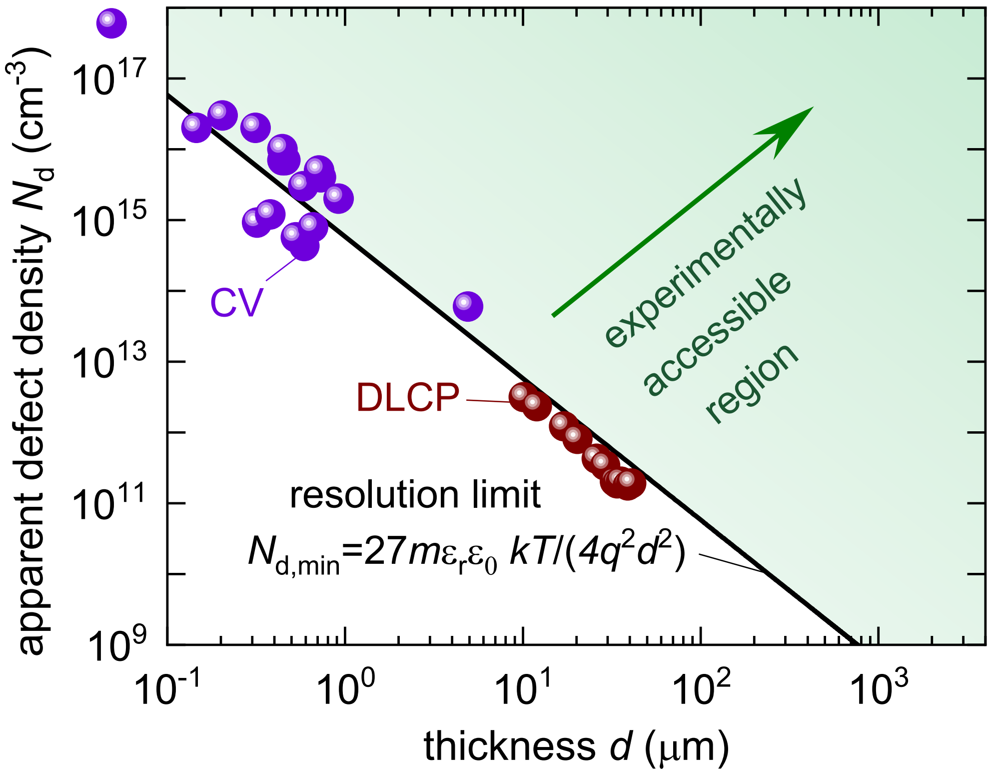

all apparent defect densities are close to the resolution limit

S. Ravishankar et al., PRX Energy **1**, 013003 (2022).

measured defect densities in literature

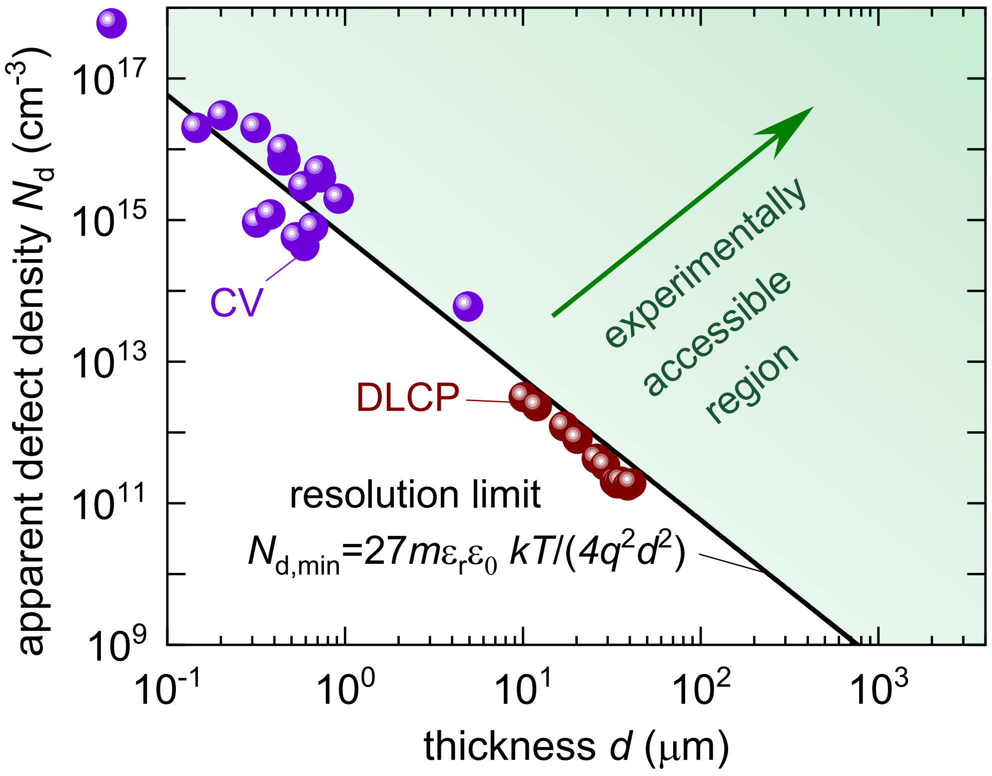

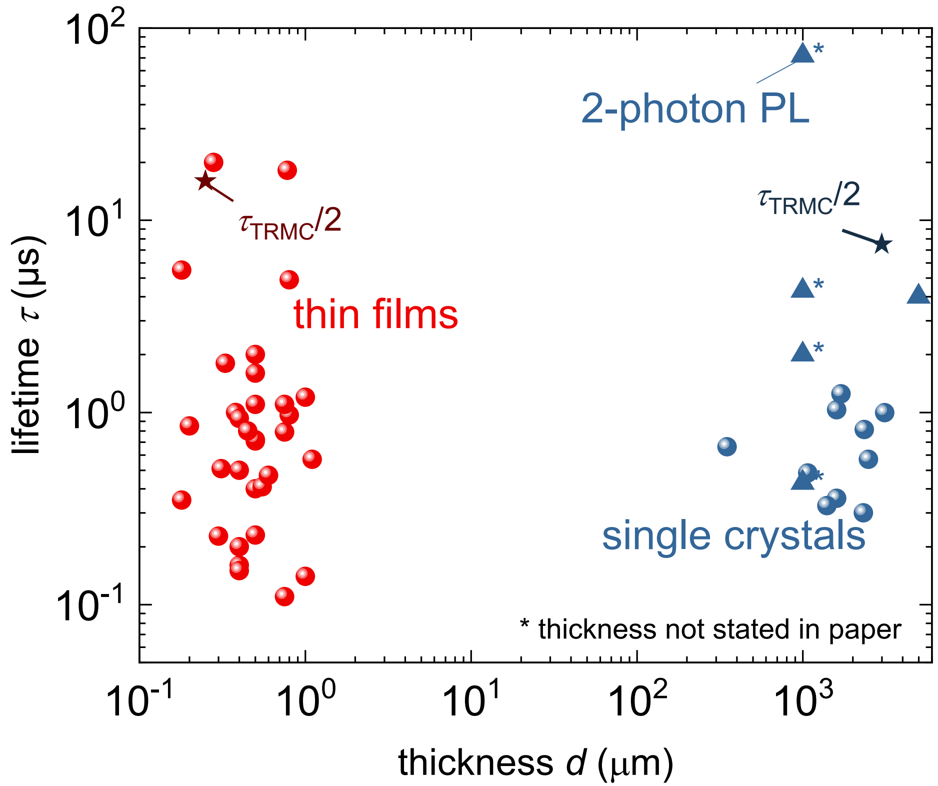

all apparent defect densities are close to the resolution limit

recombination lifetimes not correlated to apparent defect densities (ideally $\tau \propto \frac{1}{N_d}$)

J. Siekmann, S. Ravishankar, and T. Kirchartz, ACS Energy Letters **6**, 3244 (2021).

do dopants and defects have the same effect?

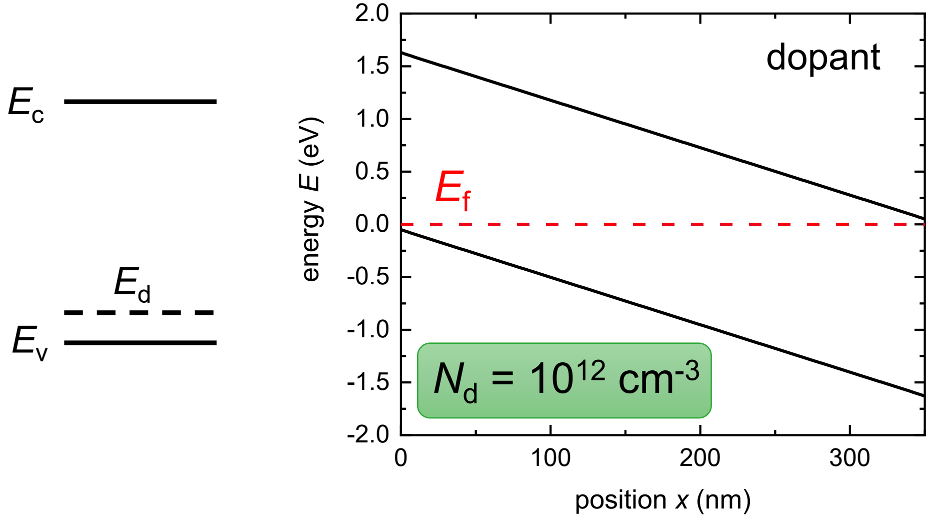

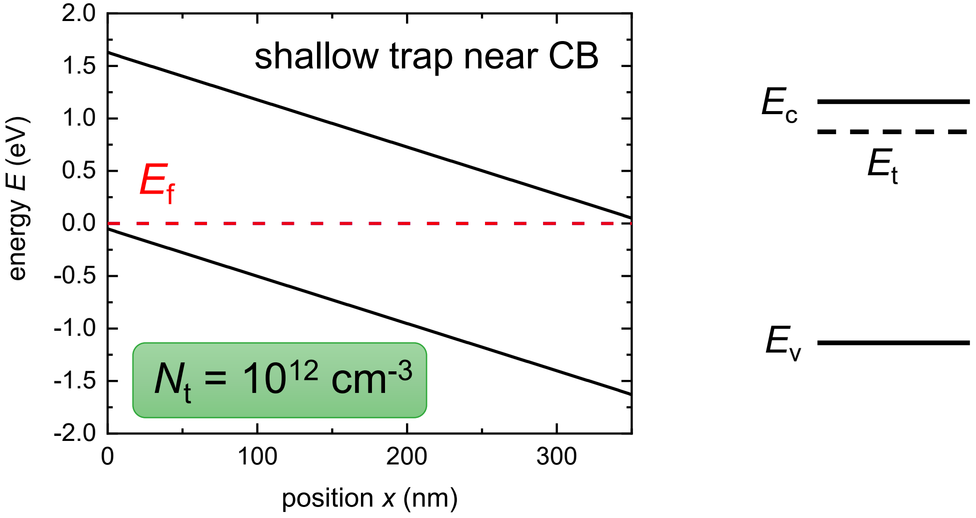

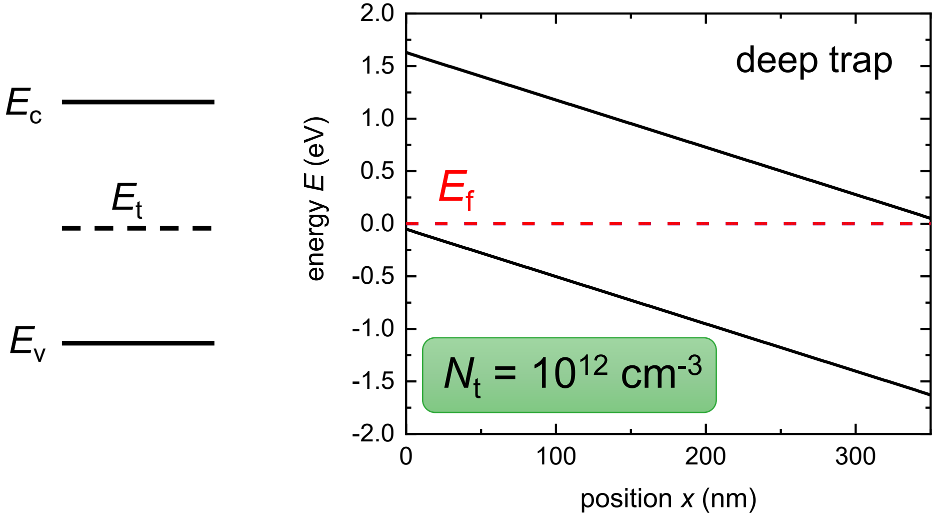

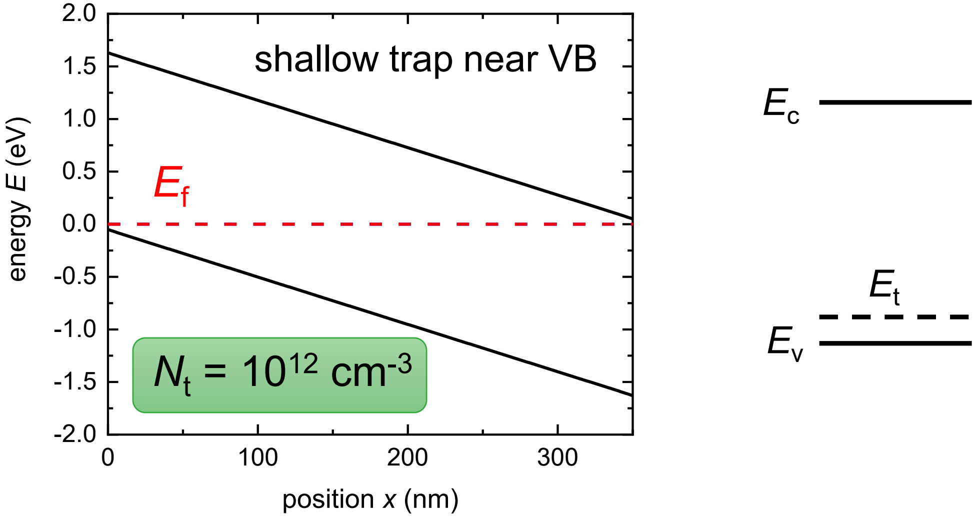

do dopants and defects have the same effect?

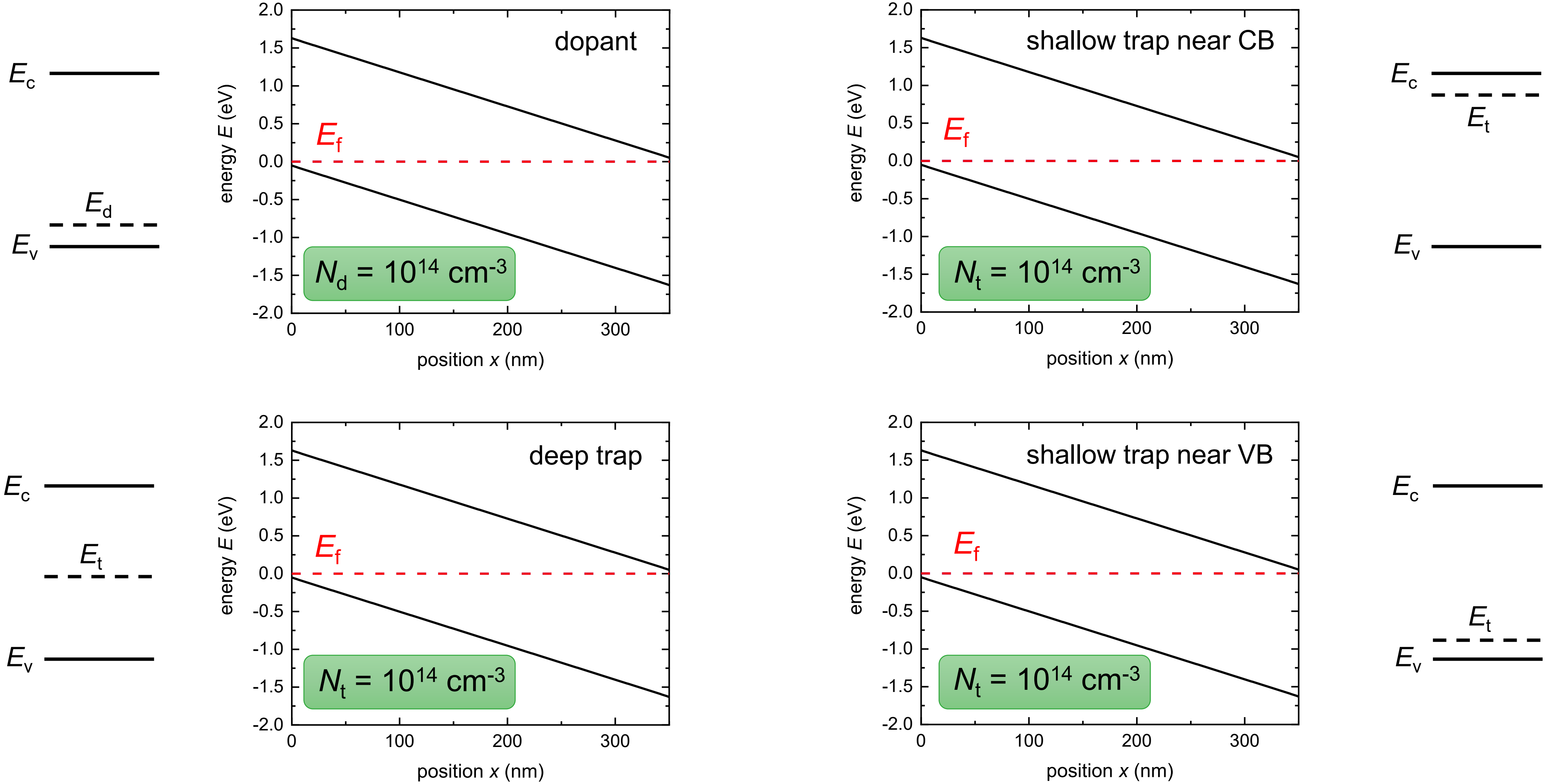

do dopants and defects have the same effect?

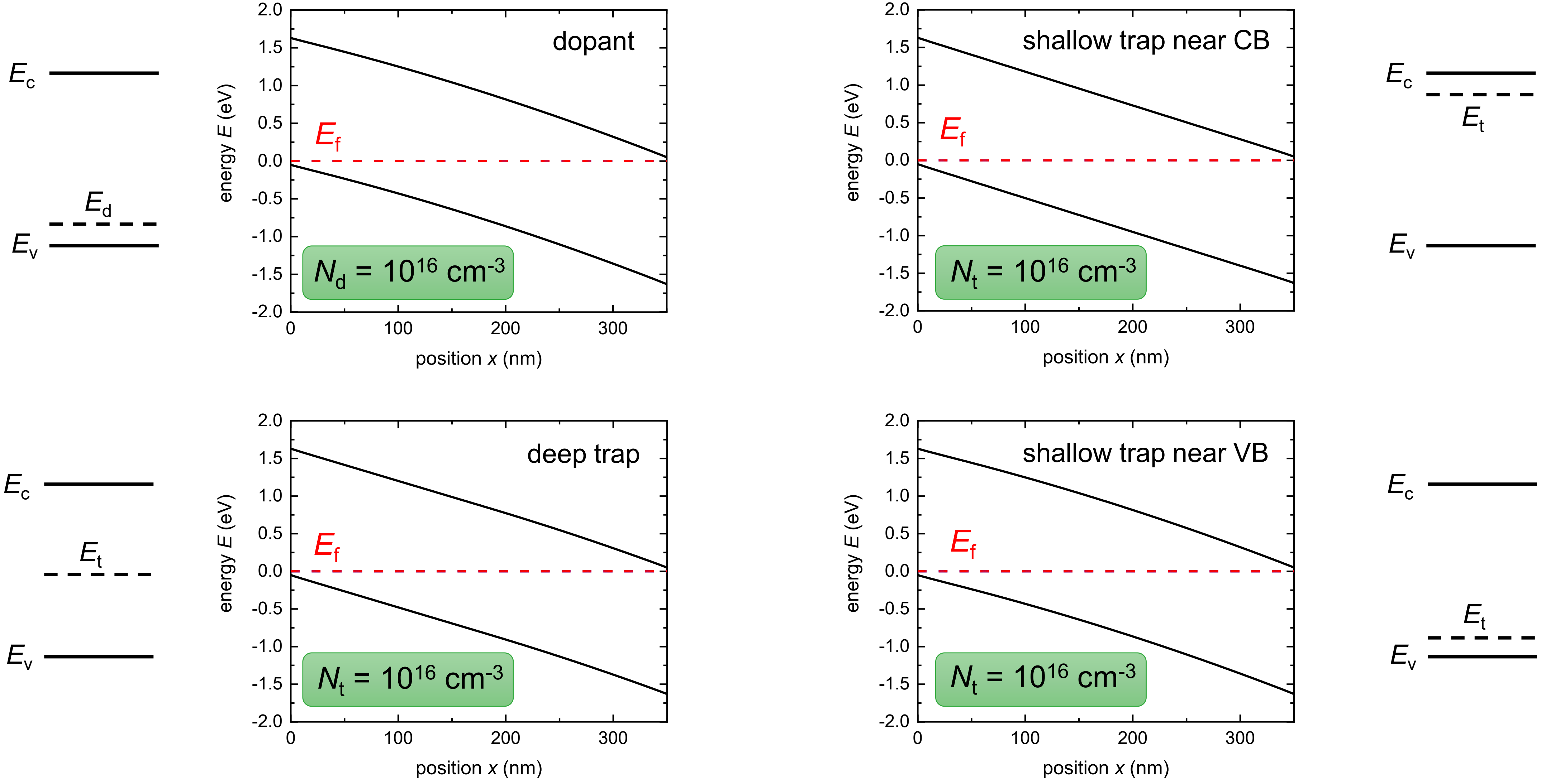

do dopants and defects have the same effect?

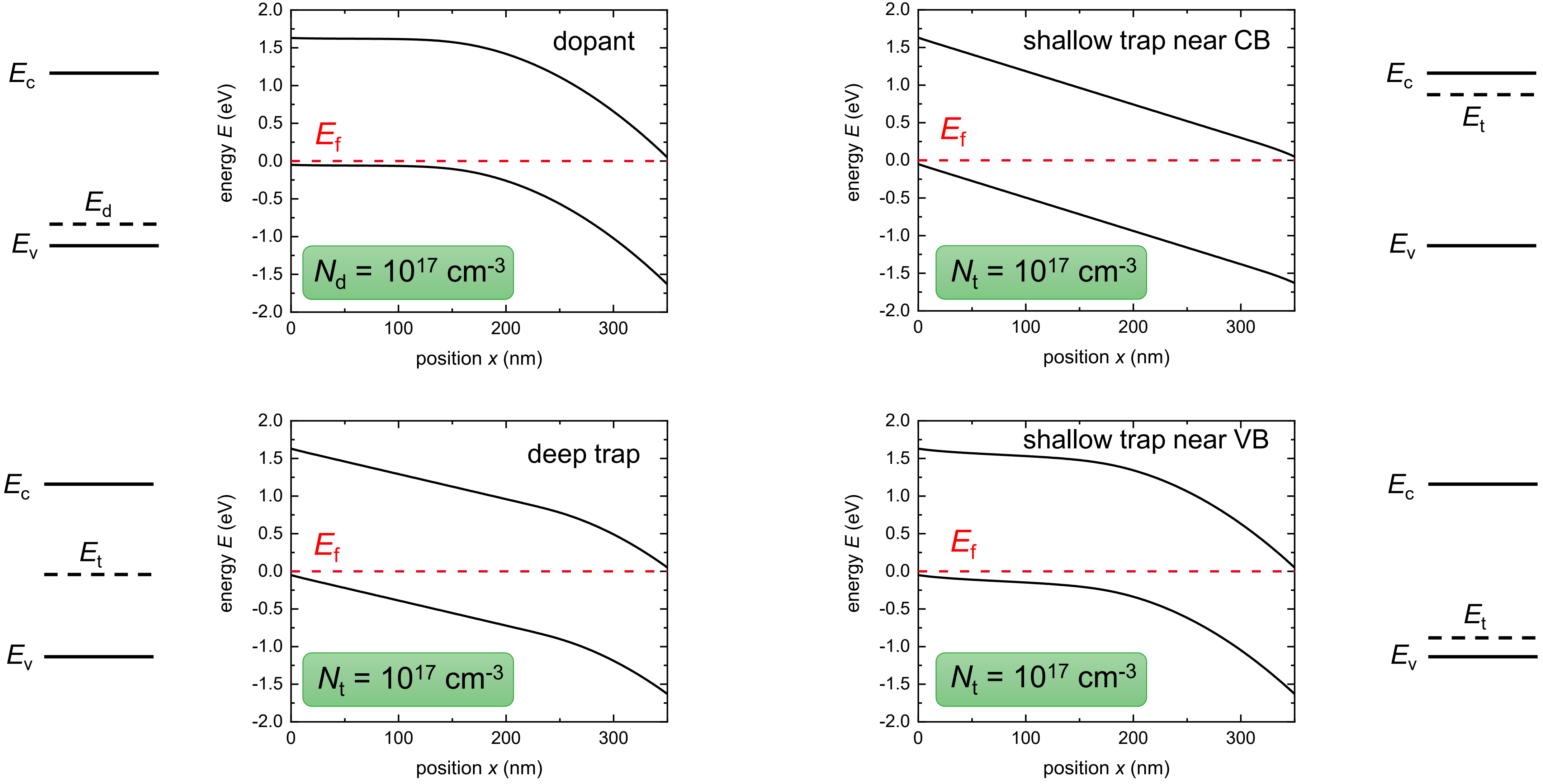

do dopants and defects have the same effect?

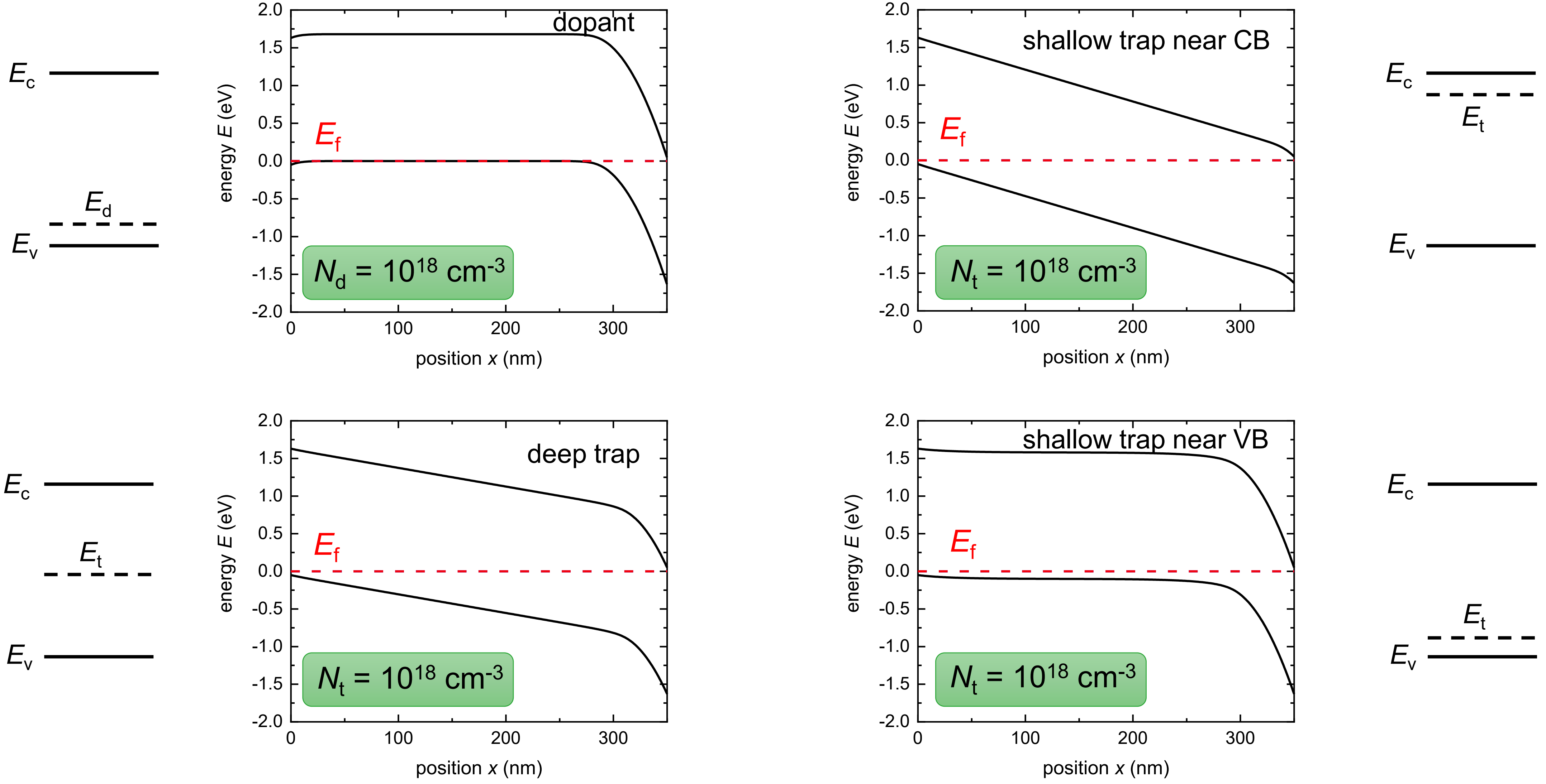

do dopants and defects have the same effect?

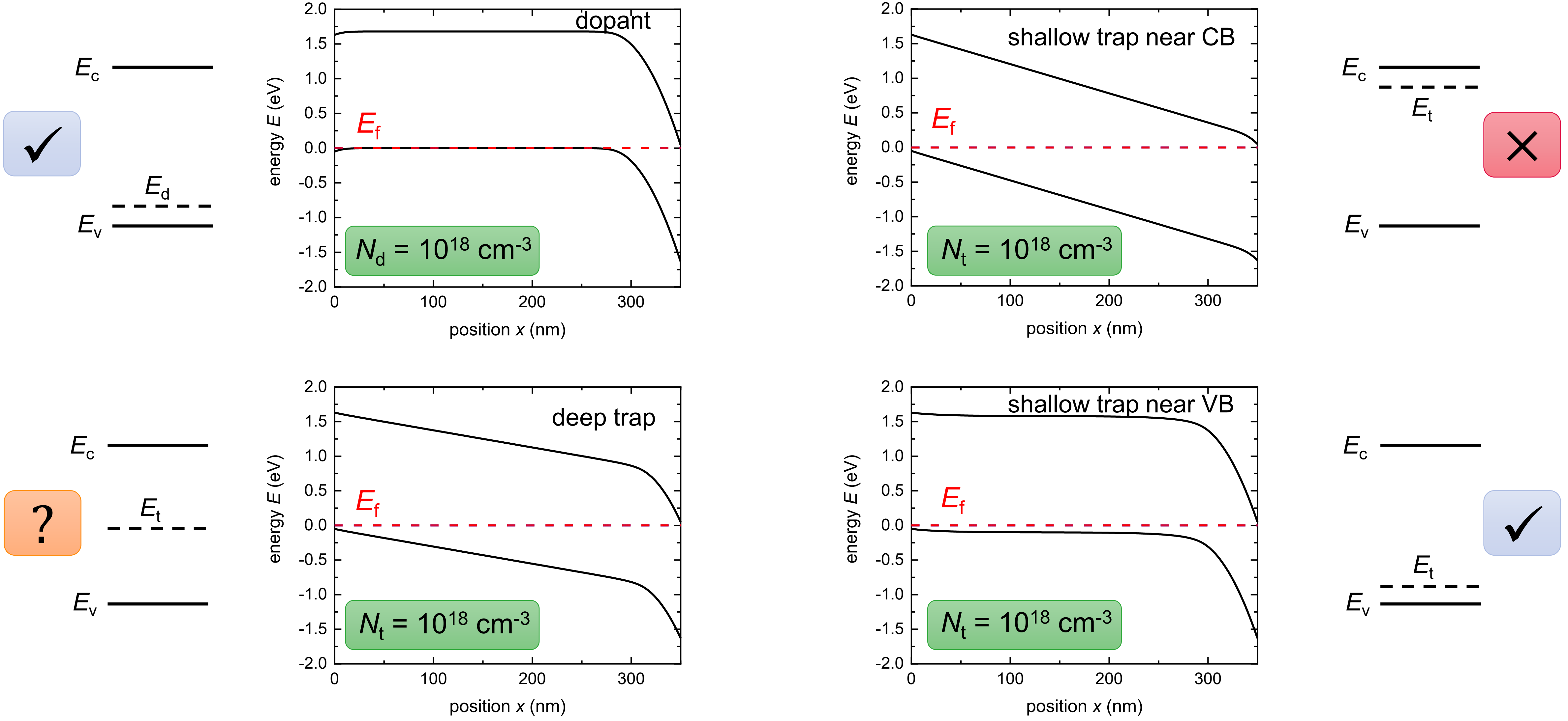

how to overcome the resolution limit?

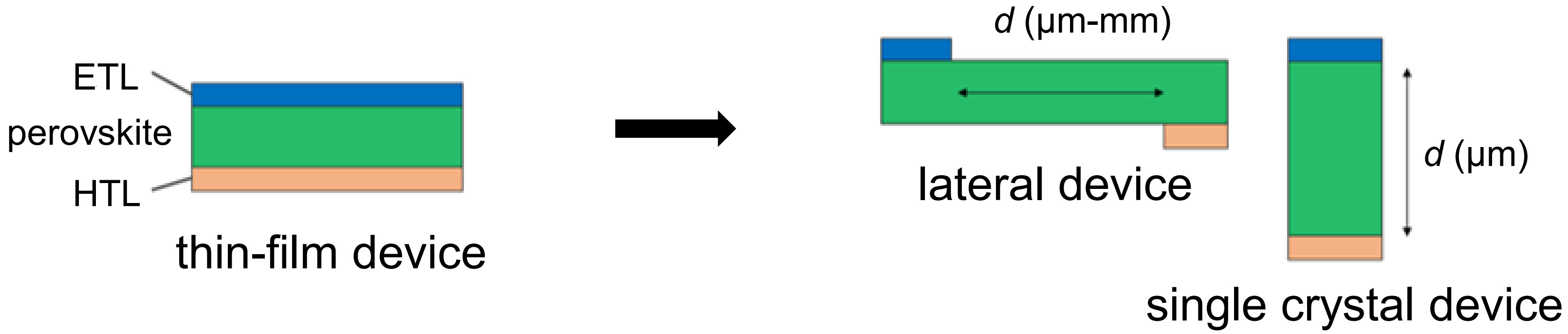

Acknowledgement: Lukas Frommel, Forschungszentrum Jülich.

how to overcome the resolution limit?

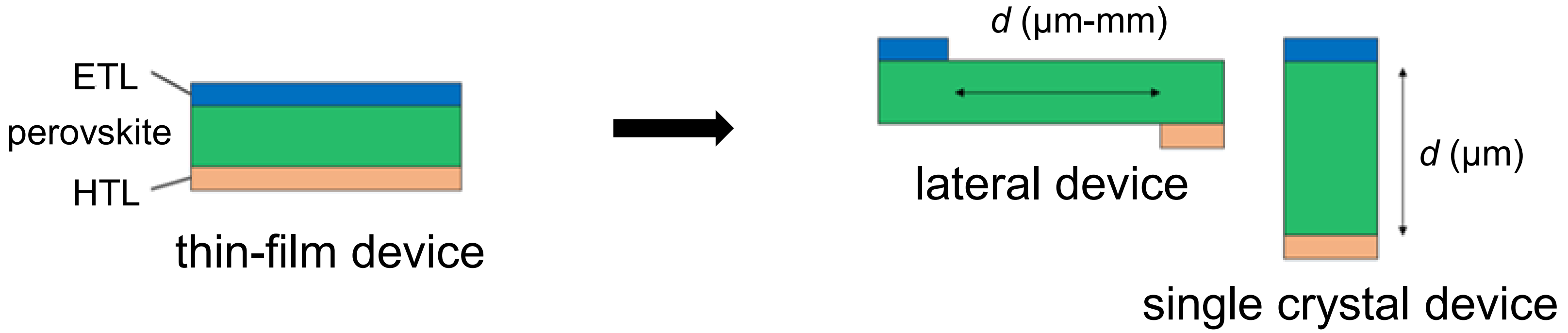

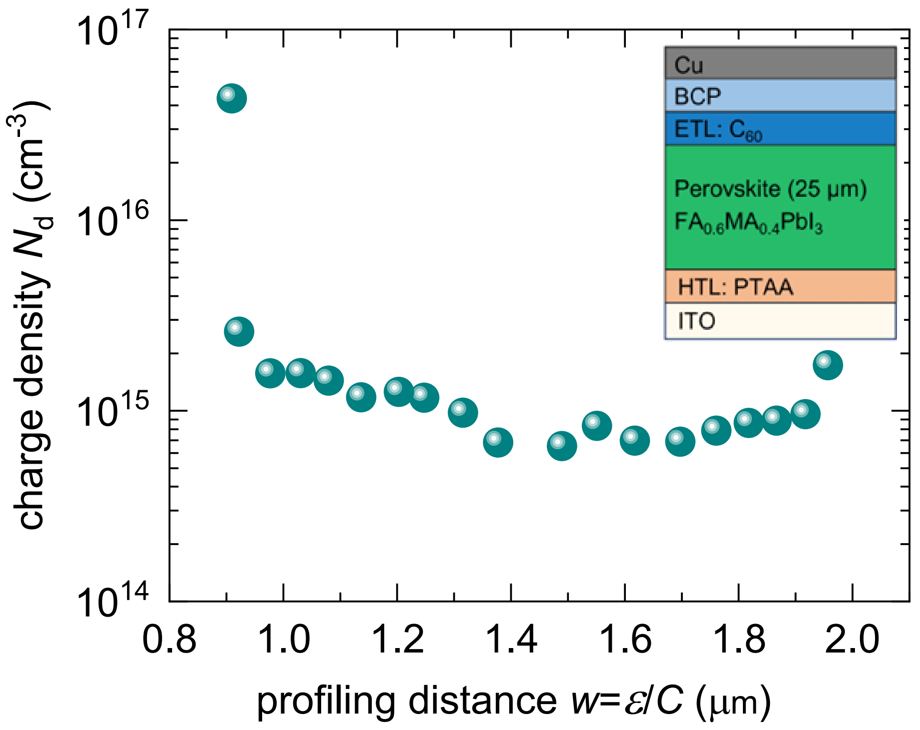

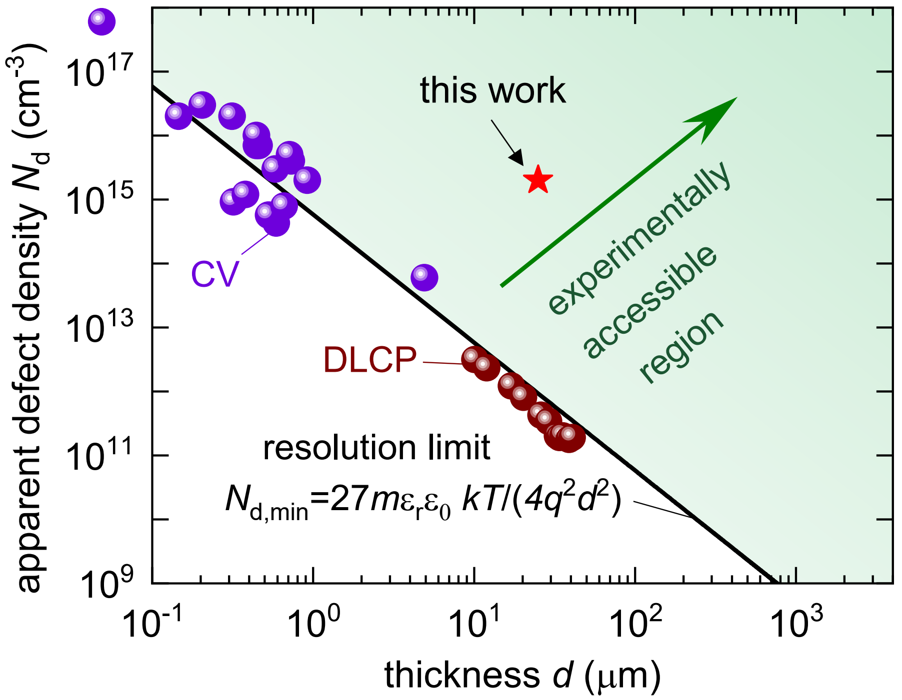

Acknowledgement: Lukas Frommel, Forschungszentrum Jülich.

how to overcome the resolution limit?

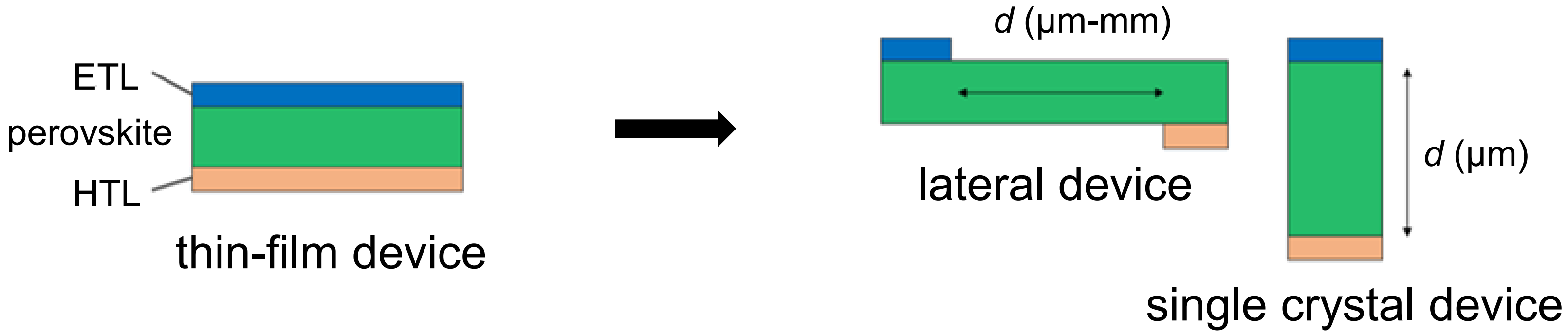

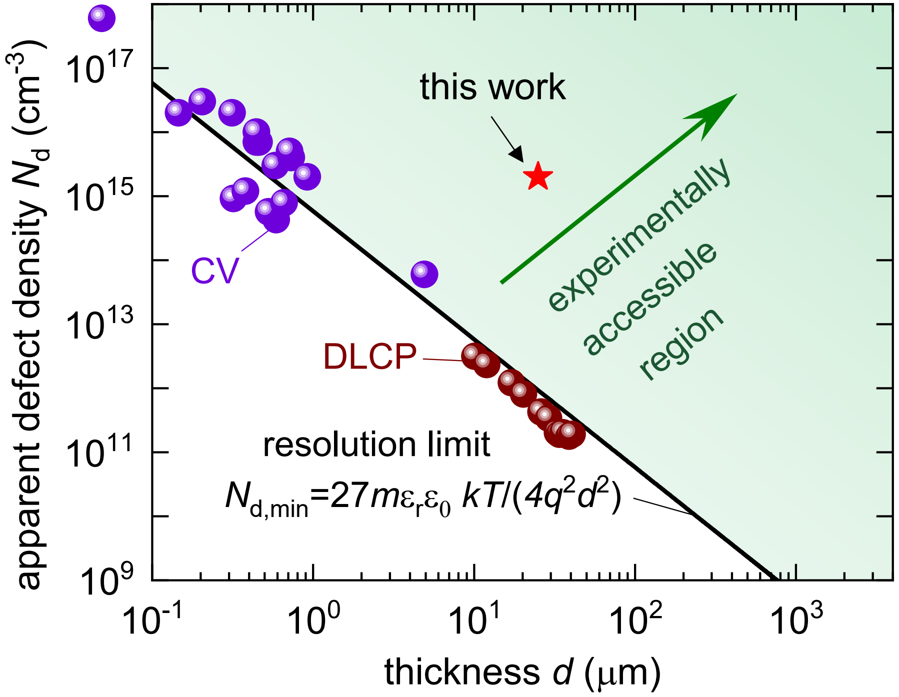

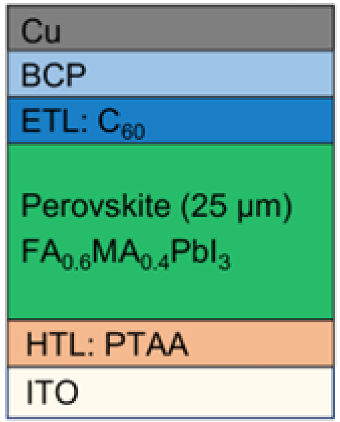

dopant-like shallow defects in single-crystal devices

Acknowledgement: Lukas Frommel, Forschungszentrum Jülich.

characterizing charge extraction losses using small-perturbation methods

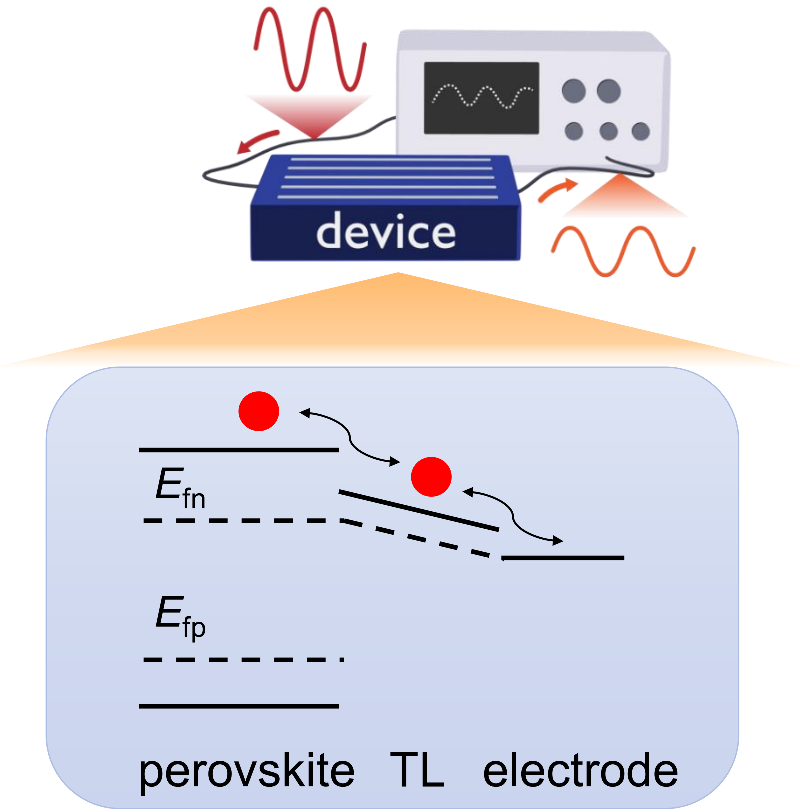

perovskite solar cell - effect of transport layers

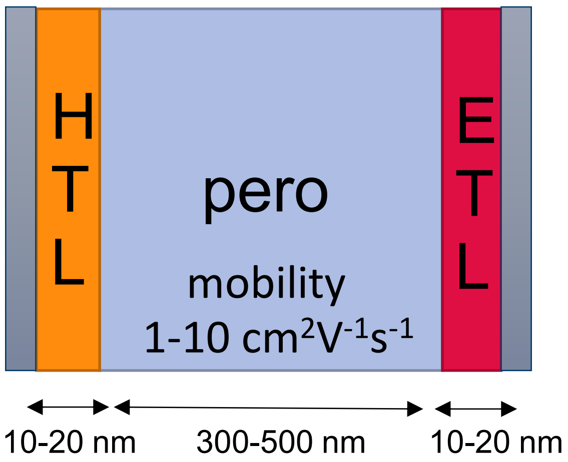

HTL	ETL
PTAA	PCBM/BCP
P3HT	C_{60}/BCP
SAMs	CMC/BCP

mobility – 10^{-5}-10^{-2} cm^{2}V^{-1}s^{-1}

perovskite solar cell - effect of transport layers

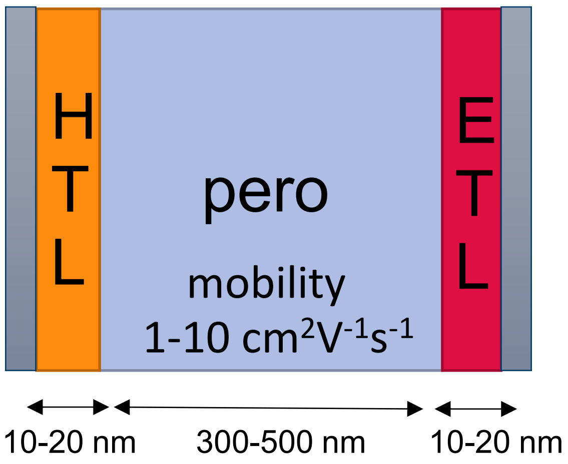

PTAA
P3HT
SAMs

PCBM/BCP
C_{60}/BCP
CMC/BCP

mobility – 10^{-5}-10^{-2} $cm^2V^{-1}s^{-1}$

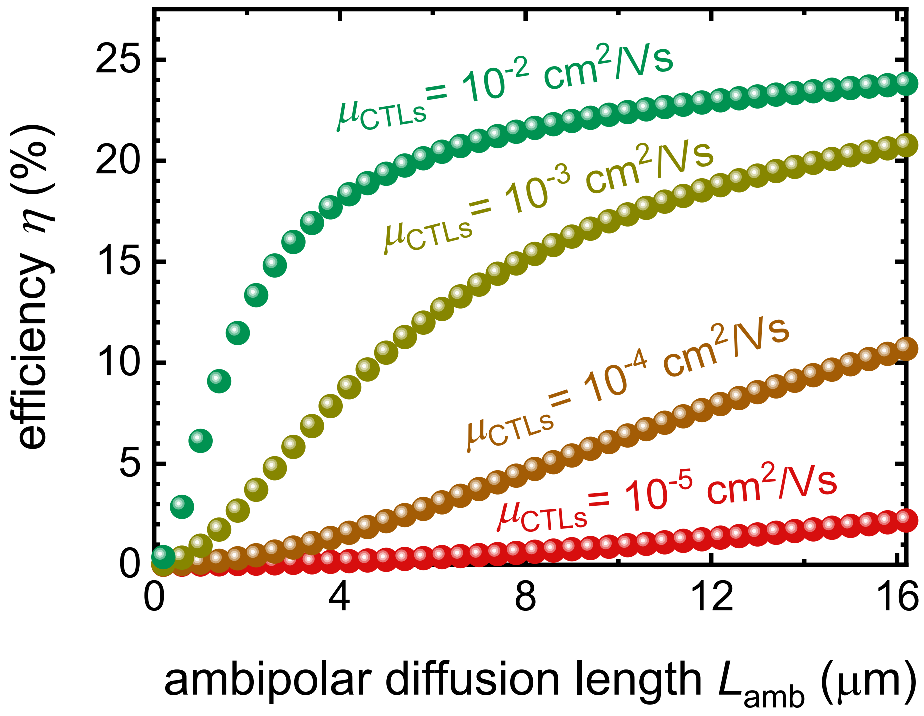

large diffusion lengths in the perovskite are irrelevant if transport layers do not extract charge efficiently

Akel, S. et al., 2023. *PRX Energy*, *2*, p.013004.

perovskite solar cell - effect of transport layers

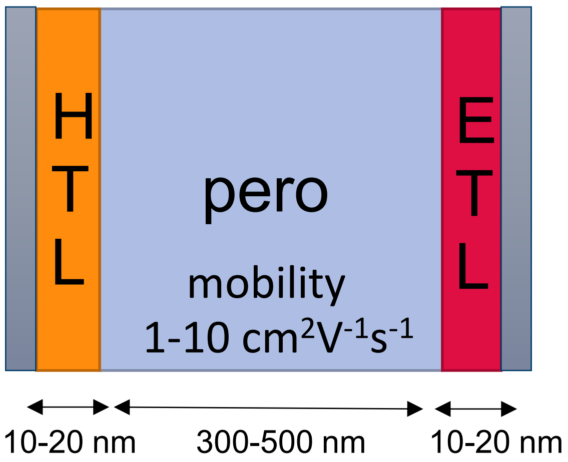

PTAA | PCBM/BCP
P3HT | C_{60}/BCP
SAMs | CMC/BCP

mobility – 10^{-5}-10^{-2} $cm^2V^{-1}s^{-1}$

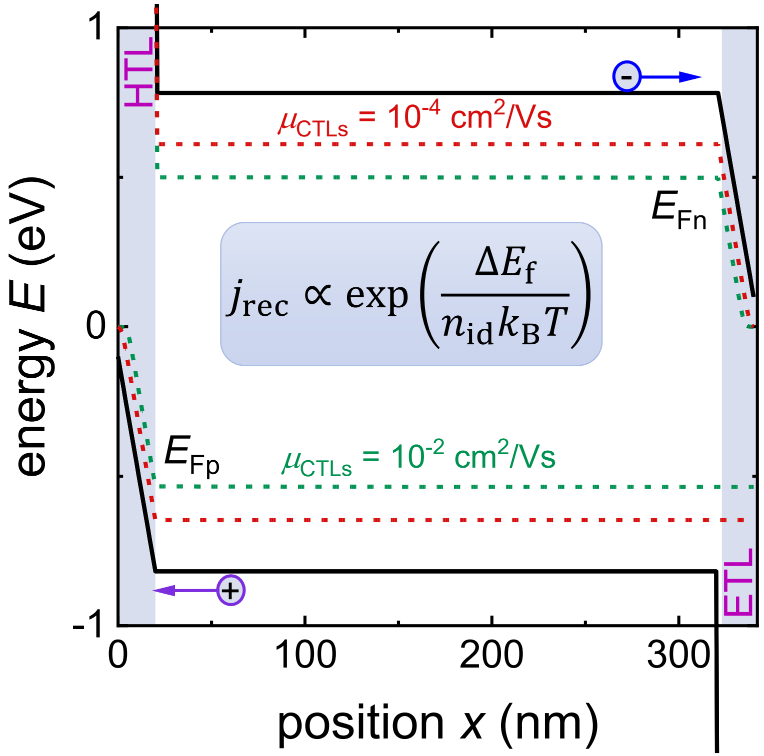

Fermi-level splitting in the perovskite is coupled to potential drop across the transport layers

Akel, S. et al., 2023. *PRX Energy*, *2*, p.013004.

key questions

can we separate transport layer effects from bulk effects in typical characterisation techniques?

can we account for the effect of the transport layers on the PSC performance?

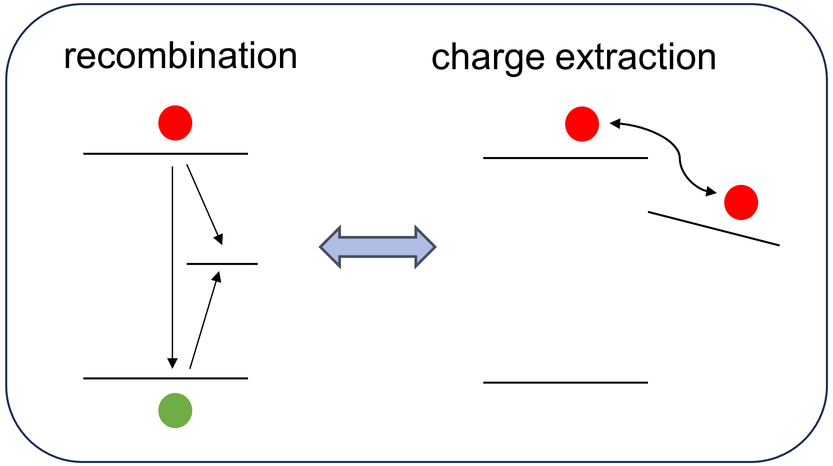

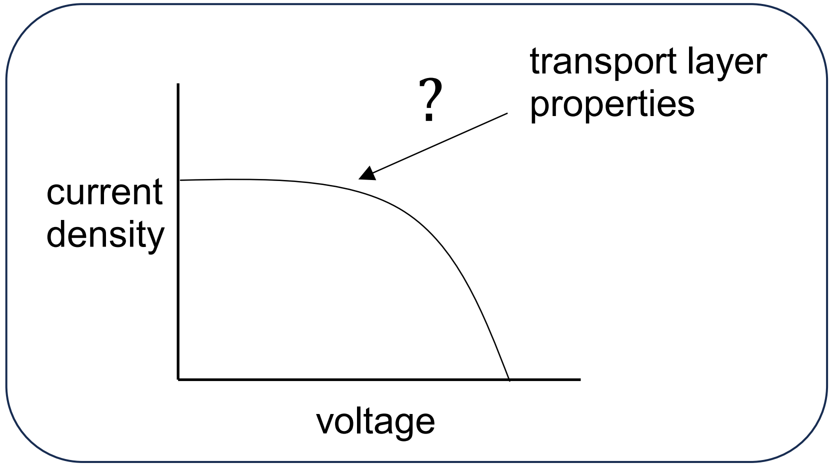

small-perturbation methods

transient photovoltage (TPV) – time domain

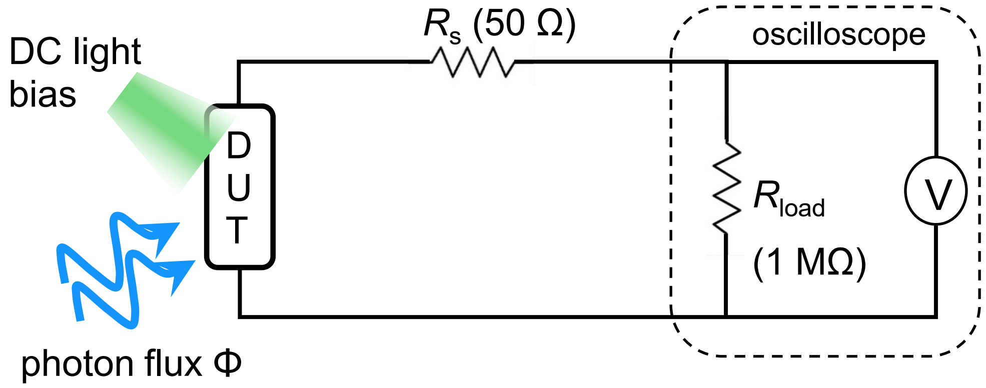

small-perturbation methods

transient photovoltage (TPV) – time domain

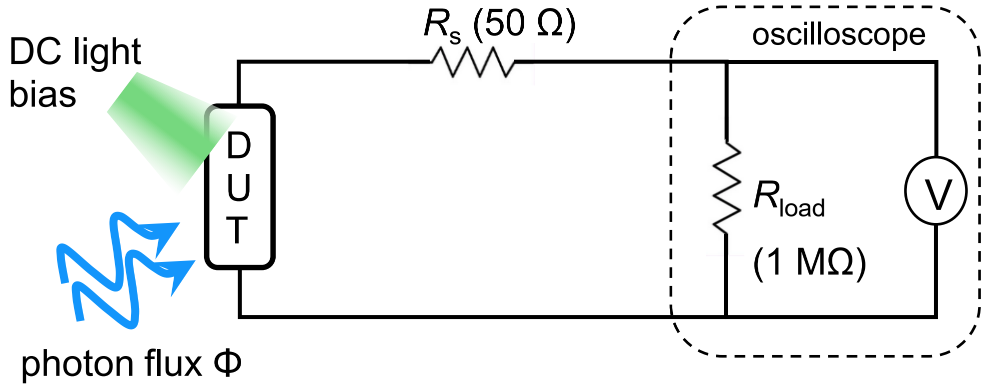

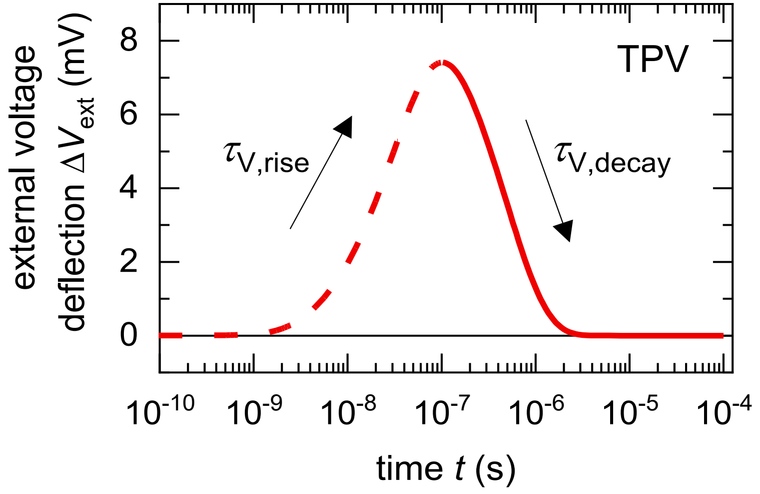

$$\Delta V_{ext}(t) = \Delta V_{ext,0}\left(e^{-t/\tau_{V,decay}} - e^{-t/\tau_{V,rise}}\right)$$

small-perturbation methods

transient photovoltage (TPV) – time domain

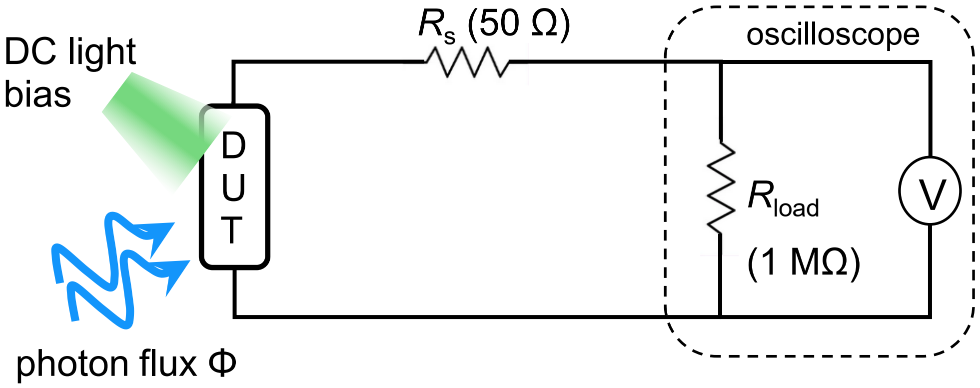

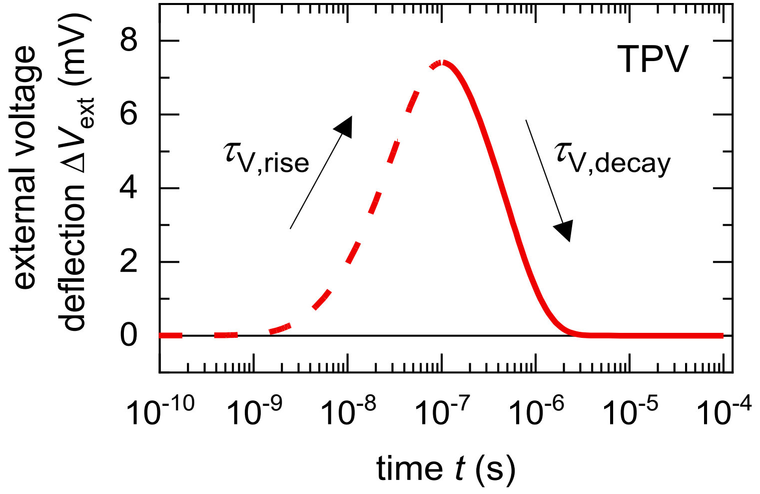

$$\Delta V_{ext}(t) = \Delta V_{ext,0}\left(e^{-t/\tau_{V,decay}} - e^{-t/\tau_{V,rise}}\right)$$

intensity modulated photovoltage spectroscopy (IMVS) – frequency domain

$$W(\omega) = \frac{\tilde{V}}{q\tilde{\Phi}} \longrightarrow \omega = 10\ \text{MHz} - 1\ \text{mHz}$$

small-perturbation methods

transient photovoltage (TPV) – time domain

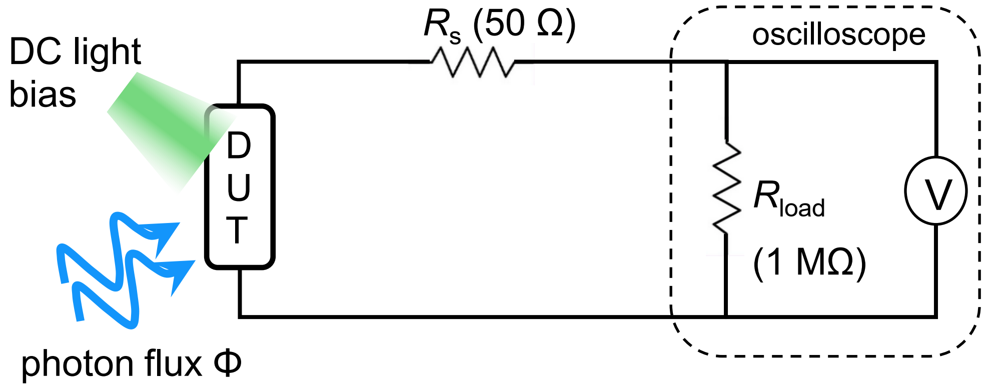

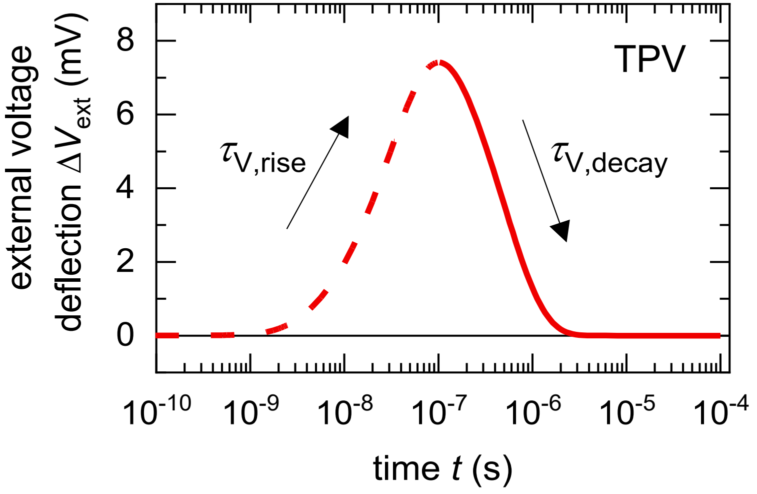

$$\Delta V_{ext}(t) = \Delta V_{ext,0}\left(e^{-t/\tau_{V,decay}} - e^{-t/\tau_{V,rise}}\right)$$

intensity modulated photovoltage spectroscopy (IMVS) – frequency domain

$$W(\omega) = \frac{\tilde{V}}{q\tilde{\Phi}} \rightarrow \omega = 10\ \text{MHz} - 1\ \text{mHz}$$

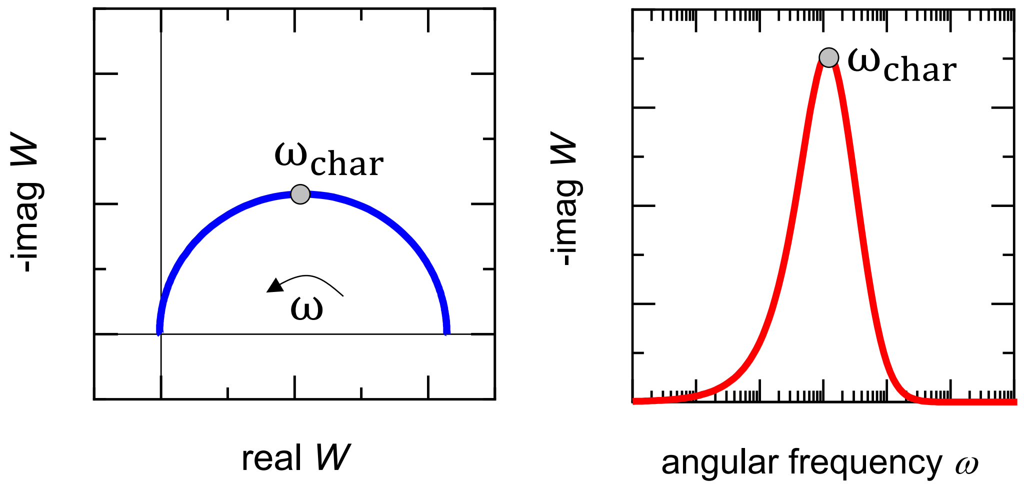

$$\frac{d(-\text{imag}\,W)}{d\omega} = 0 \rightarrow \omega_{char} = \frac{1}{\tau_{char}}$$

time constants

drift-diffusion simulations

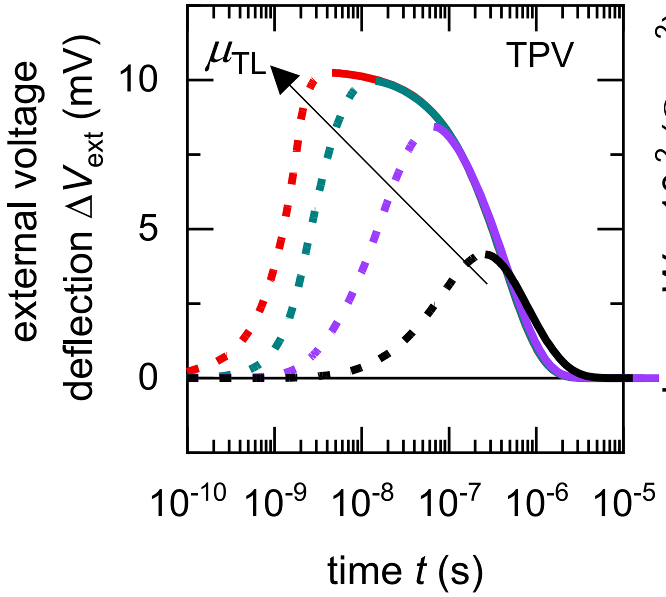

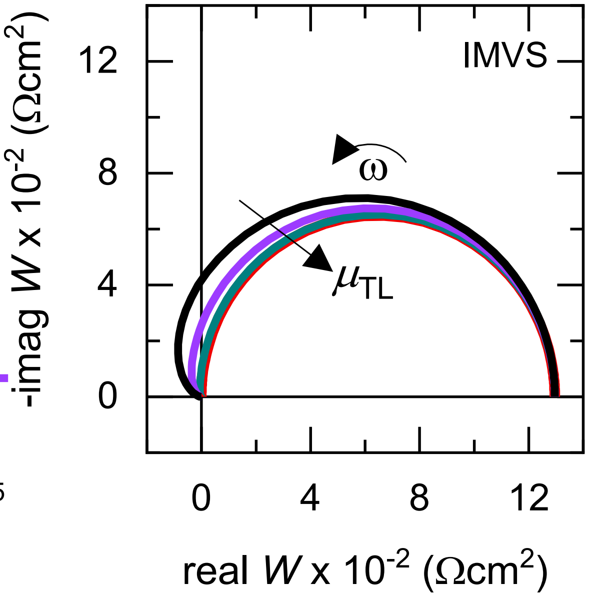

S. Ravishankar et al., 2024. *Energy & Environmental Science*, *17*(3), pp.1229-1243.

time constants

drift-diffusion simulations

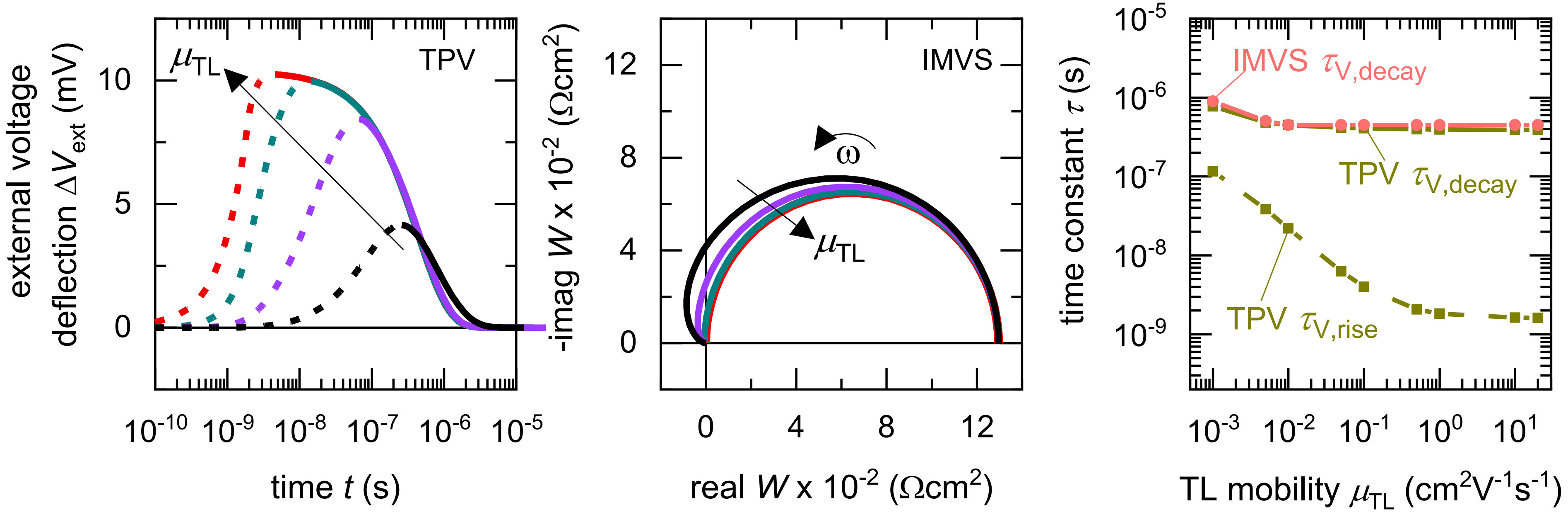

why do time domain methods show two time constants while frequency domain methods show only one time constant?

S. Ravishankar et al., 2024. *Energy & Environmental Science*, *17*(3), pp.1229-1243.

modified transfer function

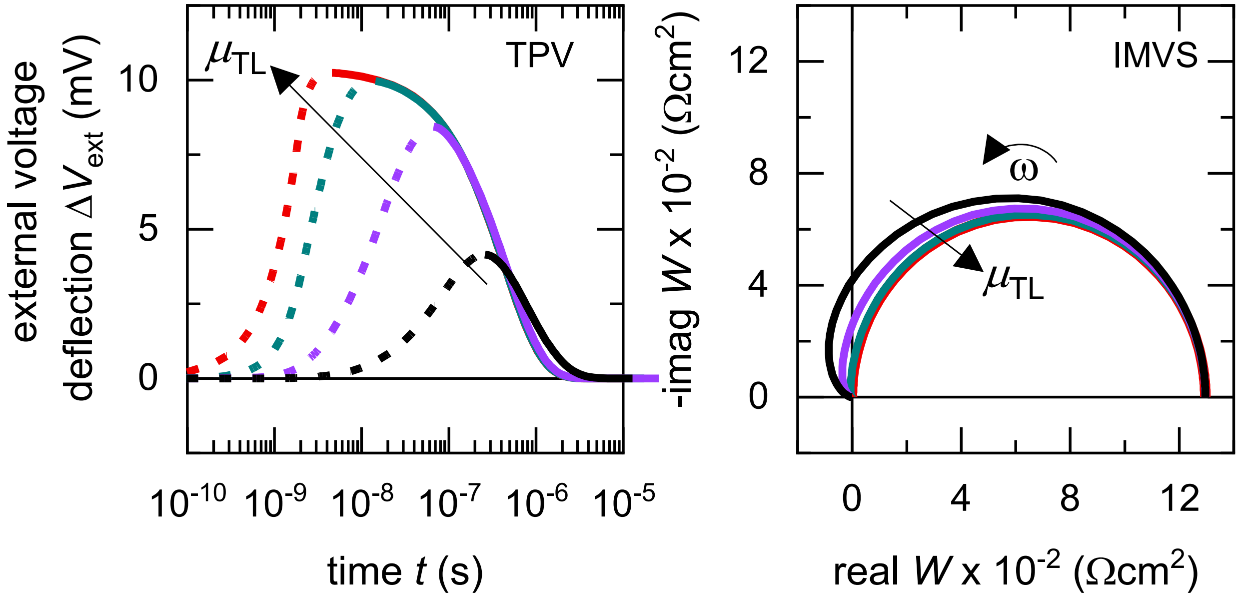

logic

time domain methods show absolute value and slope of the voltage/current

frequency domain methods show no information about the slope

$$V \rightarrow \frac{dV}{dt} \xrightarrow{\text{laplace transform}} i\omega V$$

S. Ravishankar et al., 2024. *Energy & Environmental Science*, *17*(3), pp.1229-1243.

modified transfer function

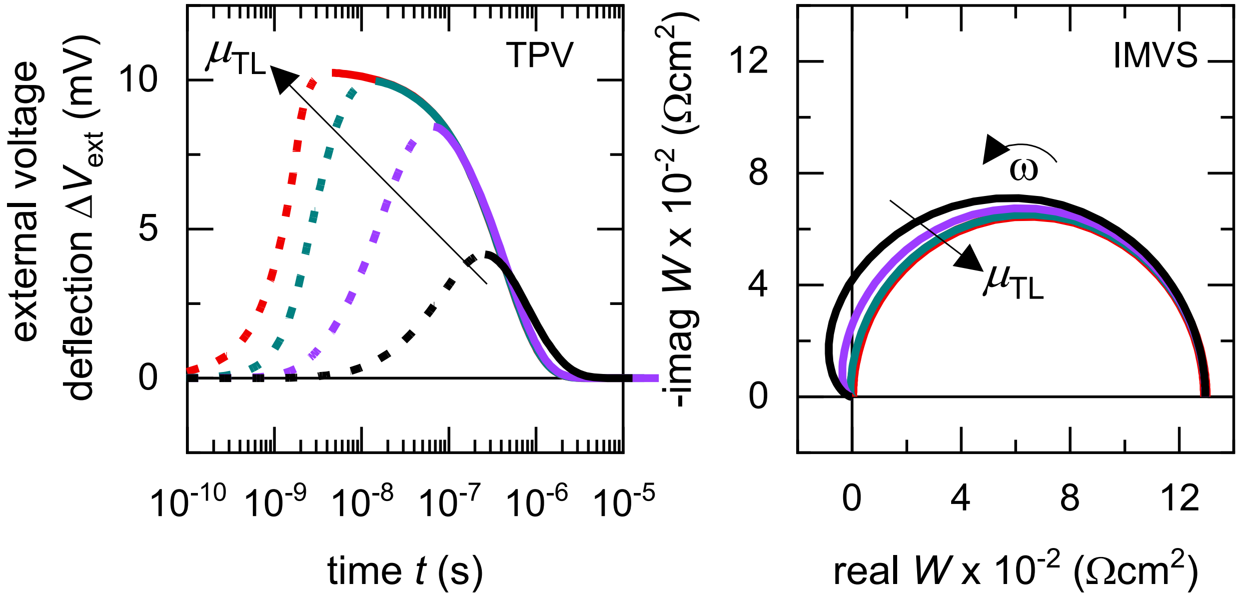

logic

time domain methods show absolute value and slope of the voltage/current

frequency domain methods show no information about the slope

$$M_W = i\omega W \longrightarrow \begin{array}{l} \text{real } M_W = -\omega \times \text{imag } W \\ \text{imag } M_W = \omega \times \text{real } W \end{array}$$

$$\longrightarrow \frac{d(-\text{imag } M_W)}{d\omega} = 0 \rightarrow \omega_{char} = \frac{1}{\tau_{char}}$$

S. Ravishankar et al., 2024. *Energy & Environmental Science*, *17*(3), pp.1229-1243.

modified transfer function

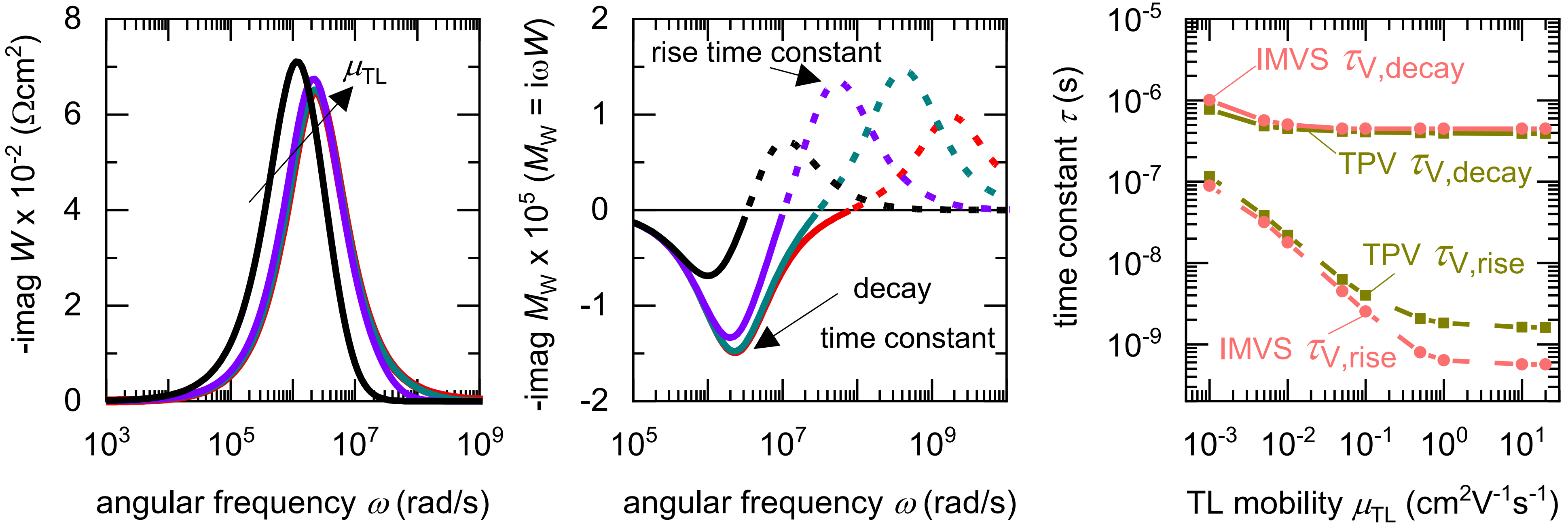

rise time constant embedded in the transition of real part of IMVS transfer function to negative values at high frequencies

S. Ravishankar et al., 2024. *Energy & Environmental Science*, *17*(3), pp.1229-1243.

modified transfer function

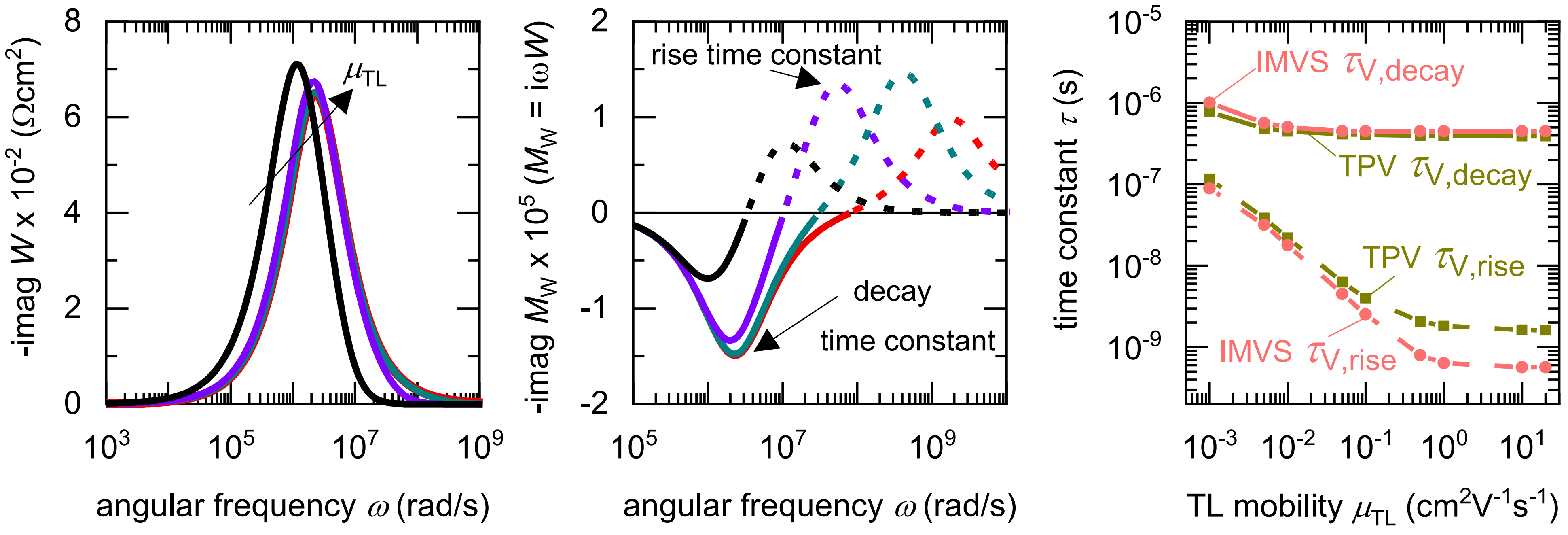

which mechanisms generate the rise and decay time constants?

S. Ravishankar et al., 2024. *Energy & Environmental Science*, *17*(3), pp.1229-1243.

charge extraction through the transport layer

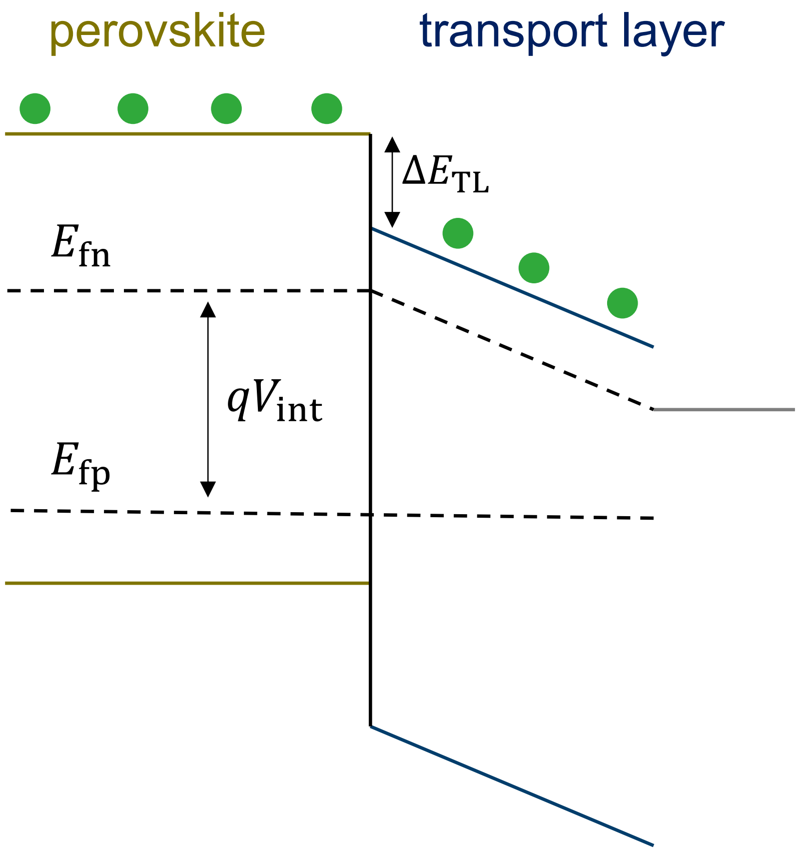

$$F_{\mathrm{TL}} = \frac{V_{\mathrm{bi,TL}} - V_{\mathrm{ext}}}{d_{\mathrm{TL}}}$$

current density

$$j = q n_{\mathrm{i}} S_{\mathrm{exc}} \times \left[\exp\left(\frac{qV_{\mathrm{int}}}{2k_{\mathrm{B}}T}\right) - \exp\left(\frac{V_{\mathrm{ext}}}{2k_{\mathrm{B}}T}\right)\right]$$

charge extraction velocity

$$S_{\mathrm{exc}}(V_{\mathrm{elec}}) \cong \mu_{\mathrm{TL}} F_{\mathrm{TL}} \exp\left(\frac{\Delta E_{\mathrm{TL}}}{k_{\mathrm{B}}T}\right)$$

charge extraction time constant

$$\tau_{\mathrm{exc}} = \frac{d_{\mathrm{pero}}}{S_{\mathrm{exc}}}$$

S. Ravishankar et al., 2023. *PRX Energy* 2, 033006.

predicted time constants

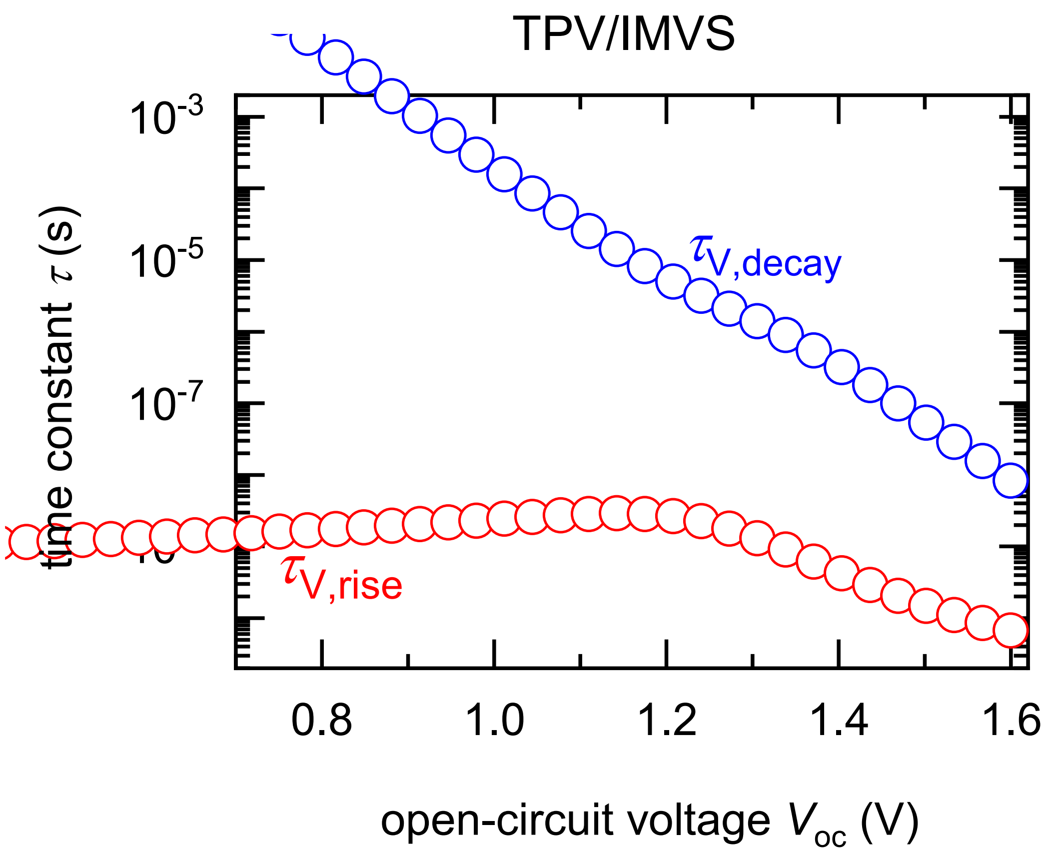

S. Ravishankar et al., 2023. *PRX Energy* 2, 033006.

predicted time constants

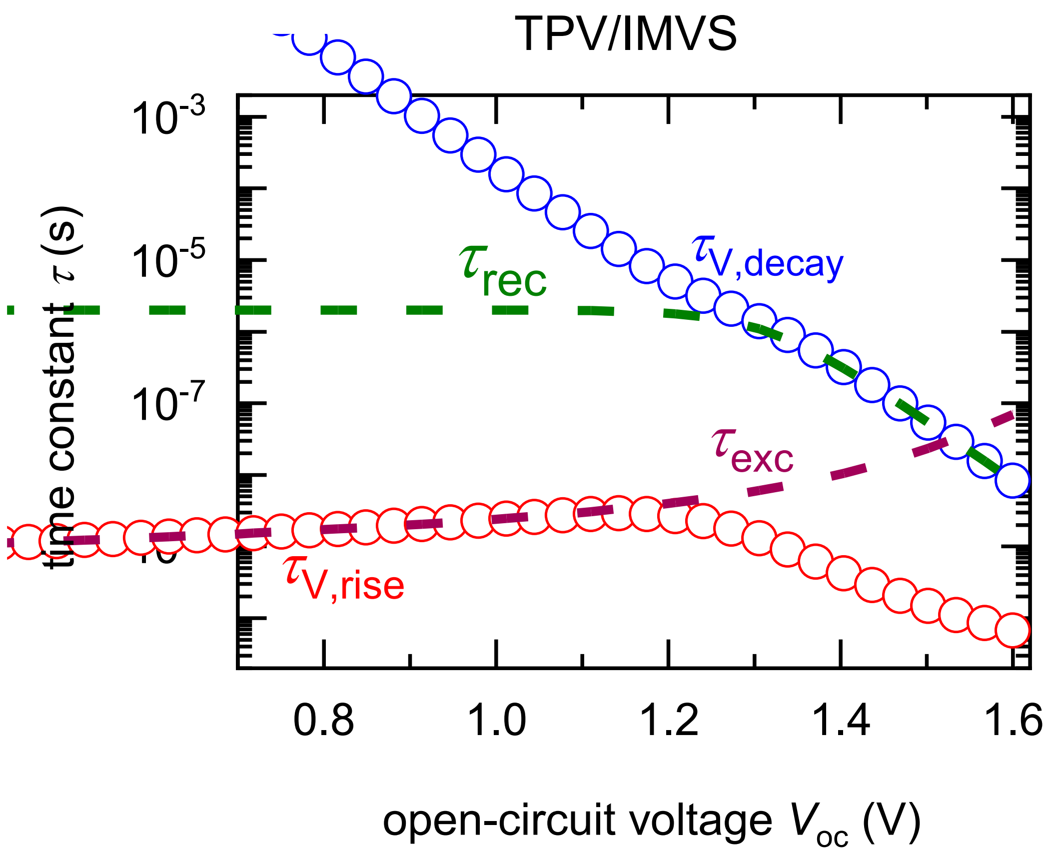

S. Ravishankar et al., 2023. *PRX Energy* 2, 033006.

predicted time constants

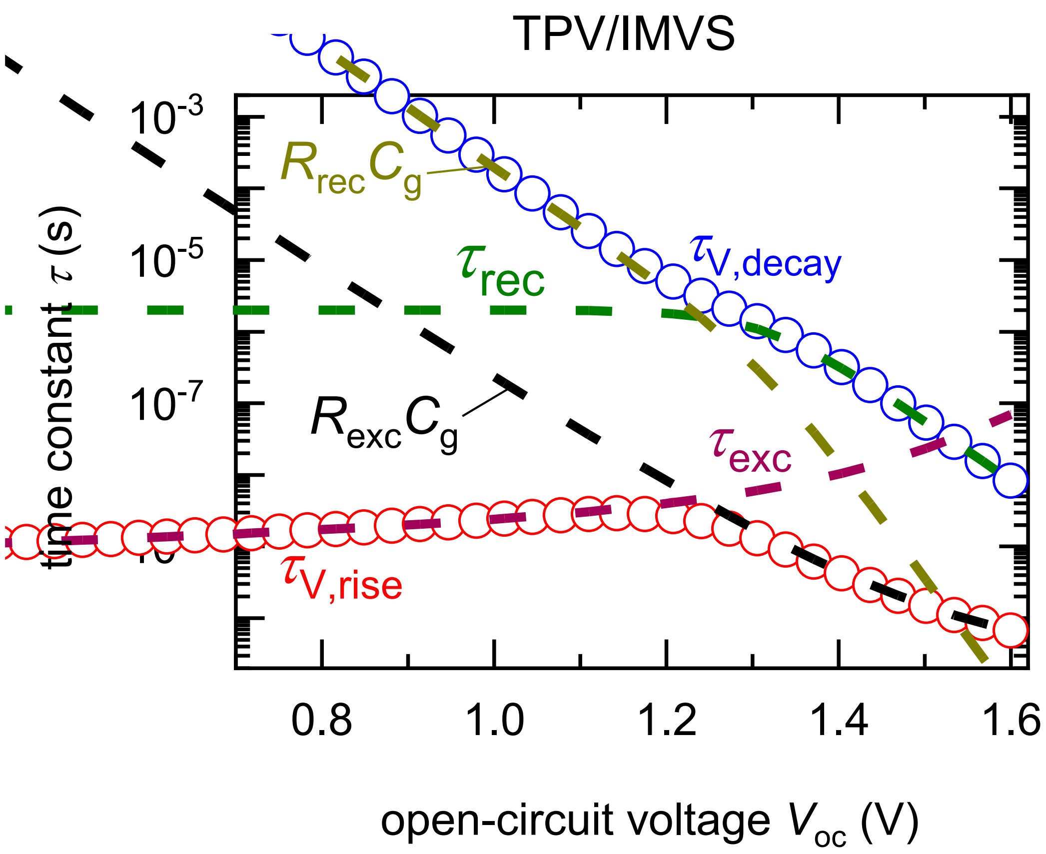

rise time constants mostly correspond to charge extraction

decay time constants correspond to recombination

S. Ravishankar et al., 2023. *PRX Energy* 2, 033006.

predicted time constants

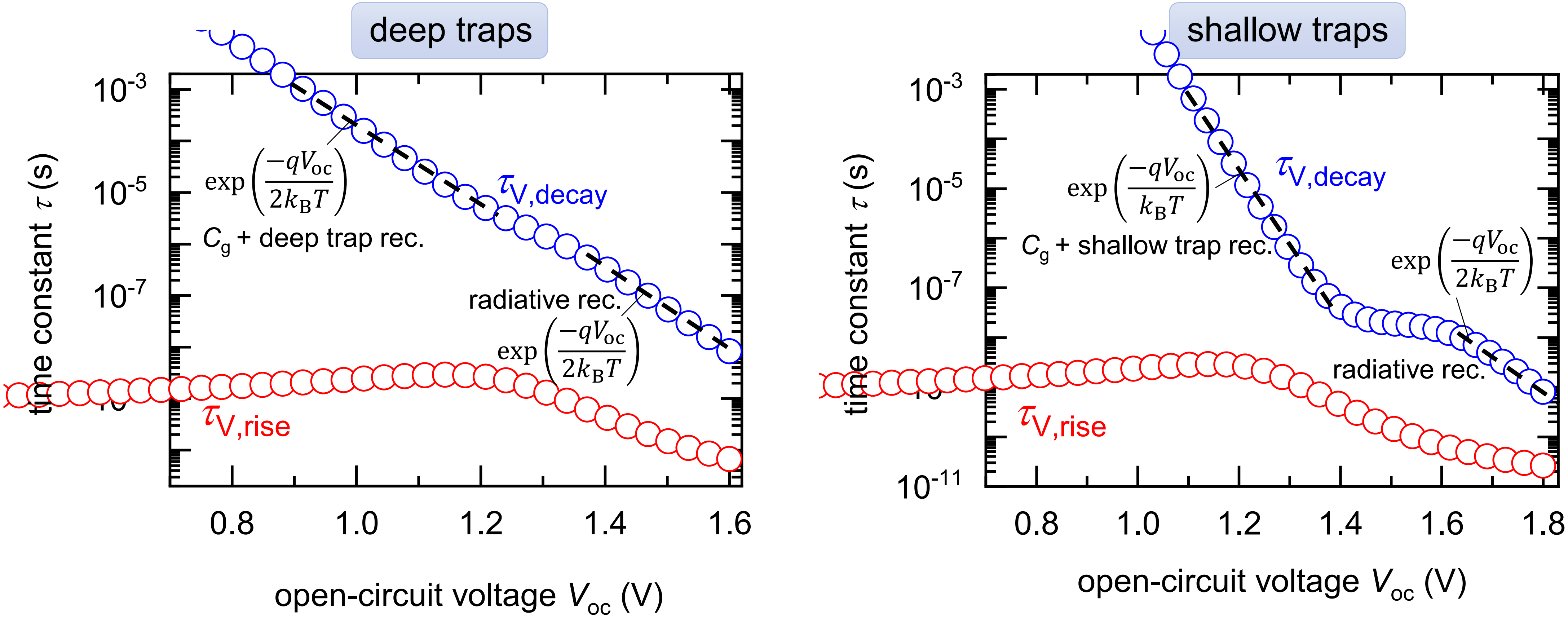

shallow traps in perovskite solar cells

transient photoluminescence (tr-PL) measurements

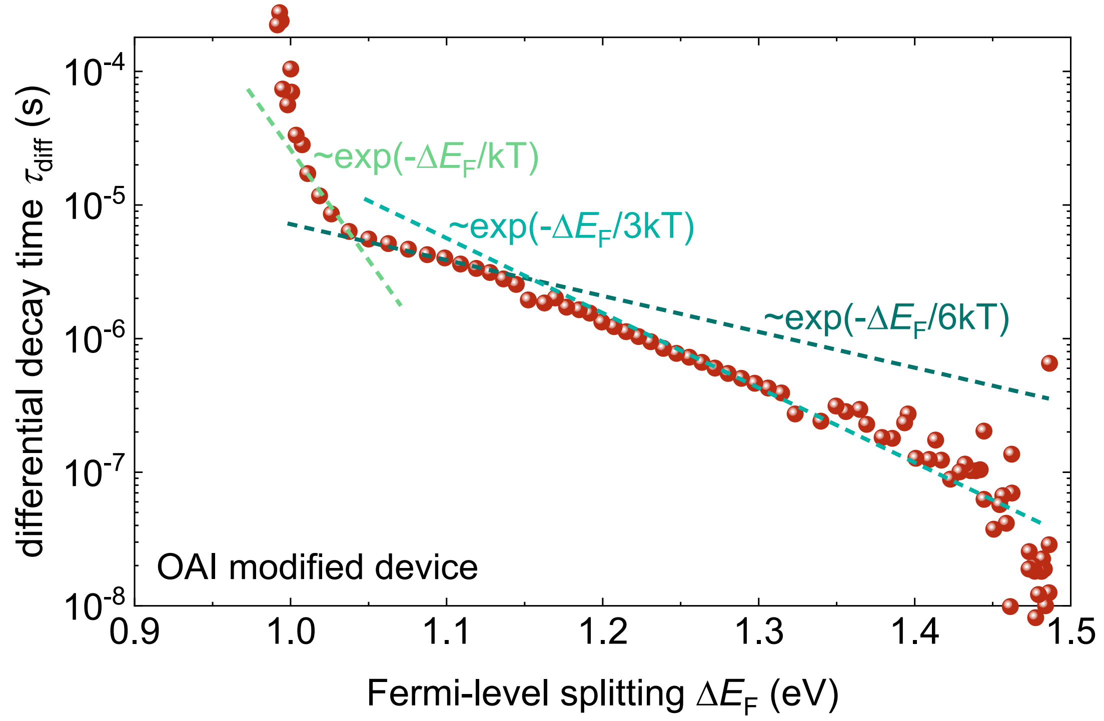

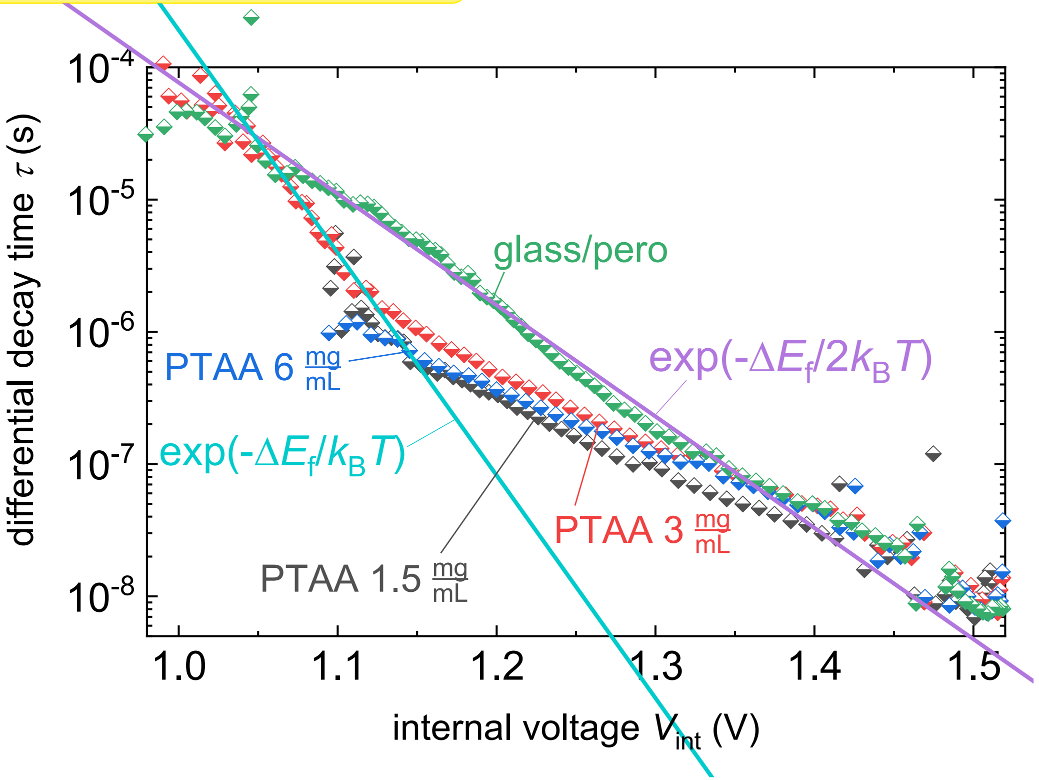

Y. Yuan et al., 2024. *Nature Materials*, *23*(3), pp.391-397. C. Dreessen et al., unpublished.

application to experimental data

ITO/SAMs/PTAA/$Cs_{0.05}FA_{0.8}MA_{0.15}PbI_{2.25}Br_{0.75}$ (1.68 eV)/C_{60}/BCP/Ag devices

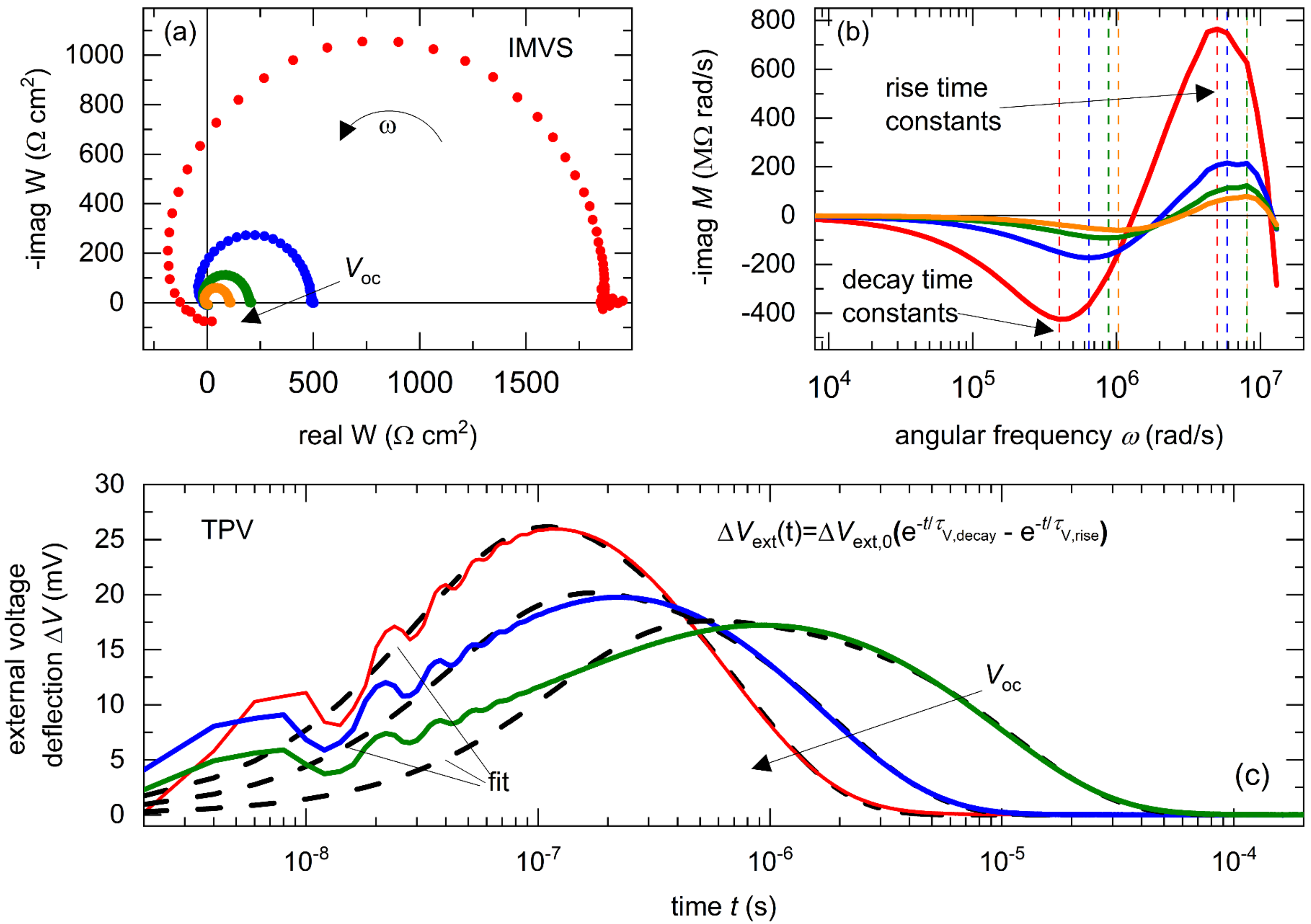

S. Ravishankar et al., 2024. *Energy & Environmental Science*, *17*(3), pp.1229-1243.

experimental rise and decay time constants

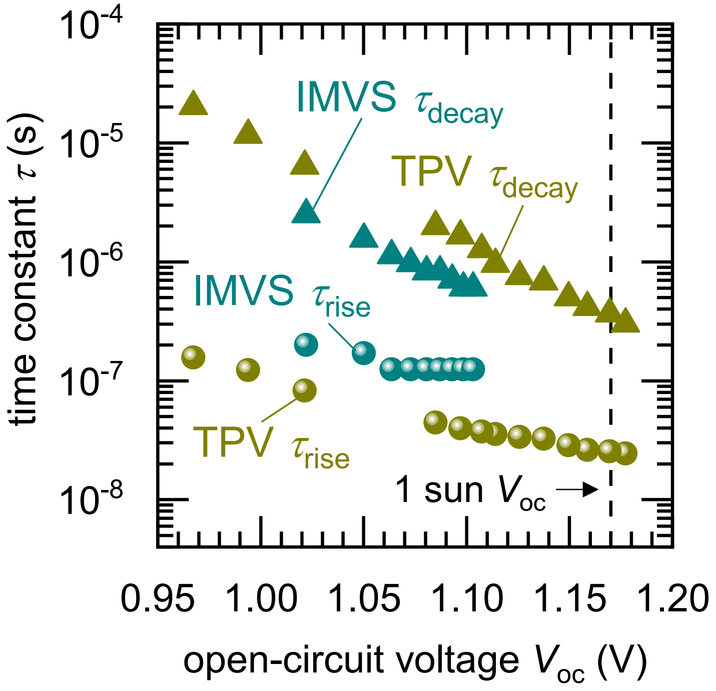

S. Ravishankar et al., 2024. *Energy & Environmental Science*, *17*(3), pp.1229-1243.

experimental rise and decay time constants

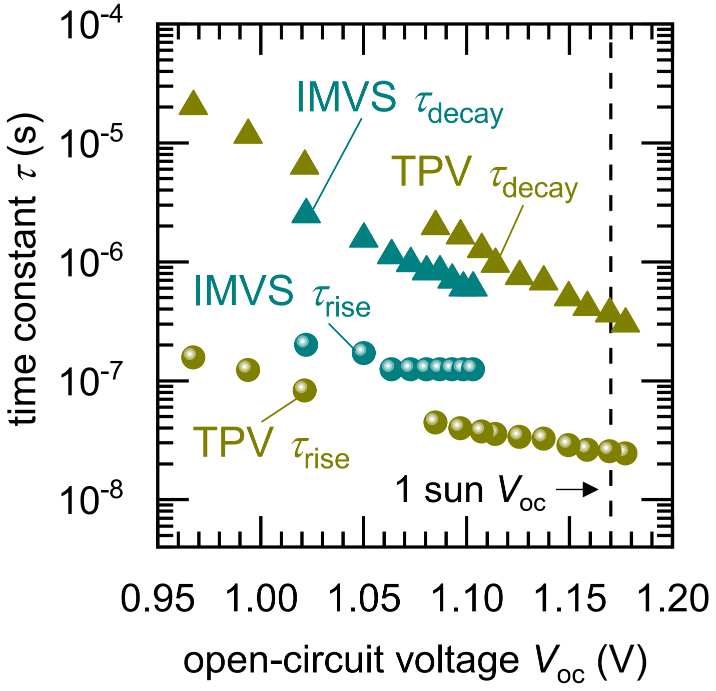

$$\tau = \tau_0 \exp\left(\frac{-qV_{oc}}{\Theta k_B T}\right)$$

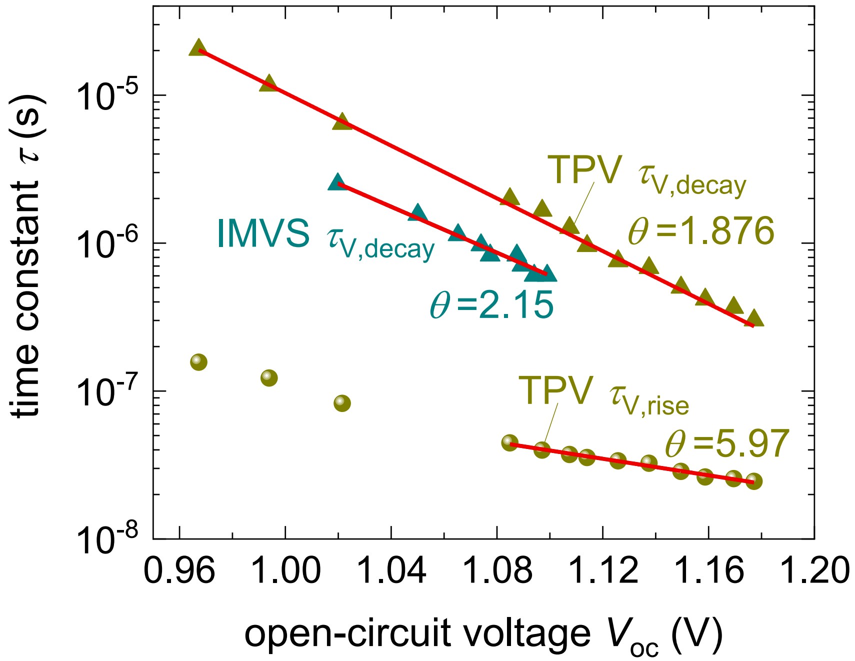

S. Ravishankar et al., 2024. *Energy & Environmental Science*, *17*(3), pp.1229-1243.

experimental rise and decay time constants

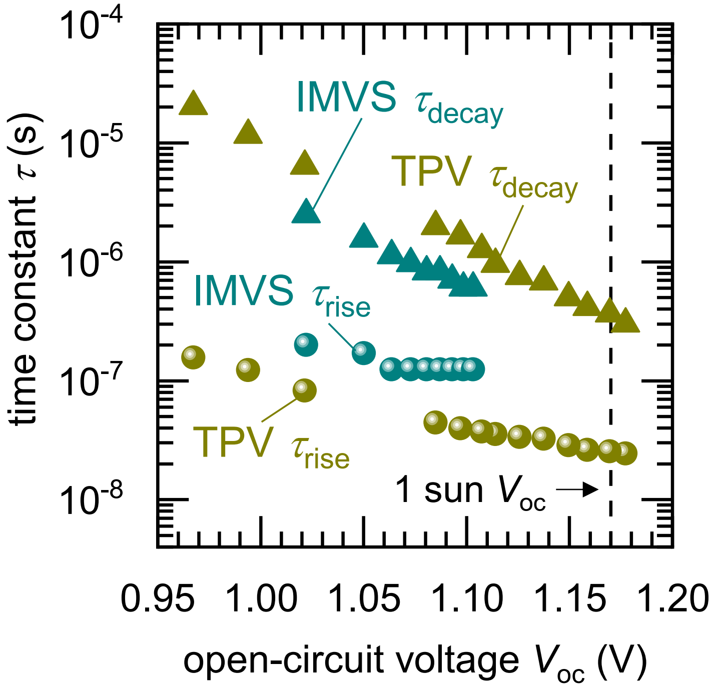

$$\tau = \tau_0 \exp\left(\frac{-qV_{oc}}{\Theta k_B T}\right)$$

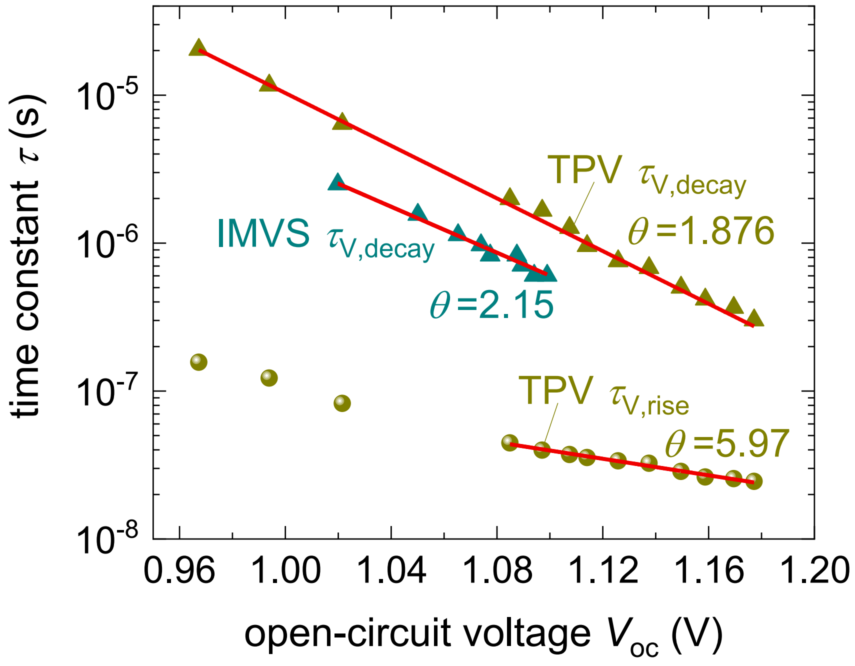

rise times correspond to charge extraction

decay times correspond to recombination limited by charge re-injection from the electrodes

S. Ravishankar et al., 2024. *Energy & Environmental Science*, *17*(3), pp.1229-1243.

figure of merit accounting for charge extraction losses

$$j = qd\left(G - \frac{n_{\mathrm{i}}}{\tau_{\mathrm{rec}}}\left[\exp\left(\frac{qV_{\mathrm{ext}}}{n_{\mathrm{id}}k_{\mathrm{B}}T}\right) - 1\right]\right)$$

current-voltage curve – balance of generation and recombination

figure of merit accounting for charge extraction losses

$$j = \left[\frac{1}{1+\frac{\tau_{\mathrm{exc}}}{\tau_{\mathrm{rec}}}}\right] qd\left(G - \frac{n_{\mathrm{i}}}{\tau_{\mathrm{rec}}}\left[\exp\left(\frac{qV_{\mathrm{ext}}}{n_{\mathrm{id}}k_{\mathrm{B}}T}\right) - 1\right]\right)$$

current-voltage curve including generation, recombination and extraction

L. Krückemeier et al., 2023. *Advanced Materials* 35, 2300872.
S. Ravishankar et al., 2024. *Energy & Environmental Science*, *17*(3), pp.1229-1243.

figure of merit accounting for charge extraction losses

$$j = \left[\frac{1}{1+\frac{\tau_{\mathrm{exc}}}{\tau_{\mathrm{rec}}}}\right] qd\left(G - \frac{n_{\mathrm{i}}}{\tau_{\mathrm{rec}}}\left[\exp\left(\frac{qV_{\mathrm{ext}}}{n_{\mathrm{id}}k_{\mathrm{B}}T}\right) - 1\right]\right)$$

↓

$$\mathrm{FOM} = \frac{1}{1+\frac{\tau_{\mathrm{exc}}}{\tau_{\mathrm{rec}}}}$$

FOM = 1
perfect charge extraction

FOM < 1
non-ideal charge extraction

L. Krückemeier et al., 2023. *Advanced Materials* 35, 2300872.
S. Ravishankar et al., 2024. *Energy & Environmental Science*, *17*(3), pp.1229-1243.

figure of merit accounting for charge extraction losses

$$j = \left[\frac{1}{1+\frac{\tau_{\mathrm{exc}}}{\tau_{\mathrm{rec}}}}\right] qd\left(G - \frac{n_{\mathrm{i}}}{\tau_{\mathrm{rec}}}\left[\exp\left(\frac{qV_{\mathrm{ext}}}{n_{\mathrm{id}}k_{\mathrm{B}}T}\right) - 1\right]\right)$$

↓

$$\mathrm{FOM} = \frac{1}{1+\frac{\tau_{\mathrm{exc}}}{\tau_{\mathrm{rec}}}}$$

$$\tau_{\mathrm{exc}} = \tau_{\mathrm{rise}} \quad \tau_{\mathrm{rec}} = ?$$

how to determine the recombination lifetime?

L. Krückemeier et al., 2023. *Advanced Materials* 35, 2300872.
S. Ravishankar et al., 2024. *Energy & Environmental Science*, *17*(3), pp.1229-1243.

experimental FOM

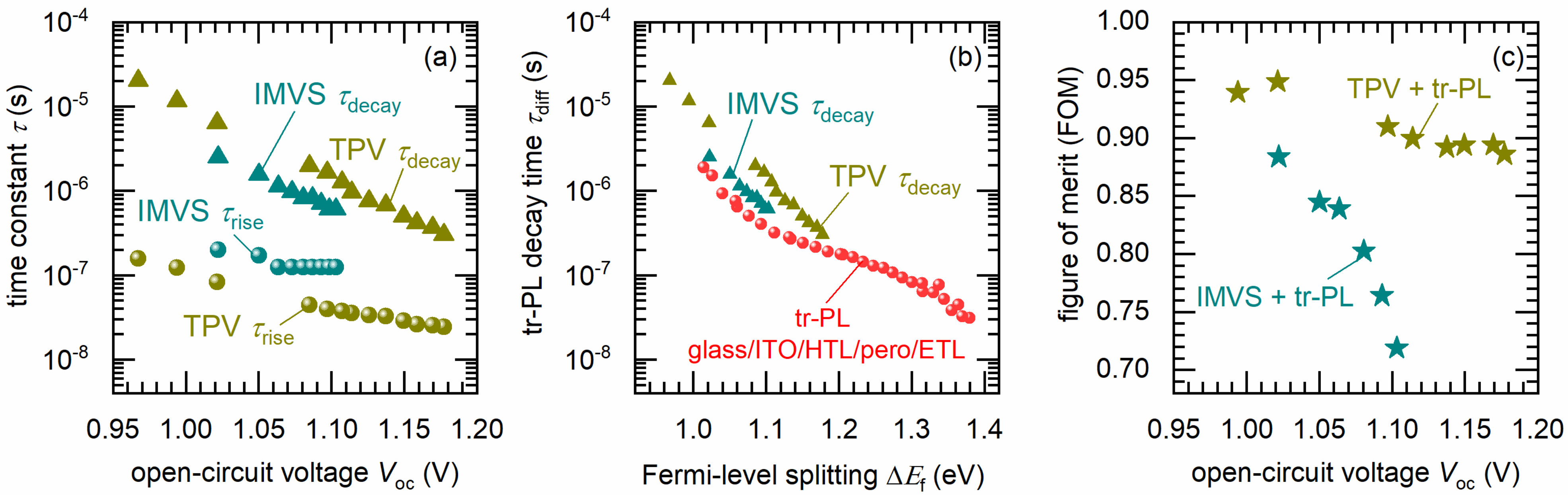

S. Ravishankar et al., 2024. *Energy & Environmental Science*, *17*(3), pp.1229-1243.

experimental FOM

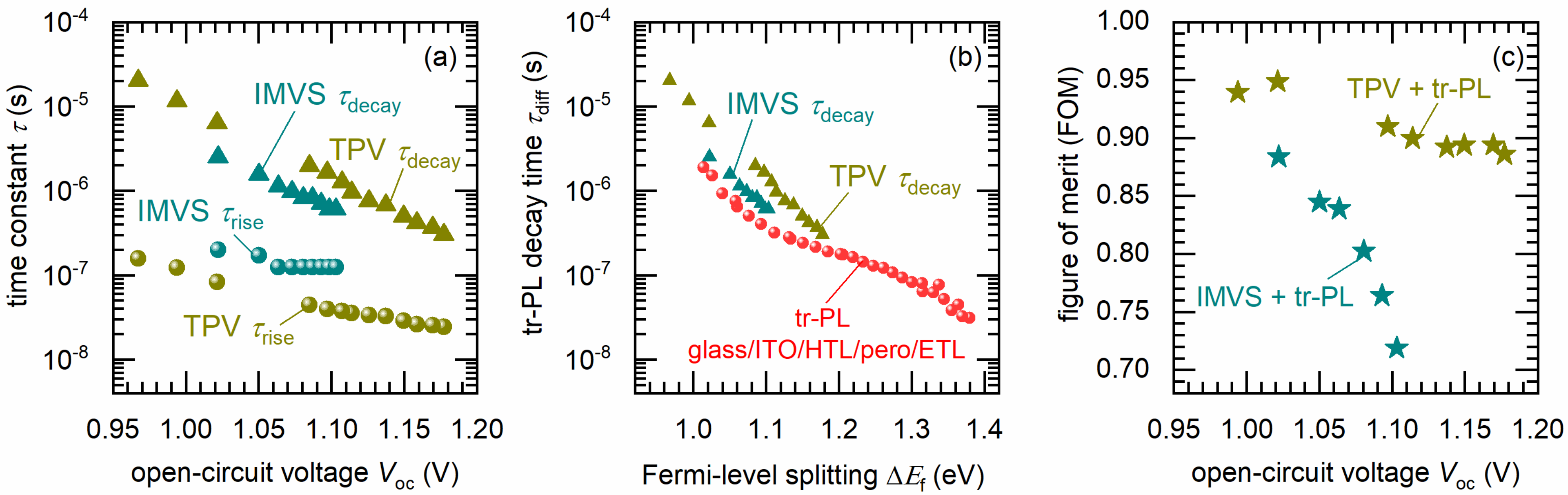

FOM values close to 1 imply a significant electric field in the transport layers that allows fast charge extraction

S. Ravishankar et al., 2024. *Energy & Environmental Science*, *17*(3), pp.1229-1243.

conclusions

JÜLICH Forschungszentrum

Can we resolve doping and defect densities from overlapping mechanisms in capacitance measurements?

→

resolution limit

$$N_{\mathrm{d,min}} = \frac{27 m_{\mathrm{CV}} k_{\mathrm{B}} T \epsilon_{\mathrm{r}} \epsilon_0}{4 q^2 d^2}$$

conclusions

Can we resolve doping and defect densities from overlapping mechanisms in capacitance measurements?

resolution limit

$$N_{\mathrm{d,min}} = \frac{27 m_{\mathrm{CV}} k_{\mathrm{B}} T \epsilon_{\mathrm{r}} \epsilon_0}{4 q^2 d^2}$$

thin-film PSCs have low deep-defect densities but significant shallow defect densities

conclusions

Can we resolve doping and defect densities from overlapping mechanisms in capacitance measurements?

→

resolution limit

$$N_{\mathrm{d,min}} = \frac{27 m_{\mathrm{CV}} k_{\mathrm{B}} T \epsilon_{\mathrm{r}} \epsilon_0}{4 q^2 d^2}$$

→

thin-film PSCs have low deep-defect densities but significant shallow defect densities

can we separate transport layer effects from bulk effects in typical characterization techniques?

$i\omega \times$ transfer function →

verify using time-domain methods

rise time constant → charge extraction

decay time constant → recombination

can we account for the effect of the transport layers on the PSC performance?

→

charge extraction efficiency

$$\mathrm{FOM}(V) = \frac{1}{1 + \frac{\tau_{\mathrm{exc}}(V)}{\tau_{\mathrm{rec}}(V)}}$$

Acknowledgements: Zhifa Liu, Yueming Wang, Lukas Frommel and the Deutsche Forschungsgemeinschaft (DFG).

Energy & Environmental Science

ROYAL SOCIETY OF CHEMISTRY

PAPER

View Article Online
View Journal | View Issue

Check for updates

Cite this: Energy Environ. Sci., 2024, 17, 1229

Discerning rise time constants to quantify charge carrier extraction in perovskite solar cells†

Sandheep Ravishankar,*[a] Lennard Kruppa,[a] Sandra Jenatsch,[b] Genghua Yan[a] and Yueming Wang[a]

Science

TECHNICAL COMMENTS

Cite as: S. Ravishankar et al., Science 10.1126/science.abd8014 (2021).

Comment on "Resolving spatial and energetic distributions of trap states in metal halide perovskite solar cells"

Sandheep Ravishankar[1], Thomas Unold[2], Thomas Kirchartz[1,3*]

PRX ENERGY 2, 033006 (2023)

How Charge Carrier Exchange between Absorber and Contact Influences Time Constants in the Frequency Domain Response of Perovskite Solar Cells

Sandheep Ravishankar,[1,*] Zhifa Liu,[1] Yueming Wang,[1] Thomas Kirchartz,[1,2] and Uwe Rau[1]

PRX ENERGY 1, 013003 (2022)

Multilayer Capacitances: How Selective Contacts Affect Capacitance Measurements of Perovskite Solar Cells

Sandheep Ravishankar,[1,*] Zhifa Liu,[1] Uwe Rau,[1] and Thomas Kirchartz[1,2]

I will lead a new junior research group at Forschungszentrum Jülich, Germany.

Candidates interested in PhD and postdoctoral positions can contact me at s.ravi.shankar@fz-juelich.de.

effect of mobile ions

single crystal device – drift-diffusion simulation

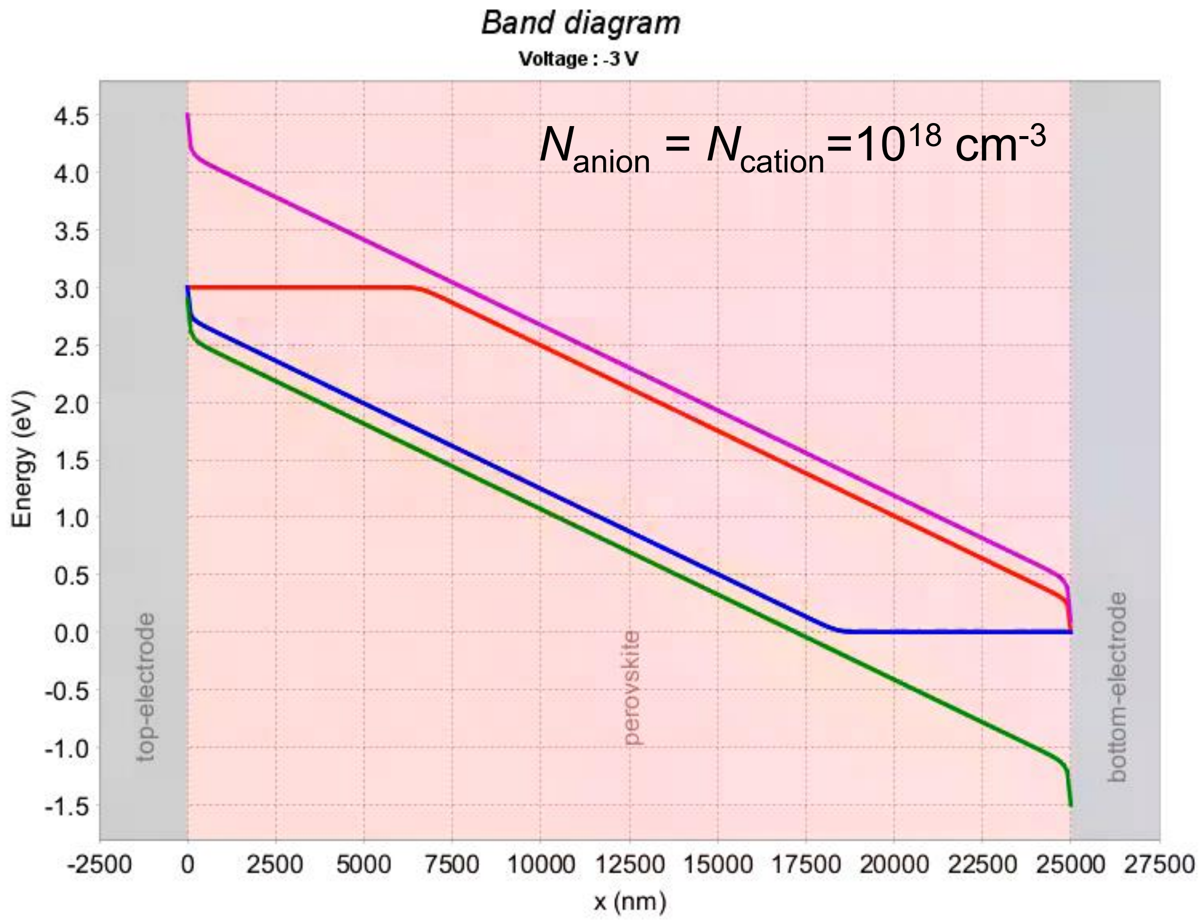

Acknowledgement: Lukas Frommel, Forschungszentrum Jülich.

effect of mobile ions

single crystal device – drift-diffusion simulation

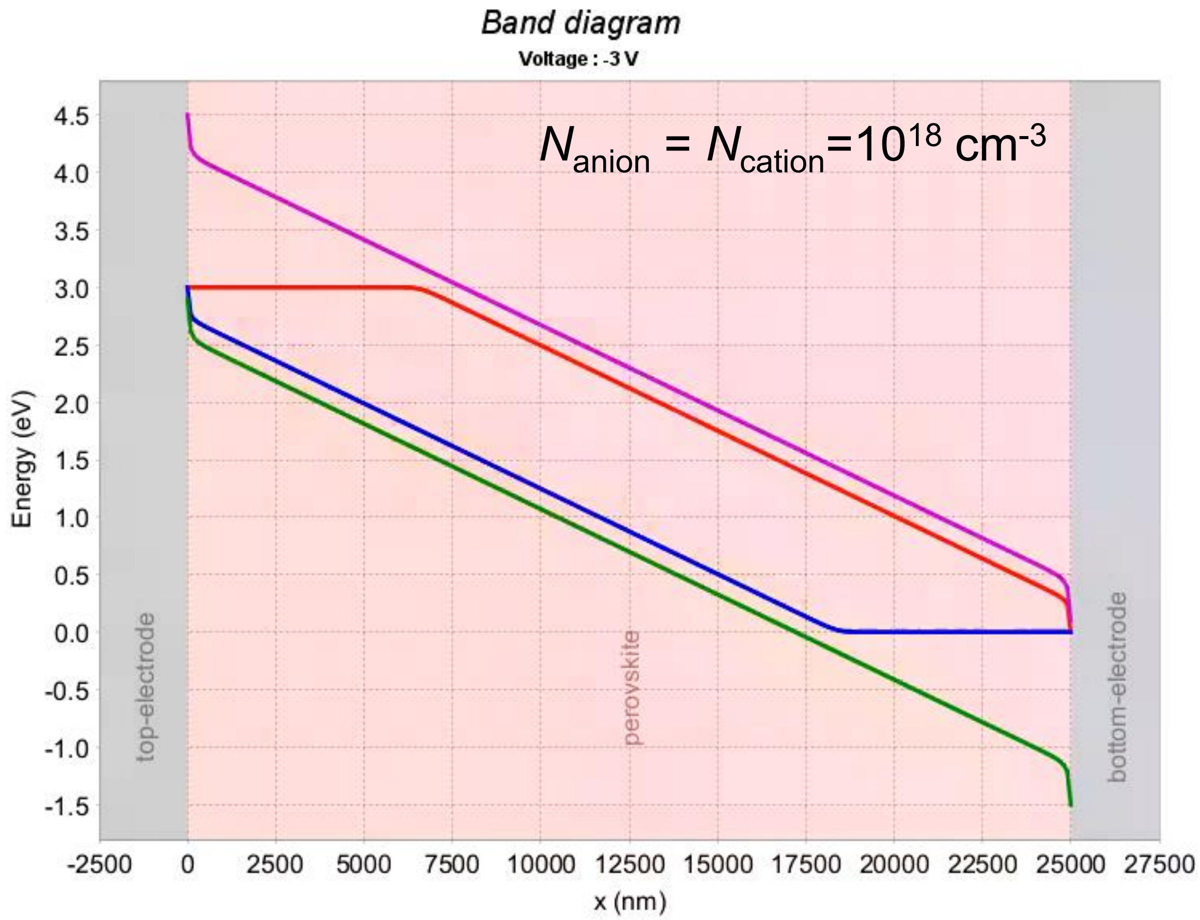

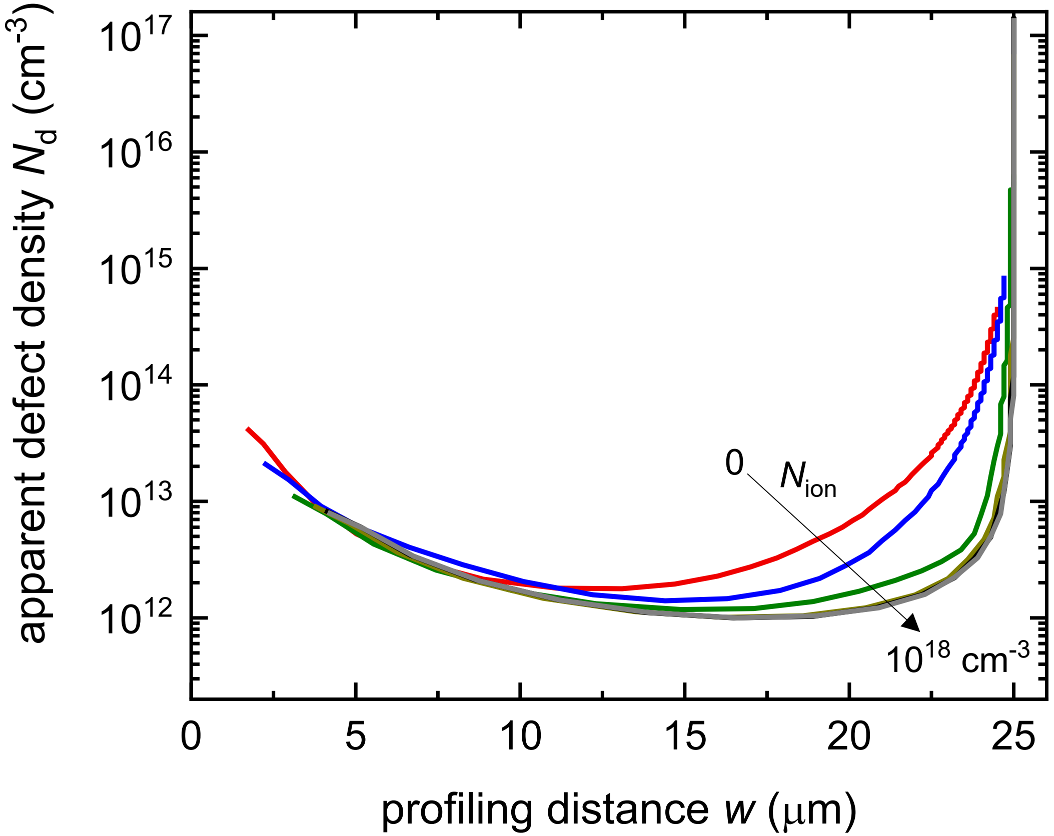

Acknowledgement: Lukas Frommel, Forschungszentrum Jülich.

influence of mobile ions

drift-diffusion simulations

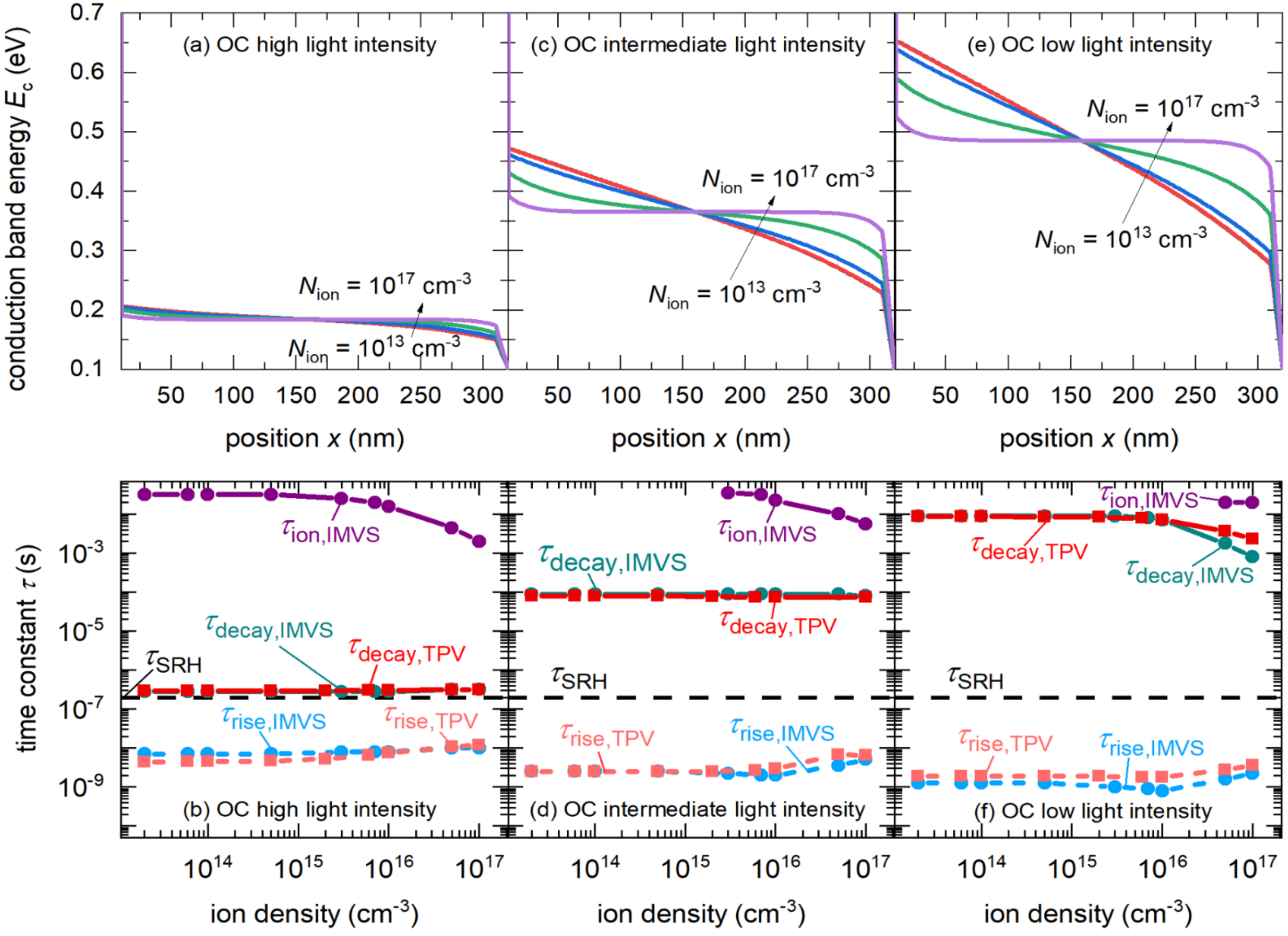

developed analysis using the modified transfer function is valid for devices with mobile ionic densities

additional time constant at low frequencies due to the slow movement of the ions

S. Ravishankar et al., 2024. *Energy & Environmental Science*, *17*(3), pp.1229-1243.

application to experimental data

ITO/SAMs/PTAA/$Cs_{0.05}FA_{0.8}MA_{0.15}PbI_{2.25}Br_{0.75}$ (1.68 eV)/C_{60}/BCP/Ag devices

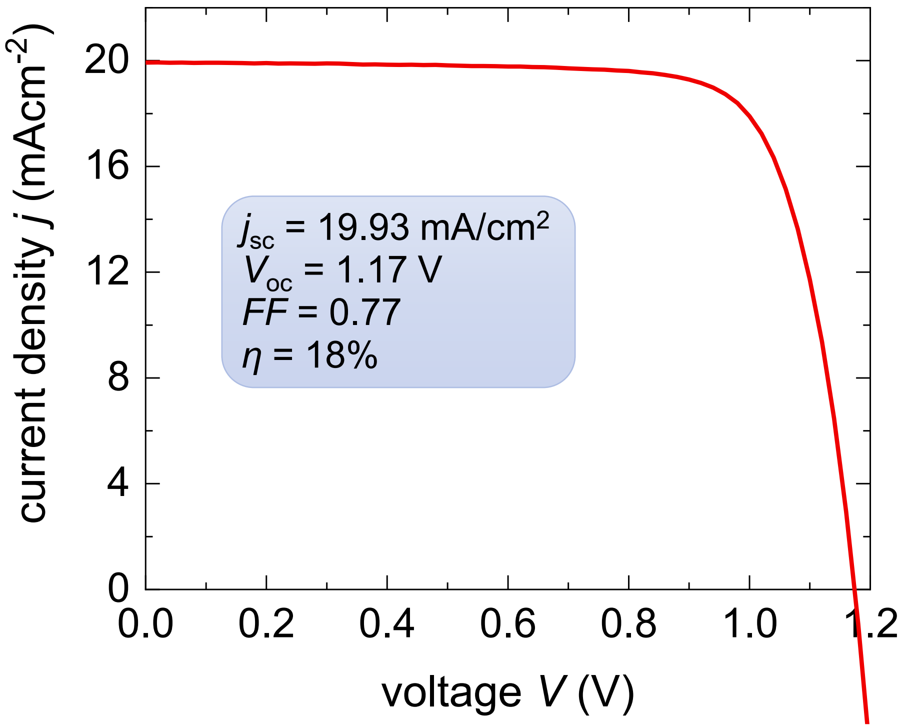

S. Ravishankar et al., 2024. *Energy & Environmental Science*, *17*(3), pp.1229-1243.

ionic influence on measured spectra

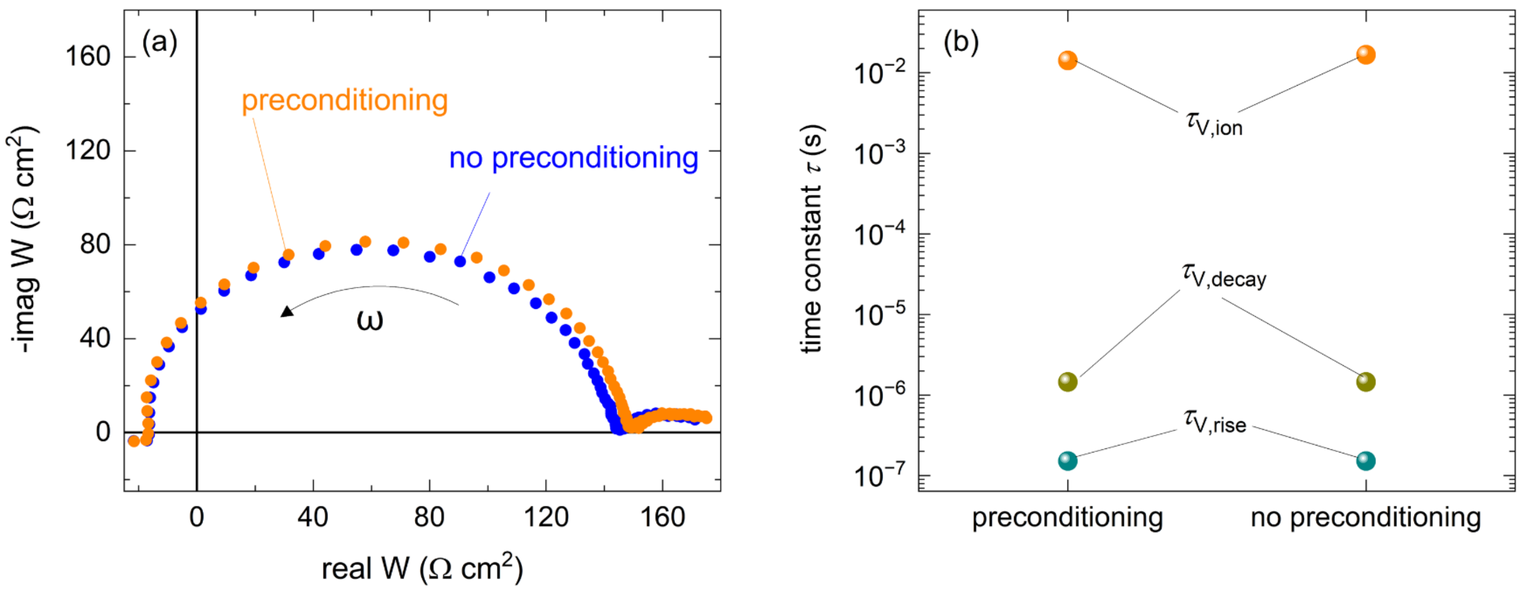

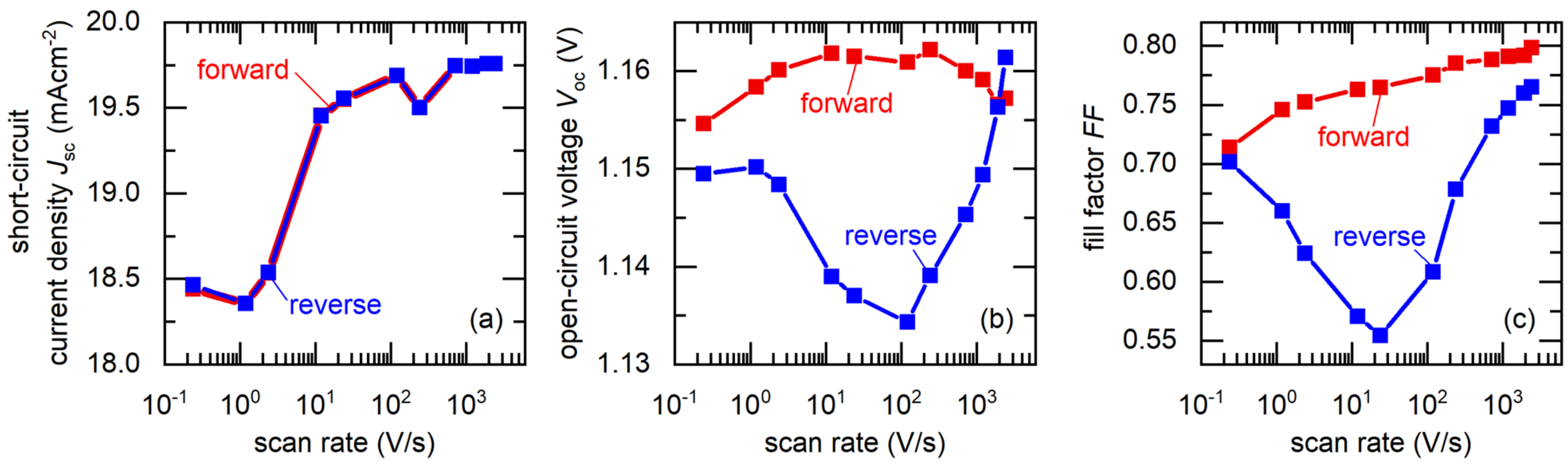

S. Ravishankar et al., 2024. *Energy & Environmental Science*, *17*(3), pp.1229-1243.

predicted time constants

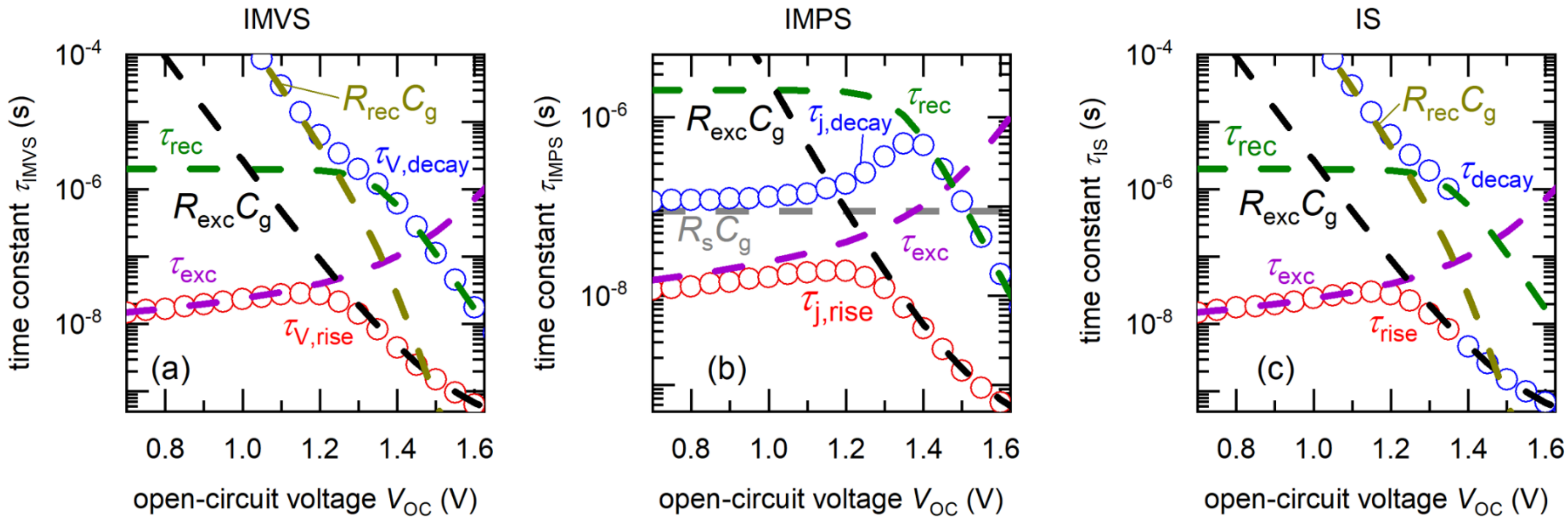

different time constants expressed due to the voltage dependence of resistances and capacitances

rise time constants generally correspond to charge extraction

decay time constants generally correspond to recombination or R_sC_g attenuation

S. Ravishankar et al., PRX Energy **1**, 013003 (2022).

derived equivalent circuit

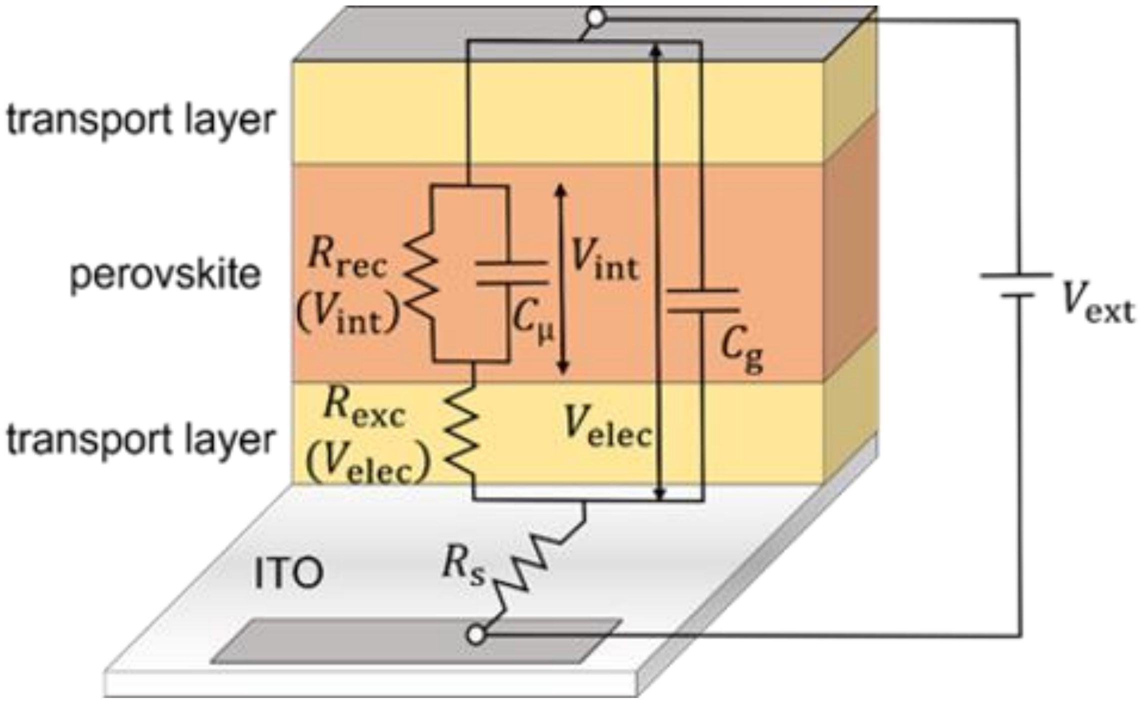

accounts for effects related to the difference between the internal voltage V_{int} (quasi-Fermi level splitting) and the external voltage under illumination

S. Ravishankar et al., 2023. *PRX Energy* 2, 033006.

IS data analysis

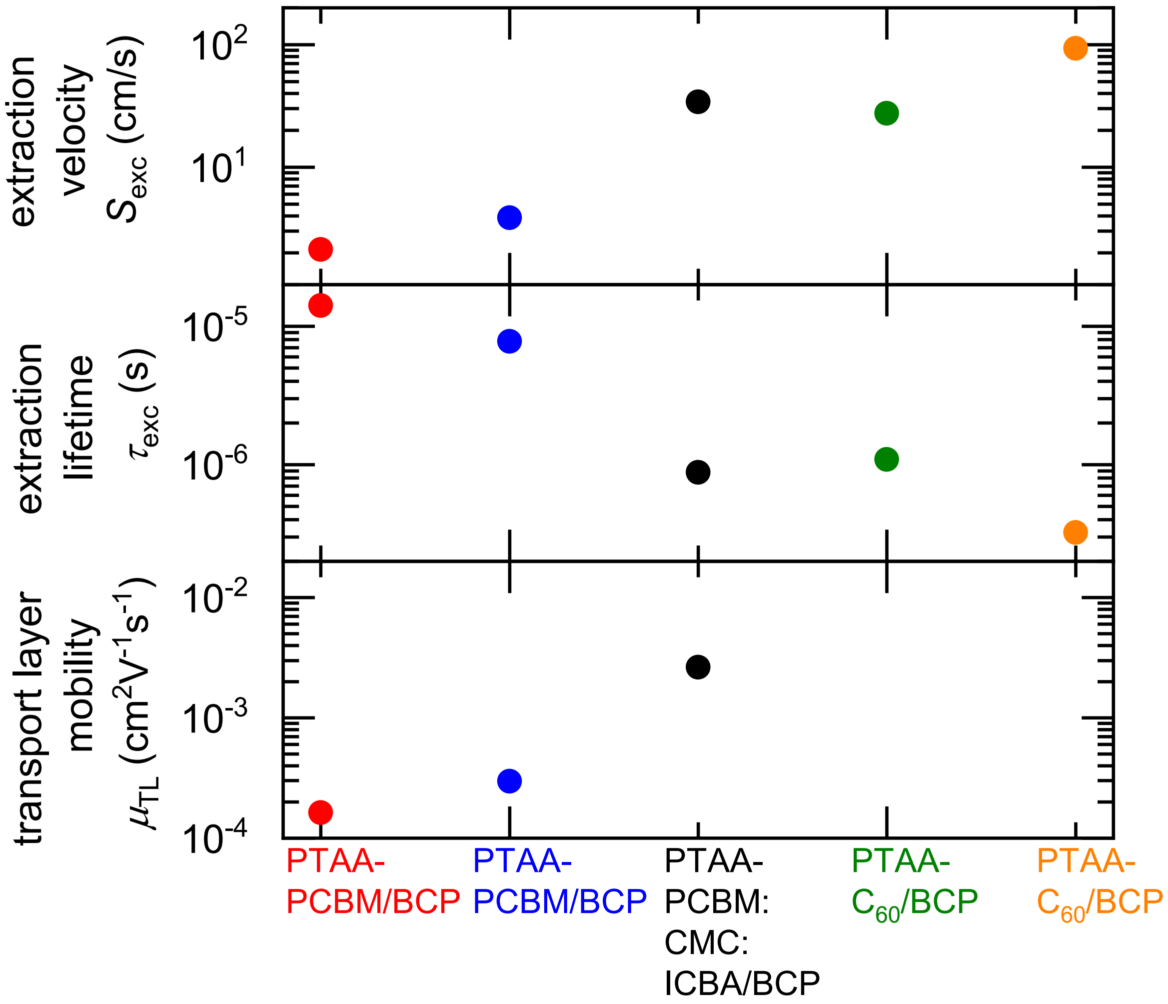

transport layer mobilities between 10^{-4} – 3×10^{-3} $cm^2V^{-1}s^{-1}$ calculated for PTAA-based PSCs

S. Ravishankar et al., PRX Energy **1**, 013003 (2022).

transport layer resistance

recombination resistance

$$R_{\mathrm{rec}} = \left(\frac{1}{R_{\mathrm{rec,SRH}}} + \frac{1}{R_{\mathrm{rec,rad}}}\right)^{-1}$$

transport layer resistance

$$R_{\mathrm{exc}} = \frac{2k_{\mathrm{B}}T}{q^2 n_{\mathrm{i}} S_{\mathrm{exc}}} \exp\left(\frac{-qV_{\mathrm{elec}}}{2k_{\mathrm{B}}T}\right)$$

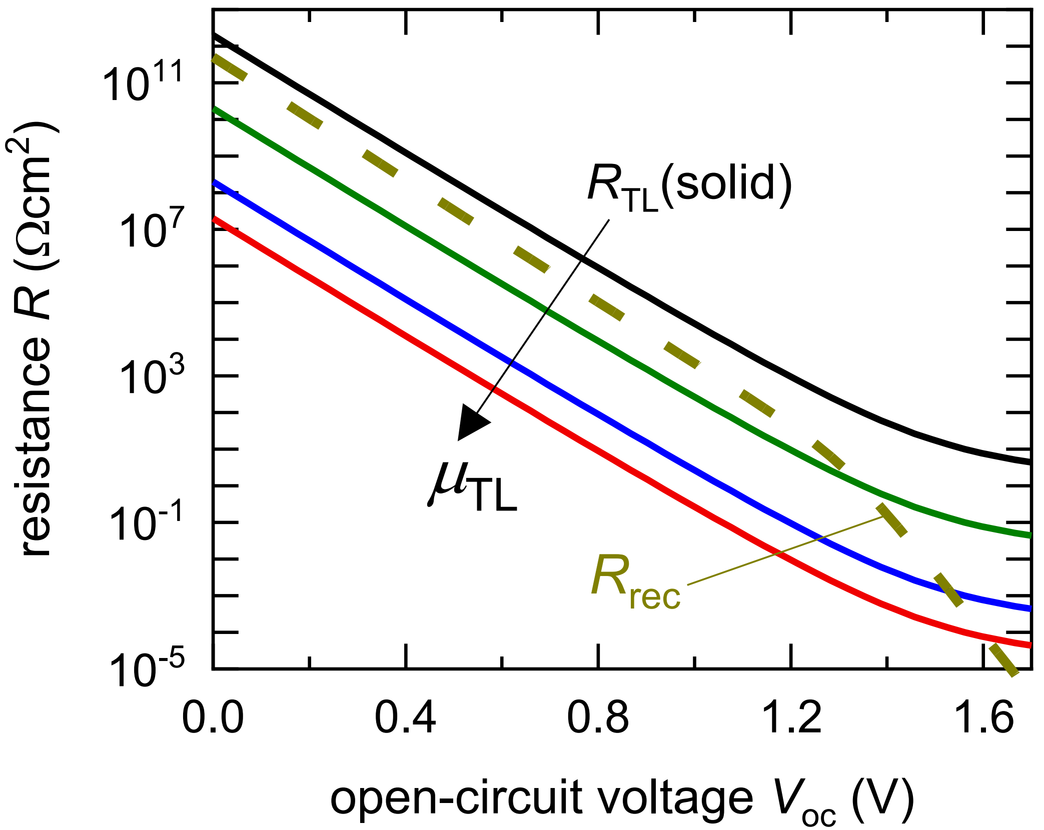

S. Ravishankar et al., PRX Energy **1**, 013003 (2022).

the internal and external voltage

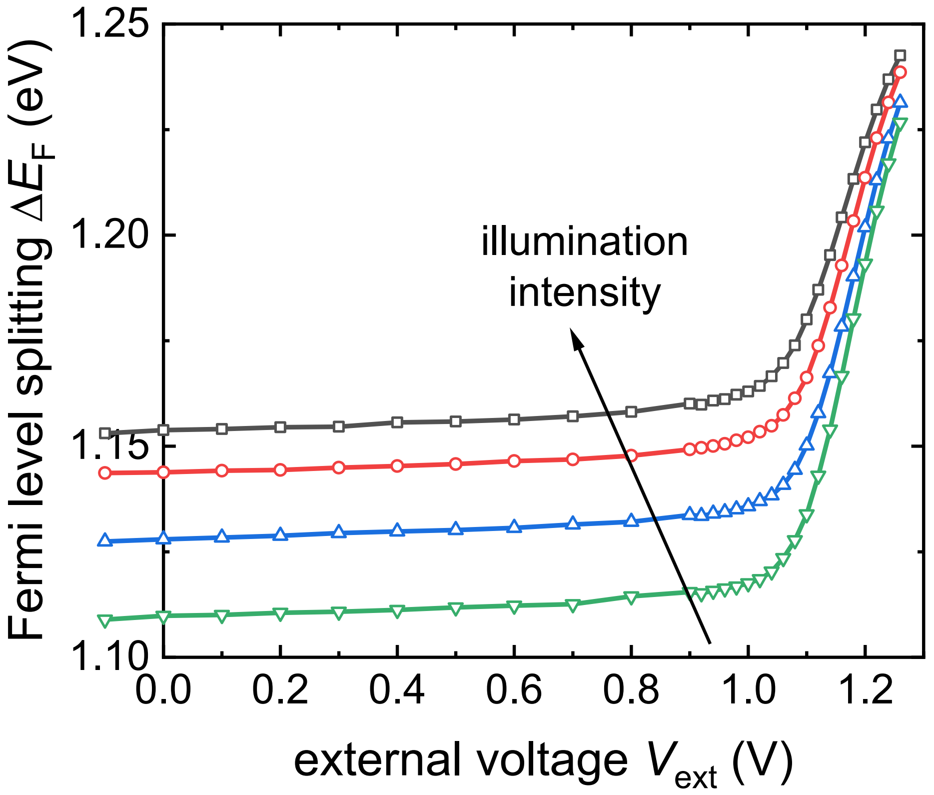

$$j_{rec}(V_{ext}) = j_{rec,0} \exp\left(\frac{\Delta E_F\,(V_{ext})}{n_{id} k_B T}\right)$$

D. Grabowski et al., 2022. *Solar RRL*, *6*(11), p.2200507.

j-V curve

$$j = j_{sc} - j_{0,sat}\left(\exp\left(\frac{qV_{ext}}{n_{id}k_B T}\right) - 1\right)$$

assumptions

quasi-Fermi level splitting is equal to the external voltage, with and without illumination

current due to photogeneration of charge carriers can be superimposed on the dark jV curve

D. Grabowski et al., 2022. *Solar RRL*, *6*(11), p.2200507.

j-V curve

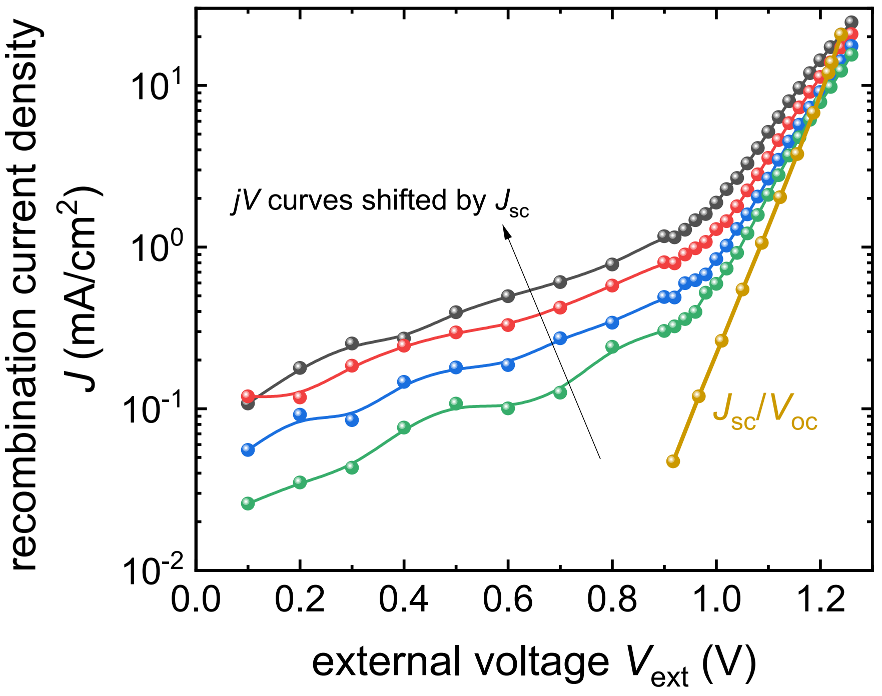

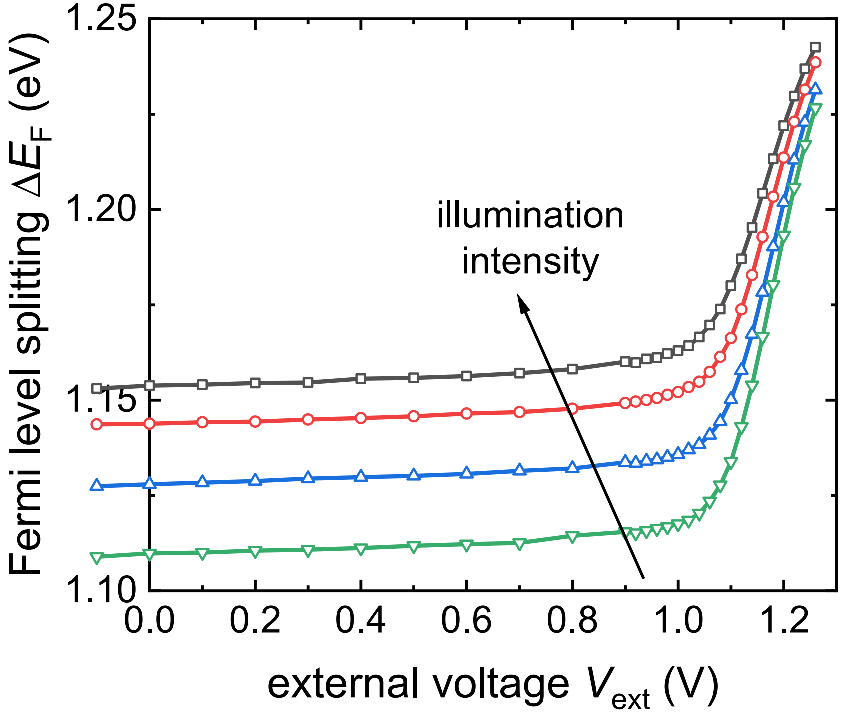

$$j = j_{sc} - j_{0,\mathrm{sat}}\left(\exp\left(\frac{qV_{\mathrm{ext}}}{n_{\mathrm{id}}k_{\mathrm{B}}T}\right) - 1\right)$$

D. Grabowski et al., 2022. *Solar RRL*, *6*(11), p.2200507.

j-V curve with influence of transport layers

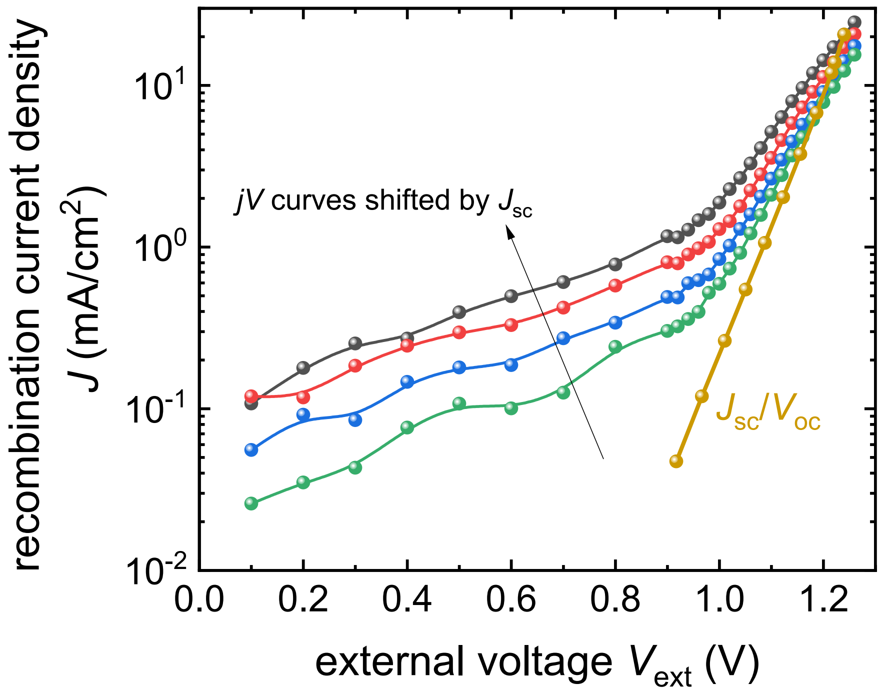

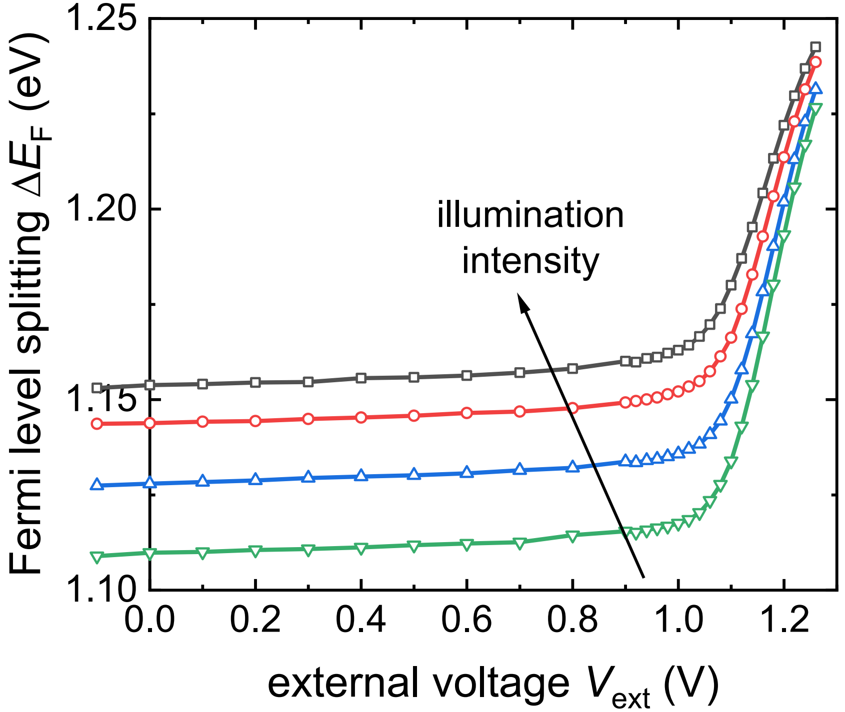

accounts for recombination losses at all points of the jV curve

$$j = qS_{\mathrm{exc}}n_0\left[\exp\left(\frac{qV_{\mathrm{int}}}{n_{\mathrm{id}}k_{\mathrm{B}}T}\right) - \exp\left(\frac{qV_{\mathrm{ext}}}{n_{\mathrm{id}}k_{\mathrm{B}}T}\right)\right]$$

O. Breitenstein, IEEE Journal of Photovoltaics **4**, 899 (2014), U. Rau et al., Physical Review Applied **14**, 014046 (2020).
S. Ravishankar et al., PRX Energy **1**, 013003 (2022).